

POLITECNICO DI MILANO  
*Department Of Electronics, Information and Bioengineering*  
Master of Science in Biomedical Engineering

# **Neuroengineering Compendium - Computational Neuroscience**

Professor: Alessandra PEDROCCHI  
Tutors: PhD. Alice GEMINIANI  
Eng. Valeria LONGATELLI  
Eng. Alessandra TRAPANI

\*\*\* Disclaimer: the content of this compendium is intended as supplementary material for students attending Neuroengineering class by prof. Pedrocchi at the Politecnico di Milano. It is based on shared notes prepared by former students and revised by the professor and the tutors. References to sources is always put, at the best of our knowledge. Circulation of this material outside the class or using any other tool but Beep channel is not permitted. \*\*\*



---

# Contents

---

<b>1 Motor Control and Motor Learning</b>	<b>3</b>
1.1 Source of Complexity in Motor Control and Motor Learning . . . . .	3
1.2 Sensory-Motor Integration . . . . .	4
1.3 Reflexes vs Voluntary Movement . . . . .	8
1.3.1 Reflexes . . . . .	8
1.3.2 Voluntary movement . . . . .	9
1.4 Motor Learning . . . . .	14
1.5 Modelling Motor Control . . . . .	16
1.5.1 Forward Model . . . . .	18
1.5.2 Inverse Model . . . . .	23
1.5.3 Forward-Inverse Model . . . . .	24
1.5.4 Multiple Paired Forward-Inverse Model . . . . .	25
<b>2 Neural Bases of Motor Control</b>	<b>29</b>
2.1 Primary Motor Cortex . . . . .	31
2.2 Ventral Stream . . . . .	37
2.3 Spinal Cord . . . . .	38
2.4 Supplementary Motor Areas and Premotor cortex . . . . .	39
2.5 Cerebellum . . . . .	41
<b>3 Focus on the Cerebellum</b>	<b>43</b>
3.1 Anatomical and Functional Structure . . . . .	43
3.2 Cerebellar Microcircuit . . . . .	45
3.2.1 Cerebellar input: mossy fibers, Granule cells and climbing fibers.	47
3.2.2 Electrical Activity of Purkinje Cells . . . . .	48
3.2.3 Cerebellar output: deep cerebellar nuclei . . . . .	49
3.3 Learning and Plasticity . . . . .	49
<b>4 Modelling and Simulation: Single Neuron Modeling</b>	<b>53</b>
4.1 Hodgkin-Huxley Model . . . . .	54
4.1.1 Markovian Stochastic Version . . . . .	57
4.2 Multi-Compartmental Models . . . . .	57

---

---

4.3	Leaky Integrate and Fire Model . . . . .	60
4.3.1	Izhikevich Model . . . . .	60
4.3.2	Adaptive Exponential LIF Model . . . . .	61
4.3.3	Generalized LIF Model . . . . .	62
4.3.4	Extended Generalized LIF Model . . . . .	64
4.3.5	E-GLIF Model: Reproducing Golgi Cell Electroresponsiveness .	67
4.4	Cerebellar Neurons Modelling . . . . .	68
<b>5</b>	<b>Modelling and Simulation: Cerebellum</b>	<b>71</b>
5.1	Cerebellum as an Inverse Model . . . . .	74
5.2	Plasticity . . . . .	76
5.2.1	Plasticity Models in Cerebellar SNN . . . . .	77
5.3	Neurorobotics . . . . .	78
5.3.1	Eye Blinking Classical Conditioning . . . . .	80
5.3.2	Vestibulo-Ocular Reflex . . . . .	81
5.3.3	Reaching Perturbed by Force Fields . . . . .	82
<b>List of Figures</b>		<b>83</b>
<b>List of Tables</b>		<b>85</b>
<b>Bibliography</b>		<b>87</b>

---

Computational neuroscience is defined as the branch of neuroscience which employs mathematical models to investigate the principles and mechanisms that guide the development, organization, information-processing and mental abilities of the nervous system. It aims both at understanding the brain functioning and advancing computational control solutions, mimicking brain performances. Models seek to capture the essential features of the biological system at multiple spatial-temporal scales from membrane currents, microcircuits, brain areas, all the way up to cognitive functions like memory, learning and behaviours. With an ever-growing progress in biological imaging techniques and computational power resources, nowadays these models can be validated through ad hoc neurophysiological experiments.

Motor control is one of the major research topic in the field of computational neuroscience, where many models have been proposed to describe the pathways for sensory signals and motor commands, and their mutual influence.

In organisms provided with nervous system, motor control is conceived as the regulation of movement. Movement is our only instrument for active interaction with the external world. Obvious examples range from expression of complex thoughts (writing, reading, talking, communicating...) to artistic production, sportive tasks, interpersonal relationships and so on. Even if most of the time it does not require any complicated conscious reasoning, movement is a really complex task to achieve. Just think of one of the movements that we all do several times a day: drink a glass of water. Even behind such a simple gesture, there is a long cascade of movements one needs to perform the drinking action:



**Figure 1:** As easy as drinking a glass of water... (From <https://it.beformentance.com/news/bicchiere-dacqua>)

1. Identification of the glass
2. Localization of the glass in relation to the external environment
3. Localization of your hand in relation to the glass

4. Reaching the glass
5. Grasping the glass without breaking it or letting it slip
6. Bringing the glass close to the mouth
7. Coordinating the arm movement and the opening of the mouth
8. Drinking

In order to achieve the final movement, we have to process and integrate different information, not only the one related to the mechanical part of the movement (i.e. motor commands), but also information related to sensation (i.e. sensory stimuli).

# Motor Control and Motor Learning

---

## 1.1 Source of Complexity in Motor Control and Motor Learning

There are several features of the human motor system that significantly complicate motor control and motor learning. There are **delays** both in the transduction of motor command from the Central Nervous System (CNS) to the muscular system and in the conduction processes of sensorial signals to the CNS. In addition, sensorial delays combine with delays associated with movement itself. These delays make the sensorial information unusable to guide at least the initial part of the movement. For this reason, the execution of fast and skilled motor tasks requires a **prediction**, thus an open loop control.

Besides delays, both sensorial inputs and motor control signals are subject to **intrinsic neural noise** that limits the motor system ability to simultaneously execute fast and accurate movements (To overcome this noise, the motor system has to combine actual sensorial data with a direct model). Therefore **motor planning** is required, as well as experience, to induct the correct information from a noisy signal.

**Time variance.** The relation between motor commands and actual executed task (dynamic) changes with time by two different points of view. First, there is an **ontogenetic factor**, which is a long term change that occurs across life span or across training i.e. living subjects growing up, and second, in a short time framework, our motor task actuation changes as we interact with different objects and in different environments. Training as well as pathologies continuously modify our actuation system and also the controlling neural mechanisms (piano players have completely different brain areas for hand control as well as tennis players have much broad brain areas for arm motion). A person suffering pain at the shoulder have a “modified” actuation

system. Of course any neurological pathology does affect motor control neural circuits. For this reason the relation between motor commands and actual movement is defined as **not stationary**.

Another level of complexity is the **non linearity** of both the environment in which the motor control works and our motor system:

- **Gravity force (external non linearity)**: the same exact motor sequence has very different effects if executed in a microgravity environment or on the Earth. Moreover the same motor command results in different configurations if executed by a lying or standing subject.
- **Joint range of motion (internal non linearity)**: our joints limit the movement in a given direction, reaching the anatomical constraint of the range of motion. At range of motion limits, higher motor commands (muscle contraction) do not result in any larger motion, achieving a saturation condition. Saturation is a straightforward example of non linearity.

Finally, the system is characterized by a significant **multidimensionality**. Considering that we have around 600 muscles in our body and let's suppose to simplify that they can be contracted or relaxed, there are  $2^{600}$  possible activation patterns (magnitude order of 10180). However, if we look at the “experience” of movements, we observe that motor tasks are actually **stereotyped**. At the motor control level, motion is managed through synergies.

To sum up, we can identify the following source of complexity in our motor control system:

1. Delays;
2. Noise;
3. Non-stationarity;
4. Non-linearity;
5. Multidimensionality (redundancy).

If we consider these features from an engineering point of view, the machine results quite complex and tackles some of the most critical points of any machine design.

## 1.2 Sensory-Motor Integration

There is a close connection and a mutual influence between sensorial brain areas and motor brain areas. Indeed actions and perceptions are involved in a loop-type of

communication, not an unidirectional one. The **sensorimotor integration** is a complex process that takes place in the CNS and that produces task-specific motor outputs based on the selective and rapid integration of sensory information from multiple sources. From a computational point of view, the brain is a processing system that converts inputs to outputs. **Inputs** are feedback **sensorial data** produced by both our sensorial organs and internal signals due to cognitive processes, **outputs** are **motor commands** that act on our muscles. Motor control can be seen as the transformation process from sensorial inputs to motor outputs. The motor control and motor learning problem is to regulate and adapt these sensory-motor transformations (through open- or closed-loop processes). The transformation from sensory to motor information is

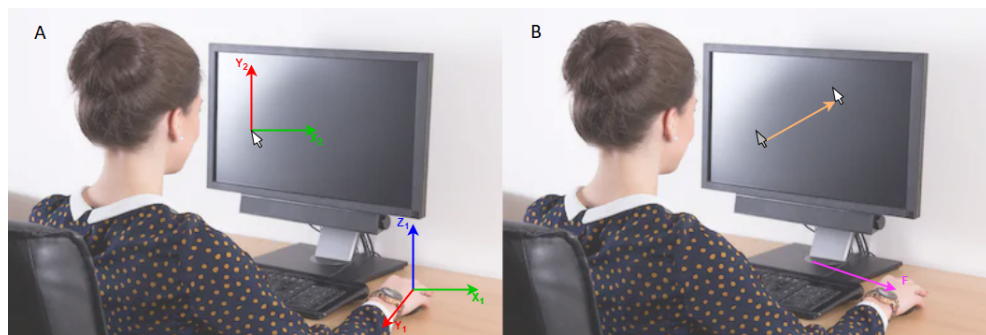


**Figure 1.1: Kinematic and Dynamic transformation:** (A) Kinematic transformation between hand position and cursor position on the monitor; (B) Dynamic transformation involves forces mechanism that control the mouse displacement on the screen, that depends on the mouse inertia and friction (Adapted from [https://www.shutterstock.com/it/search/receptionist+computer+screen?image\\_type=photo](https://www.shutterstock.com/it/search/receptionist+computer+screen?image_type=photo))

a cascade that can be subdivided into **kinematic and dynamic transformations**. Kinematic transformations convert systems coordinates, for example the transformation between hand position and arm angles (e.g. transformation between mouse position and cursor position on the monitor, Figure 1.1). Dynamic transformations link motor commands with movement (e.g. forces mechanism that control the mouse displacement on the screen, that depends on the mouse inertia and friction, Figure 1.1).

**Practical example: Taking an object with the hand.** First, we need to compute the coordinates of the object with respect to the end effector, the hand in this case, starting from the egocentric coordinates both of the end effector and the object. Then, we have to determine the joint trajectories necessary for the end effector to reach the object. Eventually we can apply the joint torques needed to obtain the desired muscle activation.

There are multiple levels of indefiniteness in this process, infinite combinations of these transformations, i.e. **level of redundancy**, 1) in the definition of the end effector

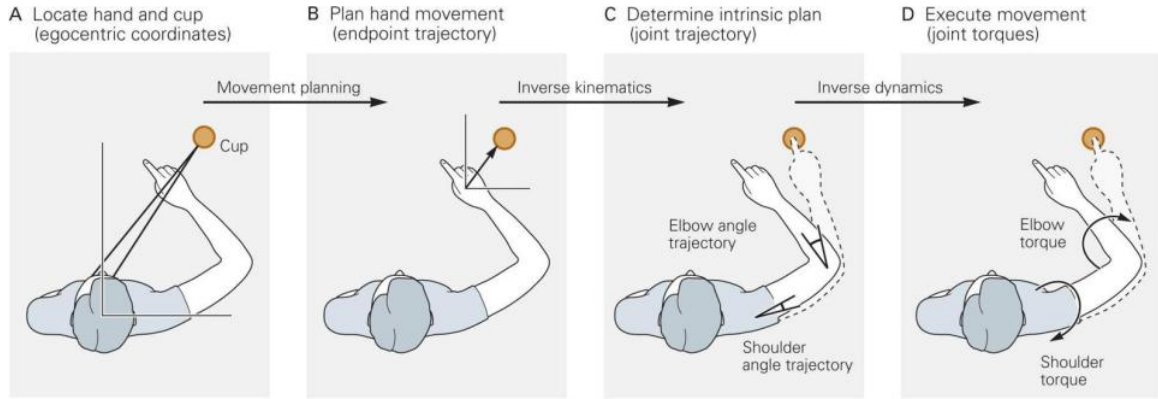


**Figure 1.2: Sensorimotor transformations in a reaching movement:** (A) **Spatial orientation.** To reach for an object, the object and hand are first located visually in a coordinate system relative to the head (egocentric coordinates). (B) **Movement planning.** The direction and the distance that hand must move to reach the object (the endpoint trajectory) are determined based on visual and proprioceptive information about the current locations of the arm and object. (C) **Inverse kinematic transformation.** The joint trajectories that will achieve the hand path are determined. The transformation from a desired hand movement to the joint trajectory depends on the kinematic properties of the arm, such as the lengths of the arm's segments. (D) **Inverse dynamic transformation.** The joint torques or muscle activities that are necessary to achieve the desired joint trajectories are determined. The joint torques required to achieve a desired change in joint angles depend on the dynamic properties of the arm such as the mass of the segments. (From [1])

path to reach the target, 2) in the joint trajectories to accomplish the end-effector path, 3) in the muscles activation once defined the joint torques. Redundancy of our neuromotor system is a very important resource of our body, it is exploited to adapt solution to specific situations (such as pain), to optimize performance, to overcome unexpected perturbations, therefore to assure **flexibility**. This is the starting point and the resource of any learning processes.

**Perception** plays a relevant role in motor control. The sensorial information is processed on the basis of the experience and carries fundamental information about objects, environments and bodies, used in organizing and executing actions and movements.

Multiple stimuli present in the visual field at the same time compete for neural representation by mutually suppressing their evoked activity throughout visual cortex, providing a neural correlate for the limited processing capacity of the visual system. These competitive interactions among multiple stimuli, present in the visual field at the same time, can be counteracted by **top-down** or **goal-directed mechanisms**, through the use of contextual information in pattern recognition, and by **bottom-up** or **stimulus-driven mechanisms**, where the perception begins with the stimulus itself.

According to [2], perception and action are linked together. Actions need perceptual information to be planned and adaptively executed, and perceptual systems needs actions to produce the relevant patterns and information. Movement is considered as



Figure 1.3: *Perception*

embedded in a continuous perception-action chain, in which perceptual information provides the basis for adaptive and prospective motor control. Active exploration is seen as the connection in the perception-action loop which generates or allows for gathering information for deciding what to do next. According to Piaget 1953 [3] , infants are exploring their own action system by performing certain movements over and over again and evaluating the continuous multimodal flow of sensory information. Likewise, Hofsten 1991 [4] proposed that exploratory movements are directed towards the infant's own action system instead on the external environment, which is traditionally expected. In a nutshell, one of the predominant driving forces of changes in behavior and development is proposed to be the exploration of the capacities of the individual.

## 1.3 Reflexes vs Voluntary Movement

Sensory-motor transformations can be subdivided in two typologies: *Reflexes* and *Voluntary movements*

### 1.3.1 Reflexes

Reflexes are involuntary movements or actions. Some movements are spontaneous, occurring as part of the baby's usual activity. Others are responses to certain actions. Reflexes help identify normal brain and nerve activity. Some reflexes occur only in specific periods of development. Reflexes are automatic non scalable responses to specific stimuli. If the stimulus is repeated, the response is always triggered in the same way, there is no modulation and no conscious capability to prevent it. Some reflexes are kept all life long. Some others are typical of newborn and are the starting point of our motor control, these latter are abandoned after a few months, letting the baby learn new and multiple solutions.

The following are some of the normal reflexes seen in newborn babies:

- *Root reflex.* This reflex begins when the corner of the baby's mouth is stroked or touched. The baby will turn his or her head and open his or her mouth to follow and "root" in the direction of the stroking. This helps the baby find the breast or bottle to begin feeding.
- *Suck reflex.* Rooting helps the baby become ready to suck. When the roof of the baby's mouth is touched, the baby will begin to suck. This reflex does not begin until about the 32nd week of pregnancy and is not fully developed until about 36 weeks. Premature babies may have a weak or immature sucking ability because of this. Babies also have a hand-to-mouth reflex that goes with rooting and sucking and may suck on fingers or hands.
- *Moro reflex.* The Moro reflex is often called a startle reflex because it usually occurs when a baby is startled by a loud sound or movement. In response to the sound, the baby throws back his or her head, extends out the arms and legs, cries, then pulls the arms and legs back in. A baby's own cry can startle him or her and trigger this reflex. This reflex lasts about 5 to 6 months.
- *Tonic neck reflex.* When a baby's head is turned to one side, the arm on that side stretches out and the opposite arm bends up at the elbow. This is often called the "fencing" position. The tonic neck reflex lasts about 6 to 7 months.
- *Grasp reflex.* Stroking the palm of a baby's hand causes the baby to close his or her fingers in a grasp. The grasp reflex lasts until about 5 to 6 months of age.

- *Babinski reflex.* When the sole of the foot is firmly stroked, the big toe bends back toward the top of the foot and the other toes fan out. This is a normal reflex up to about 2 years of age.
- *Step reflex.* This reflex is also called the walking or dance reflex because a baby appears to take steps or dance when held upright with his or her feet touching a solid surface.

### 1.3.2 Voluntary movement

Differently from reflexes, voluntary movements are planned by the intention of the subject and they can be modulated by external or internal events. They are independent from the effector, goal-directed and, differently from reflexes, can answer differently to the same stimulus depending on the goal and can be generated by internal instructions, not only as a response to an external stimulus.

**Practical Example: *Reaching task.*** Reaching tasks are typical volitional movements [1].

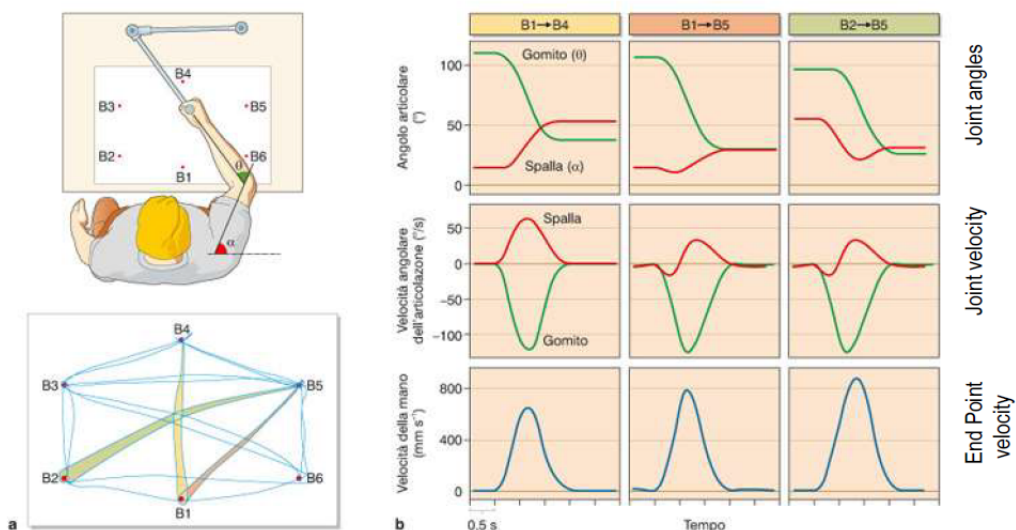


**Figure 1.4: Reaching task:** (a) The subject is required to make reaching tasks to multiple targets on the horizontal plane. Lower plot: End Point trajectories are quite rectilinear. (b) Different shoulder rotation (red traces) are used to get to the different targets, while very similar elbow joint traces (green) are shown (first raw). Also the joint velocity (second row) are modulated to achieve a very similar end-point velocity (third row). (From [1])

In order to perform a voluntary task, the brain needs to solve the levels of redundancy, mentioned before. However, we can easily observe that, as seen in Figure 1.4, there are important similarities in the execution of reaching tasks to different targets. Some features are stable across different target positions and across multiple subjects. These features are for reaching tasks: 1) the quasi-rectilinear endpoint path and 2) the

bell-shaped endpoint and joints velocities. These experimental observations suggest that, besides the infinite possible solutions, there is a tendency to solve redundancy in stereotyped solutions [1].

All paths are roughly straight and all hand speed profiles have the same shape and scale in proportion to the distance covered. In contrast, the profiles for the elbow and shoulder angles for the three hand paths differ. The straight hand paths and common profiles for speed suggest that motor planning is done with reference to the hand because these parameters can be linearly scaled. Planning with reference to joints would require computing nonlinear combinations of joint angles.

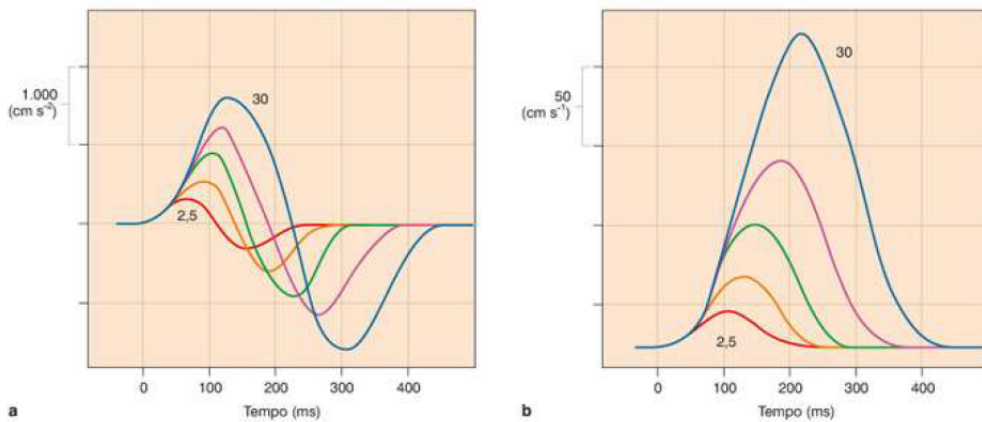


**Figure 1.5: Velocity and acceleration** change with the distance of the target. (a) Hand acceleration over time (b) Hand velocity over time. (From [1]).

If the brain forms a representation of a movement before its execution, does it plan the extent of the movement or does it continuously assess the distance between the hand and the target and use visual information to stop movement once the target is reached? If the brain relied primarily on vision to stop, the initial speed of the hand might be relatively similar in movements of different extents [1].

Instead, both the speed and the acceleration of the hand movement are scaled proportionately to the distance of the target (Figure 1.5). This means that the extent of a movement is planned before the movement is initiated. The representation of this plan for movement is called a **motor program**. The motor program specifies the spatial features of the movement and the angles through which the joints will move. These are collectively known as movement kinematics. The program must also specify the forces required to rotate the joints (torques) to produce the desired movement. This is known as movement dynamics.

## Laws of voluntary movement

### *I law: Voluntary movement shows invariant features*

The CNS plans in abstract way the final output of the movement independently from the mechanisms which will be carried out to accomplish it. Performance does depend

A Right hand Able was I ere I saw Elba

B Right hand (wrist fixed) Able wasl ere I saw Elba

C Left hand Able was I ere I saw Elba

D Teeth Able wasI ere I saw Elba

E Foot Able war& ere I saw Elba

**Figure 1.6: Motor equivalence:** It is possible to write using different parts of the body. The examples shown in figure are written with the right hand (A), with the right hand but with the wrist fixed (B), with the left hand (C), with the pen between the teeth (D), and with the pen fixed to the foot (E). The capacity to perform the same motor behavior with different muscular groups is called motor equivalence. (From [5])

on the effector, thus the natural solution chooses the effector which gets the best performance (“*the more the use, the better the performance*”). In the early 1950s the psychologist Donald Hebb [6] observed that individual motor actions share important characteristics even when performed in different ways. For example, our handwriting appears about the same regardless of the size of the letters or of the limb or body segment used to produce them (Figure 1.6).

Hebb called this **motor equivalence**. Motor equivalence suggests that a purposeful movement is represented in the brain in some abstract form rather than as a series of joint motions or muscle contractions.

The continuous motion of drawing a figure eight consists of regular increases and decreases in the angular motion of the hand. These changes in angular motion occur at regular intervals during which the hand describes approximately equal angles, a feature termed **isogony**. The duration of each hand movement is the same regardless of the length of the hand path, a feature termed **isochrony**. Studies of more complex movements, such as those made during random continuous scribbling, show a similar segmentation. Such studies also reveal a consistent relationship between the speed of hand motion and the degree of curvature of the hand path: velocity varies as a continuous function of the curvature raised to the  $2/3$  power. This two-thirds power law governs virtually all movements and expresses an obligatory slowing of the hand during

movement segments that are more curved and a speeding up during segments that are straight [1].

### ***II law: Reaction time increases with quantity of information that has to be processed***

A process that brings with it a lot of external inputs, necessarily needs more time in

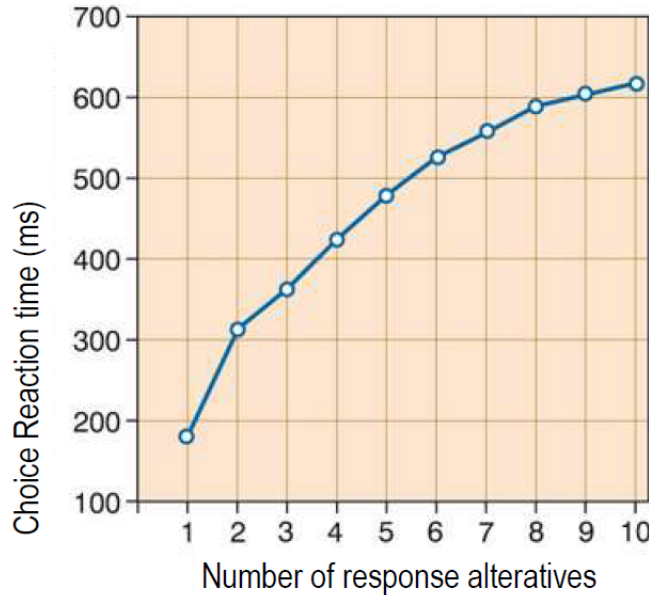


**Figure 1.7: Reaction time increases with the information content:** Reaction time increases non-linearly with the number of response alternatives available to the subject. (From [1])

order to evaluate a higher number of possible answers. The reaction time, i.e. the time that pass between the external stimulus and the motor response, increases non-linearly with the number of alternative answers available to the subject, thus information to be processed: → *External Stimulus* → *Identification of the Stimulus* → *Selection of the answer* → *Motor Output*.

### ***III law: Speed-accuracy trade off (also called Fitt's law)***

The accuracy of a movement varies in direct proportion to the speed of movement. The higher the velocity, the lower the accuracy. Multiple factors concur to the worsening of accuracy for fast motions:

1. If the available time is short, feedback loops does not enter into play
2. Signal dependent noise: higher speed means more recruited motor units that result in higher signal-dependent noise, thus lower accuracy
3. Higher speed means more recruited motor units, thus more variance

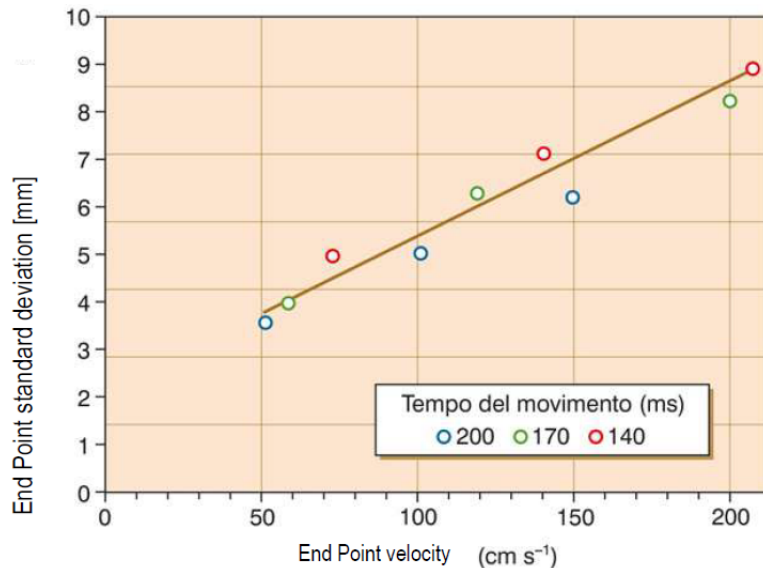


**Figure 1.8: Fitt's law: speed-accuracy trade-off:** Subjects held a stylus and had to hit a straight line lying perpendicular to the direction in which they moved the stylus. Subjects could not see their hand and thus were unable to correct their movement. The variability in the motion of the subjects' arm movements is shown here as the standard deviation of the extent of movement plotted against average speed (for three different movement times). The variability in movement increases in proportion to the speed and therefore to the force producing the movement. (From [1])

Minimum variance is an important criterion of optimization for movement learning. In the 1890s the psychologist Robert Woodworth showed that fast movements are less accurate than slow ones [7]. This is in part because fast movements leave less time for feedback corrections. In fact, the fastest movements are shorter than the reaction time itself. However, lack of time for correction does not explain fully why fast movements are less accurate and more variable than slow ones; faster movements made without visual feedback are also more variable in both extent and speed.

Several factors contribute to the increase in variability with speed. One of these is the recruitment of additional motor neurons to produce rapid increases in force, since the excitability of motor neurons is subject to random variations. A constant incremental increase in force is produced by progressively smaller numbers of motor neurons. Therefore, as force increases, fluctuations in the number of motor neurons lead to proportionately greater fluctuations in force and thus velocity. This proportional relationship is maintained over most of the range of contractile force and corresponds to the proportional increase in variability with the speed of movement and the distance of the target. [8]

#### **IV law: Movement efficiency grows with experience and learning**

Variability also arises because subjects may be uncertain about the forces and

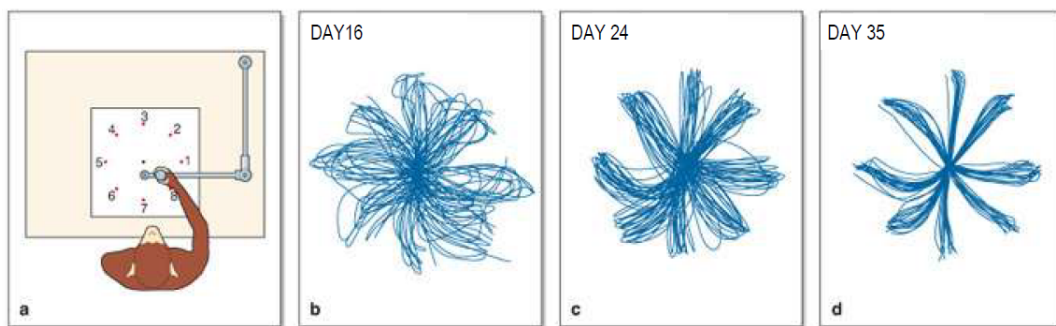


**Figure 1.9: Learning induced by repetitive training:** (A) A monkey was made to sit at a table and move a handle at the end of a manipulandum (starting from the position shown) over the surface toward targets arranged in a circular array (numbered 1-8). The monkey was required to move the handle from the center of the array to whichever one of the targets lit up, covering the target with a clear plexiglass circle on the end of the manipulandum. (B) Records of movement trajectories for a monkey are shown at successive stages of training. The trajectories become straighter with practice, and increasing accuracy is reflected in the decreased dispersion (variability) of the trajectories. (The persistent curvature of the trajectories to targets 4, 5, and 6 is a result of mechanical constraints of the apparatus.) (From [1])

loads that are needed to oppose movement. This uncertainty decreases with practice, however, so that both the accuracy and the speed of movement increase. For example, a monkey that is trained to grasp a handle and move it to a series of targets learns to anticipate opposing forces and to program its movements accurately before initiating a movement. With time, movement paths to each target become straighter and less variable [8].

## 1.4 Motor Learning

Learning involves changes in behavior that arise from the interaction with the environment and is distinct from maturation, which involves changes that occur independently from interaction. The goal of learning in general is to **improve performance**. Even if some species show no motor learning, the need for motor learning arises in species in which the organism's environment, body or task change. Specifically, when such changes are unpredictable, they cannot be pre-specified in a control system, and therefore **flexibility** in the control process is required.

Motor learning requires a compromise between:

**Innate capacities:** hard-wired, robust, fast

**Learned capacities:** adaptable, slow, flexible

The **innate capacities** are the abilities everyone was born with. In order to execute them, pre-specified neural connections are needed and their presence make them stable and very insensitive to perturbations. These capacities are not learnt and they establish a fixed relationship between the stimulus and the related response. A clear example is

given by reflexes.

The robustness of innate capacities can reduce available flexibility to learn new motor tasks because motor learning could require the interruption or change of reflexes and synergies at the CNS level. The learned capacities are all the abilities humans put besides the innate ones. They are obtained through the motor learning process as there are no pre-codified neural connections. Voluntary movements are related to learned capacities.

The learning process is composed by a co-adaptation of neural and anatomic structure; therefore, it takes place in everyone life and from generation to generation as well. For example, human manual skill has a very fine controller, but it is possible thanks to the opposable thumb. Anatomical body adaptation occurs both in everyone alive (e.g. tennis players' hypertrophies) and from generation to generation.

Learning and information code and transfer occur in a very different way in humans neurons with respect to other animals. There are many evidences of these huge differences, including the size of the brain wrt to the number of neurons as well as some studies about intercommunication between neurons.

### **From literature: Communication between pairs of neurons in humans [9].**

The authors studied the communication between pairs of neurons (pre-post synaptic) in humans (temporal cortex neurons from acute brain slices of epileptic patients and brain tumors patients) and they compared them to mice neurons (young and adult murine models). They show that adult human neurons can transfer information faster (@ ten times higher rates than mouse neurons, because of faster recovery from depression. Human neurons can thereby reliably encode high input frequencies in their output. Thus, neuronal information transfer can have a substantially higher bandwidth in human neocortical circuits than in rodent brains.

As a matter of fact, we have to always consider with some caution what we know about details of brain microcircuits because most of this knowledge is based on murine or primate animal models... Indeed across species the brain is different and mental ability, too. Humans have bigger brain and at the same time a higher mental ability.

Humans have: (i) a higher rate of brain mass wrt body mass ii) an expansion of frontal areas (iii) more neurons in the brain and in the cortex. These structural features are also accompanied by functional features: i) larger dendrite trees; ii) more synapses per neurons iii) faster action potentials. These considerations suggest that from murine model to humans you need to multiply by  $10^{11}$  neuron and  $10^{14}$  synapses.

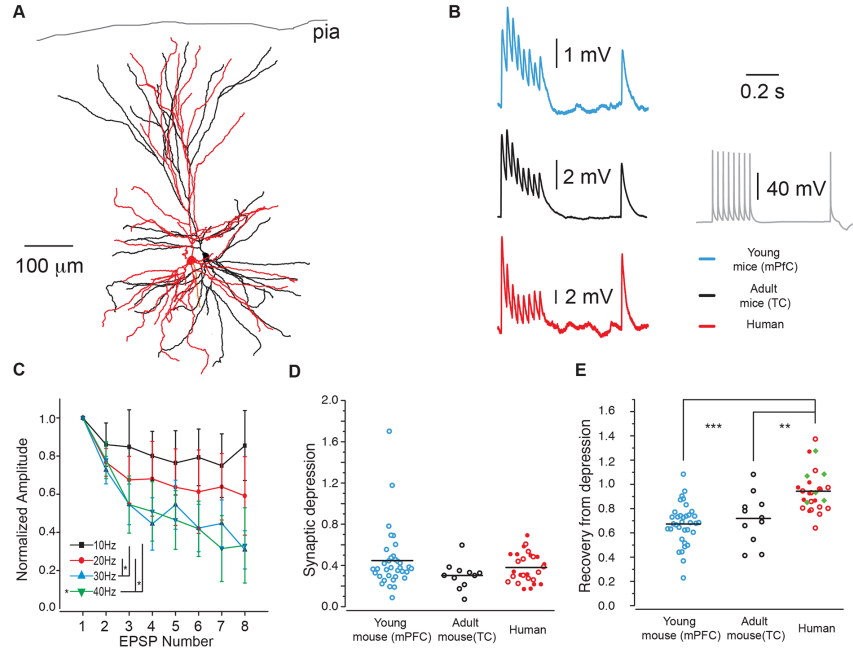


**Figure 1.10: Synapses in adult human neocortex rapidly recover from depression:** (A) Digital reconstruction of a biocytin-filled, synaptically connected pair of layer 2/3 pyramidal neurons in human temporal cortex. (B) Experimentally recorded EPSPs, generated by presynaptic timed APs at 30 Hz followed by a recovery pulse, 500 ms after the 8th pulse. Traces in blue are from young murine medial prefrontal cortex (mPFC) (P12–36), black, from murine temporal association cortex (10–11 weeks) and red from human temporal cortex. Grey is an example of a train of human presynaptic APs. Examples are averages of 30 repetitions. (C) Activity dependence of human short-term synaptic depression. Normalized average EPSPs (three pairs) generated in response to different frequencies (10–40 Hz). (D) Ratio 8th/1st EPSP (mean  $\pm$  SEM)  $0.38 \pm 0.03$  human,  $0.44 \pm 0.05$  for young mouse synapses and  $0.30 \pm 0.04$  for adult mouse synapses ( $p > 0.05$ ). (E) Ratio 9th/1st EPSP (mean  $\pm$  SEM)  $0.94 \pm 0.03$  for human, whereas young mouse EPSPs were still depressed  $0.67 \pm 0.03$  ( $p < 0.001$ ) and adult mouse EPSPs  $0.72 \pm 0.06$  ( $p < 0.001$ ). Difference between young and adult mouse ratios were not significant ( $p = 0.7$ ). Human  $n=27$  (14 from tumor patients and 13 from epilepsy patients, see Materials and Methods); young mouse  $n=35$ ; adult mouse  $n=11$ . Filled red circles, human tumor patients; open red circles, human temporal lobe epilepsy patients (300 ms interval between 8th and 9th EPSP). Open blue circles, young mouse group p12-p36; open black circles, adult mouse group 8–11 weeks. Filled green diamonds, human patients with 500 ms interval between 9th and 8th EPSP. (From [9])

## 1.5 Modelling Motor Control

Motor control is a highly complex physiological mechanism and the entire process is decomposed by the CNS in different functional modules each one with different input-output features. In order to model the general functioning of the brain during motor control, we have to refer to the so-called **internal models**. The word “internal” implies that the model is within the brain, so it a neural network in the brain, while the word “model” implies that the neural network simulates a target dynamical process [10].

These model mimics the functions of the system to be controlled and are a representation of the sensory-motor and motor-sensory transformation present within our

brain. Internal models can be controlled through either **feedforward** or **feedback control**. Internal models represent the necessary steps that the brain need to put in place for an effective motor control.

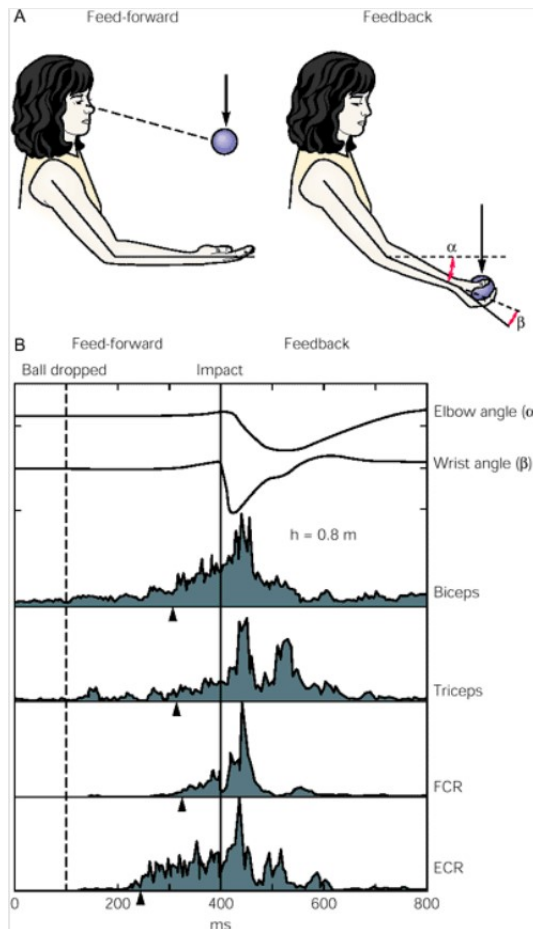


**Figure 1.11: Feedback and Feedforward motor control** To get a ball, we need feedforward and feedback control. (A) Experiment: the ball is falling from different starting point at different height, chosen by the experimenter. (B) Mean responses of a subject that had to get a ball falling from 0.8m. The plots refer to the angle of the elbow and wrist joints and rectified EMG activity of biceps, triceps, flexor carpi radialis (FCR) and extensor carpi radialis (ECR). The anticipatory answers (e.g. before ball impact) are constituted by the co-activation of biceps and triceps and of FCR and ECR. After the impact there is a transient modification of strain reflex with a further co-activation of flexor and extensor muscles (with respect to mutual inhibition). (From [1]).

In **feedforward control** the input is the mere current state and the model of the system. In motor control, it exerts an **anticipatory control** (open loop control) by combining sensorial actual information and previous experience.

In **feedback control**, the input is the error signal given by the current state and a reference signal, and the output is an action that compensates for the error. In motor control, it exerts an **actual control** (close loop control) based on sensory information due to actual executed movement. It provides a motor command that should be able to compensate the error given by the difference between the desired output and the

actual state. This compensation is characterized by a gain value.

Open loop control is essential for most natural movements, where the eventual timing of closed loop control would be available too late to effectively guide the movement.

There are two primary types of **internal models** used for modelling the brain functioning in motor control:

- **forward model** to capture the causal relationship between inputs to the system and the outputs;
- **inverse model** to estimate the motor commands required to achieve the desired sensory feedback (anticausal direction).[11]

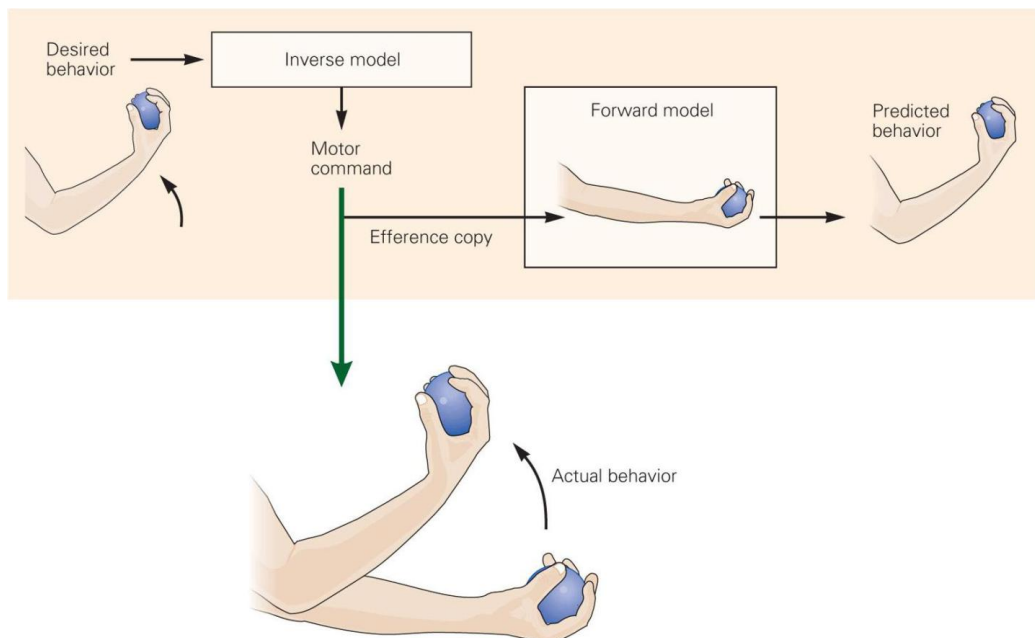


**Figure 1.12: Inverse and Forward model:** Forward model maps motor commands in the sensory space; Inverse model estimates motor commands to obtain a desired sensory feedback. (From [1]).

### 1.5.1 Forward Model

The **forward model** mimics both the **external world** and **motor system** aspects to predict a causal relationship between actions and their consequences. It takes as input the **efference copy**, an internal copy of the motor command, and gives as output the **predicted behaviour**, i.e. the predicted trajectory together with the predicted sensory feedback resulted from the action. Thanks to this model, we can estimate the precise state, avoiding delays and noise, and reduce the sensory feedback caused by our own action. By detecting the consequences of our own actions, we can distinguish them from the consequences due to the external environment, gaining in perceptual

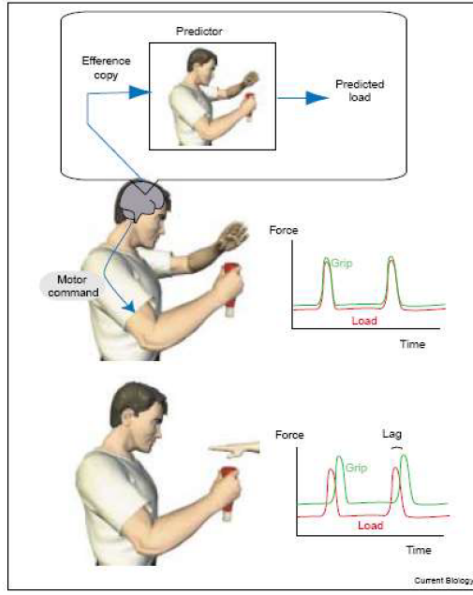


**Figure 1.13: Forward model:** To prevent a ketchup bottle from slipping sufficient grip force must be exerted to counteract the load. (top) When the load is increased in a self-generated manner (left hand strikes the ketchup bottle), a predictor can use an efference copy of the motor command to anticipate the upcoming load force and thereby generate grip which parallels load force with no delay. (bottom) When the load is externally generated (another person strikes the ketchup bottle), then it cannot be accurately predicted. As a consequence, the grip force lags behind the load force and the baseline grip force is increased to compensate and prevent slippage (From [12])

stability and different attention.

#### From literature: *Localize visual objects* [13]

The concept of motor prediction was first considered by Helmholtz when trying to un-

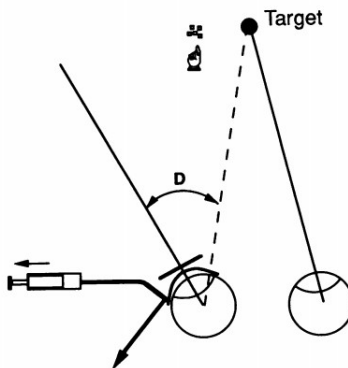


**Figure 1.14: Localize a visual object** (From [13])

derstand how we localize visual objects. To calculate the location of an object relative to the head, the CNS must take into account both the retinal location of the object and also the gaze position of the eye within the orbit. Helmholtz's ingenious suggestion was that the brain, rather than sensing the gaze position of the eye, predicted

the gaze position based on a copy of the motor command acting on the eye muscles, termed efference copy. He used a simple experiment on himself to demonstrate this (Figure 1.14). When the eye is moved without using the eye muscles (cover one eye and gently press with your finger on your open eye through the eyelid), the retinal locations of visual objects change, but the predicted eye position is not updated, leading to the false perception that the world is moving [13].

**From literature:** *Two eyes for one eye* [14] Shergill, Frith and Wolpert proved and measured the existence of forward model into the human brain. They demonstrated that when two kids fight, each one says that the other kid kick him harder, both of them are telling the truth. This is because the escalation of perception is a consequence of their natural neural elaboration.

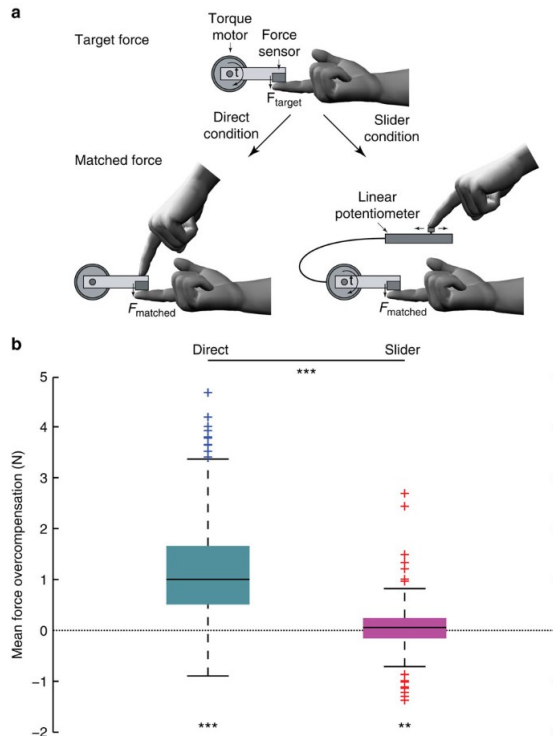


Figure 1.15: *Two eyes for one eye* experiments (Adapted from [14])

**First experiment:** A force transducer is linked to a lever where a motor can command the output force on the lever itself. When the experiment starts, the motor generated a force equal to 0.25N on the first subject's finger. Then this first subject had to press his/her index finger on the lever for 3 seconds on the index finger of the second participant. Then the second subject had to produce on the lever the force he/she received from the first subject on the index finger of the third subject and so on.

**Second and Third experiment:** Each subject is individually tested (12 subjects).

The motor produced a given force on the index finger of each participant and they had to produce the same force sensed by:

- Their right hand index finger on the lever (second experiment)
- Their right hand index finger on a joystick (third experiment).

### Experimental results:

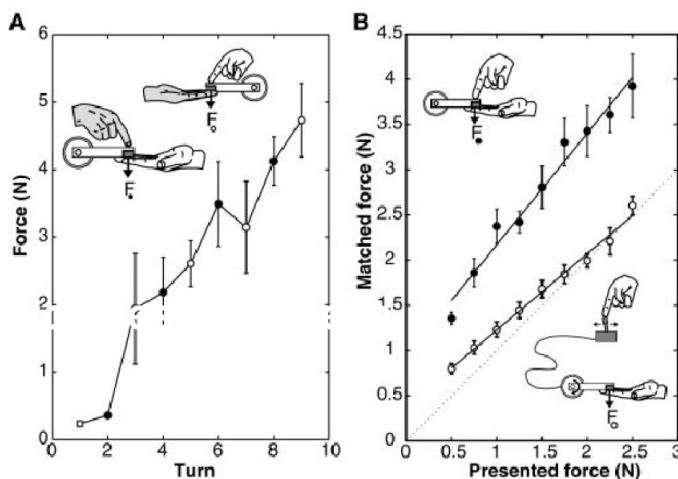


**Figure 1.16: Two eyes for one eye experimental results (From [14])**

**First experiment** (Figure 1.16A): Force escalation is occurring rapidly. To understand the cause, we analyze the second experiment.

**Second experiment** (Figure 1.16B-black dots): Self generated forces are perceived as weaker than externally generated forces of the same magnitude. A possible reason is that this process comes from a predictive step where consequences of our own movements are anticipated and used to attenuate the perception of the related sensations.

**Third experiment** (Figure 1.16B-white dots): The hand does not directly generate the force, whereas the hand movement is transduced through the joystick in force produced by the motor. In this (unusual) condition, predictive mechanisms are not used, and therefore the produced force matches with the received one.

The hand does not directly generate the force, whereas the hand movement is transduced through the joystick in force produced by the motor. In this (unusual) condition, predictive mechanisms are not used, and therefore the produced force matches with the received one.

### From literature: *Why can't you tickle yourself?* [15]

Another example is given in the paper “*Why can't you tickle yourself?*” by Blakemore, Wolpert and Frith [15]. In this paper they explain that the consequences of our actions are perceived in a different way compared to the same action done by someone else. When there is a difference between the predicted movement and the actual exe-

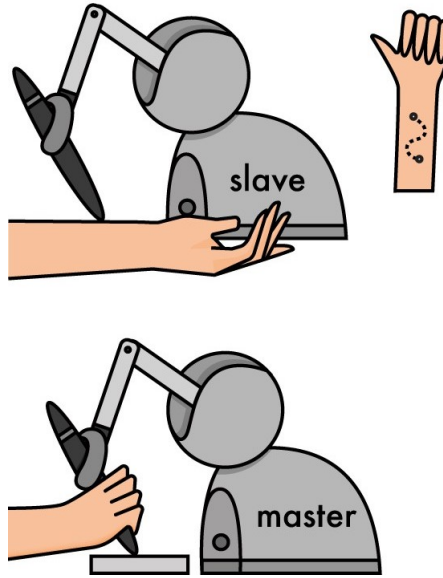


**Figure 1.17: Why can't you tickle yourself** (Adapted from [15])

cuted one, there is a growing difference between prediction and sensorial feedback and therefore perceived sensation is not attenuated (or less attenuated).

#### Experiment:

- Cond .1: robot generates movement (external tickling)
- Cond. 2: robot is moved by the left hand of the subject (=self tickling)
- Cond. 3: robot is moved by the left hand but with a delay (100, 200, 300 ms)
- Cond. 4: robot is moved by the left hand but the robot motion is rotated with respect to the hand motion

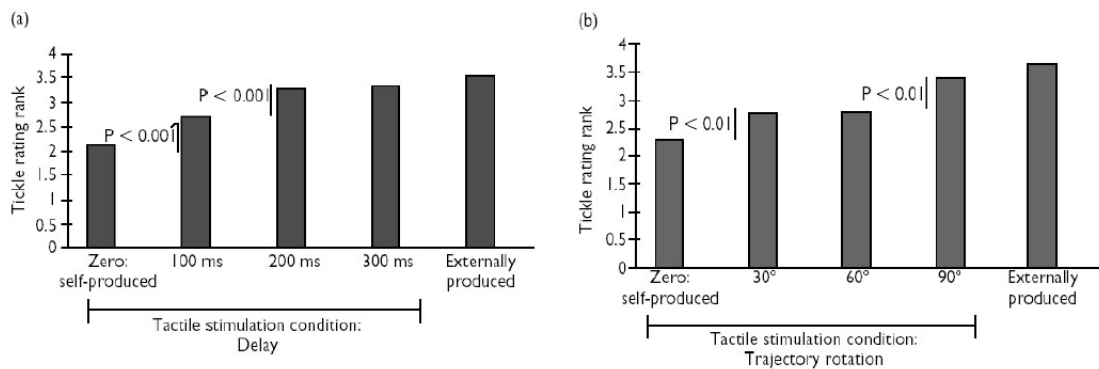


**Figure 1.18: Experimental results:** Graph show that the tickliness of a tactile stimulus increase with increasing delay (a) and trajectory (b) between the movement of the left hand and the tactile stimulus on the right palm. These results suggest that the perceptual attenuation of self-produce tactile stimulation is based on specific sensory predictions made by a forward mode (from [15]).

These results support the hypothesis that tactile perception attenuation is self-produced, it is due to tactile prediction correlated to stimuli. It is the correlation (and not the movement itself) between movement and produced sensation (self-produced) that determines the attenuation of the perceived sensation.

### Further proof: pathological behaviour [15]

If we consider pathological condition, such as schizophrenia, auditory hallucinations can make a person erroneously interpret the internal voices as external, and passivity of experience leads to the incapability to distinguish between action caused by the subject himself or someone else. In that case the predictor of the model is not working properly.

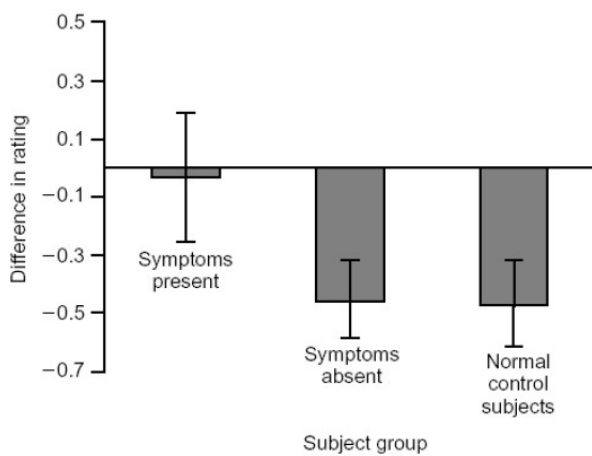


**Figure 1.19: Experimental results for pathological condition:** Graph showing the mean perceptual rating difference between self-produced and externally produced tactile stimulation conditions for three subjects groups: patients with auditory hallucinations and/or passivity, patients without these symptoms and normal control subjects. There was no significant difference between the perceptual ratings in the two conditions for patients with auditory hallucinations and/or passivity, hence the mean rating difference was close to zero. In contrast, there was a significant difference between the perceptual ratings in the two conditions for patients without these symptoms and in normal control subjects: both groups rated self-produced stimulation as less tickly, intense and pleasant than externally produced stimulation (from [15]).

## 1.5.2 Inverse Model

The **inverse model** estimates the motor commands required to achieve the **desired sensory feedback**, actuating a **feedforward control**(Figure 1.20). They use the desired and actual position of the body as inputs to estimate the necessary motor commands that would transform the current position into the desired one. The model is built with learning and experience: errors in the output of the model can be used to correct the model itself not the current motor action.

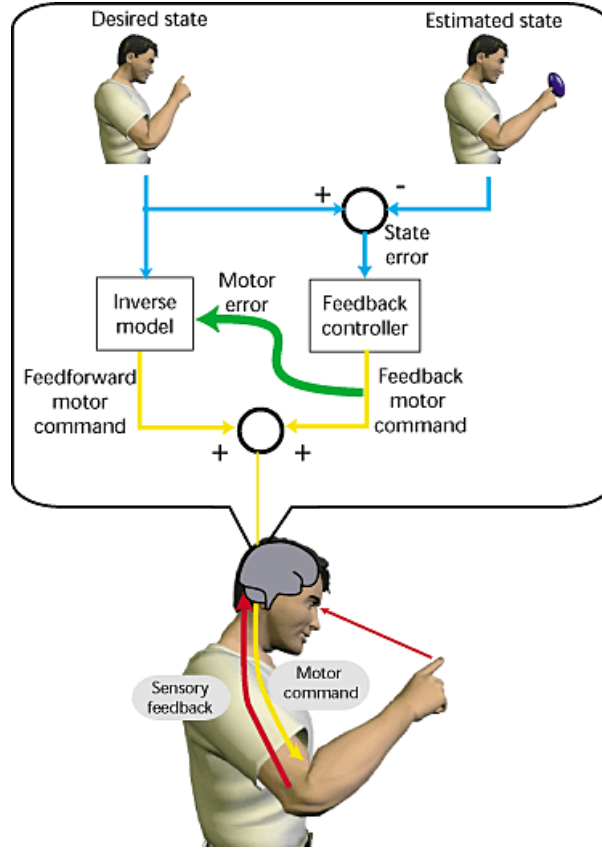


**Figure 1.20: Inverse model.** (From [16].)

### 1.5.3 Forward-Inverse Model

The two models (**inverse and forward**) can be combined to achieve efficient motor control, thus realizing the general model for the reproduction of motor control (Figure 1.12). The movement can be initiated through the inverse model, that produces the motor command. The motor command, more specifically a copy of its efference copy- is given in input to the forward model, that produces an estimation of the sensory feedback resulting from the action.

Skilled motor behavior relies on accurate predictive models of both our own body and the tools we interact with. As the dynamics of our body change during development and as we experience tools which have their own intrinsic dynamics, we need to continuously acquire new models and update existing models.

The problem of training an inverse model is strictly linked to the unavailability of a **physical error** on model output, thus an error on motor commands is unavailable. In fact, we do have an error signal measured by sensorial data (e.g. if we move an arm, we can have visual error feedback), but we do not have any information about the error on motor commands that generated the movement.

For instance, when we speak, we perceive the error in terms of acoustic stimulus,

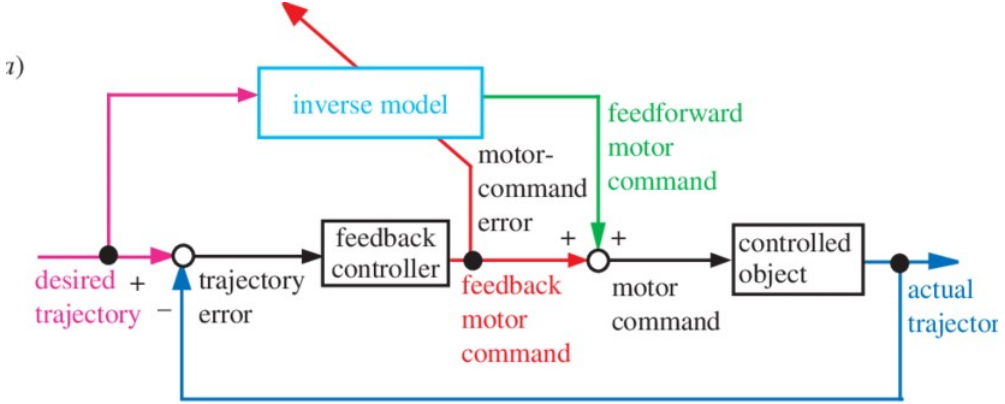


**Figure 1.21: General feedback-error-learning model.** (From [17]).

but not as muscle error. Kawato et al. proposed the existence of a feedback controller [17]. The feedback controller transforms trajectory errors (e.g. sensorial coordinates) in motor command feedbacks, that are used to update inverse models. Training signals represent sensorial error signals converted in the motor coordinates.

Also forward models are not fixed entities but must be learnt and updated through experience. Forward models can be trained and updated using prediction errors, that is by comparing the predicted and actual outcome of a motor command. Well established computational learning rules can be used to translate these errors in prediction into changes in synaptic weights which will improve future predictions of the forward model.

A Kalman filter module can be added to the scheme, as in Figure 1.22, with the role of weighting the contribution of this prediction and of the actual sensory feedback in establishing the current state. The Kalman filter mimics the capability of our brain to base the action either on sensory afferences or on a-priori models depending on the current reliability of the afferences.

#### 1.5.4 Multiple Paired Forward-Inverse Model

In Figure 1.23 the multiple paired forward-inverse model is represented. It aims at modelling the motor learning and motor control function with a modular network. In this network forward models include the correspondence of a certain module to the current context and, accordingly, the corresponding inverse model contributes to the formation of the overall feedforward motor command [18]. Its distinctive tract is that multiple models learn to subdivide experience so that at least a forward model could predict the consequences of a given action in a given context.

It is composed of N modules and each module is composed by three main elements: the **forward model**, the **responsibility predictor** and the **inverse model**.

The *forward model* and the *responsibility predictor* are used to determine module

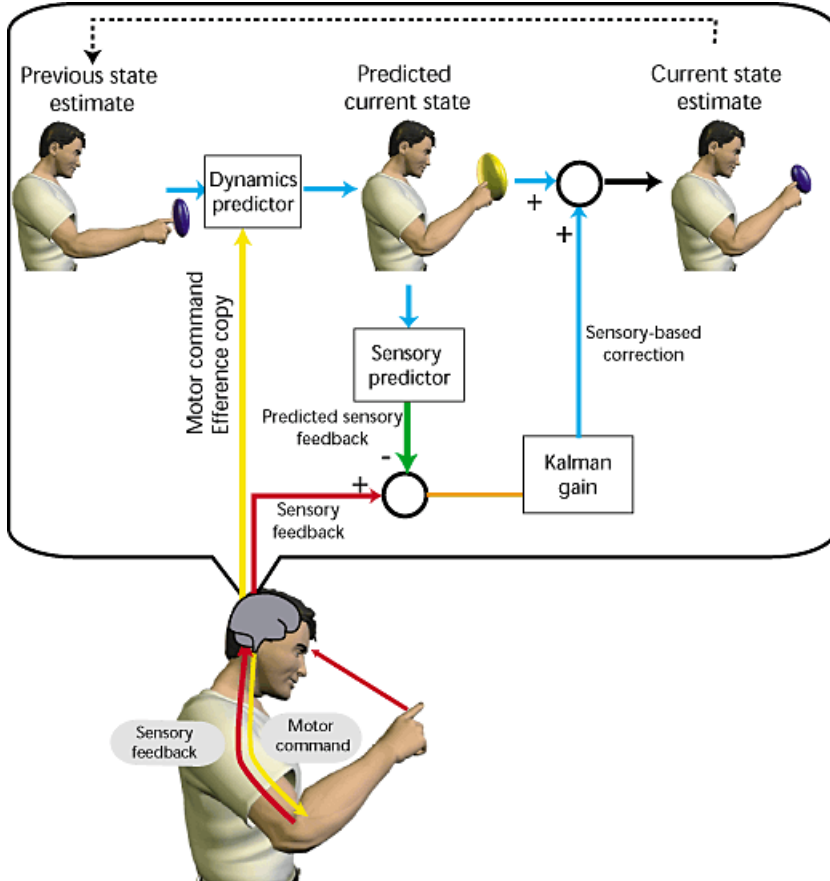


**Figure 1.22: Re-afference and Kalman Filter (From [16].)**

responsibility, which is inversely proportional to how much the sensory feedback and the efference copy of the model are suited for the present context and to the prediction error.

The value of responsibility is used to control forward model learning, where the error received by each module is proportional to the responsibility weight, and also to weight the output of each module and form the general feedforward motor command.

Instead, the *inverse model* generates the motor commands, given a desired trajectory, and has to learn the control signal of the context. For the inverse model, the error signals are weighted with the same responsibility degree and so, the better the prediction of the paired forward model is, the more the paired inverse model gains part of the error signal.

The selection of the appropriate modules is solved by generating a responsibility signal for each module based both on the consequences of performed actions, as estimated by the forward models, and on sensory signals, as estimated by the responsibility predictor.

Within each module, the inverse and forward models are tightly coupled, by the responsibility signal, during motor learning. This architecture allows to simultaneously

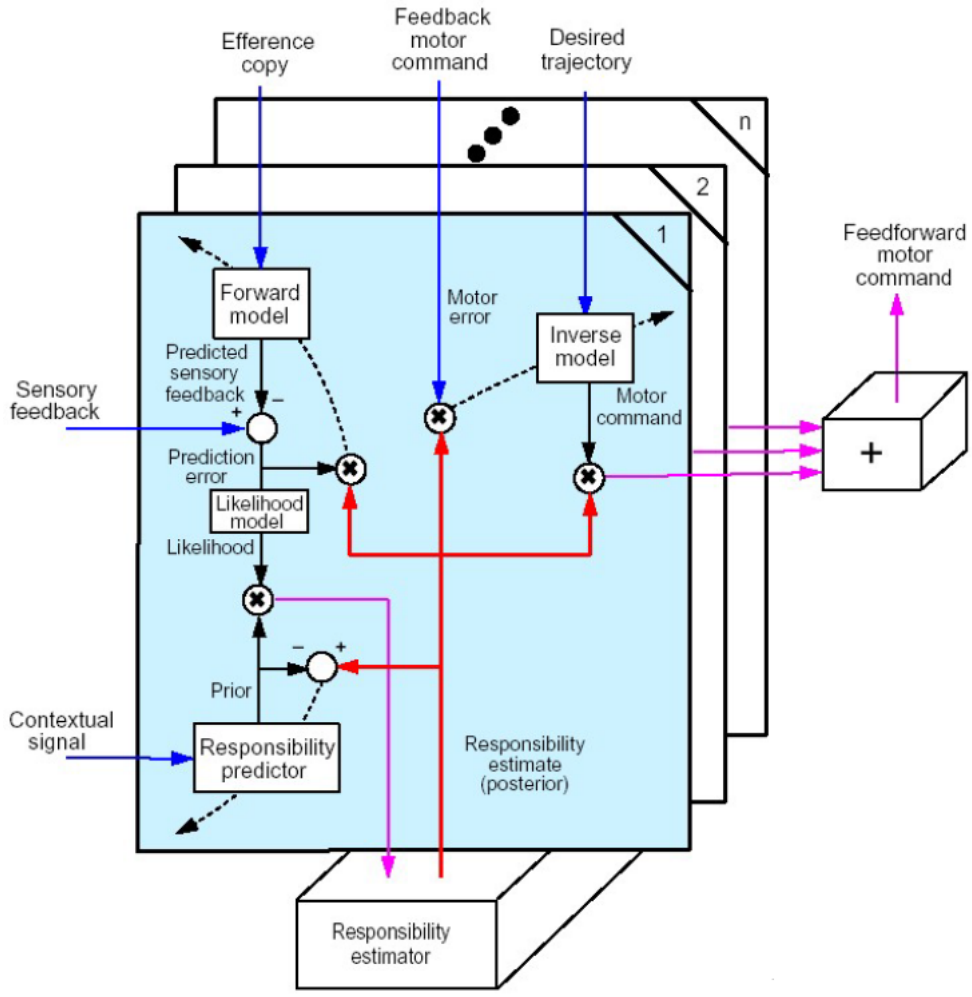


**Figure 1.23: Multiple Paired Forward-Inverse Model:** There are  $N$  modules that are represented as different sheets. Here are shown details for the first module and the interaction between different modules are possible thanks to the responsibility estimator. Each module is composed by three parts that interact. The first two parts, the forward model and the responsibility predictor, are used to determine module responsibility. This “responsibility signal” (fuchsia line) reflects the degree to which the single module gets the actual context and therefore to which degree it should participate to motor command. (From [18]).

learn the multiple inverse models necessary for control and also to select the appropriate inverse models for a given environment.

#### Final remarks on internal models:

On the one hand, we applied control theory to understand human motor control behavior and we draw from this approach of investigation the existence of internal models. On the other hand, we need to go back to neurophysiology to prove that the organization of human brain indeed includes these models.

As a matter of fact, the demonstration is not so straight forward, the human brain is still mysterious to neuroscientists, and a lot of research in neuroscience is currently

ongoing on these topics.

# Neural Bases of Motor Control

---

There are many areas of our brain that are involved in motor control. This is because a lot of information need to be processed in order to achieve the desired movement. Each motor area has a specific role and gives a precise contribution, even though modifications and substitutions are known to happen when a pathology is present for example in case of Brain trauma or Cerebrovascular accidents. Redundancy of neural pathways as well as plasticity in the brain is an enormous resource. Plasticity is the process of adaptation of brain circuits and connections due to internal and external stimuli.

Motor systems are organized hierarchically and parallelly. Figure 2.1 shows a schematic representation of the connections between different brain areas involved in motor control.

Motor areas of the cerebral cortex can influence spine directly or through the Brain Stem (Encephalic trunk). Sensorial afferences reach the motor cortex through Thalamus, either directly or after a pre-processing of the Basal Ganglia and/or the Cerebellum. We can highlight five loops:

- Spine loop (arc reflex)
- Spinal-cortex loop
- Cerebro (cortex)-cerebellum loop
- Cerebellum-spine loop
- Cortex- basal ganglia loop

Motor cortex receives the desired trajectory from premotor cortex and frontal lobe, also receives information about sensory data from the sensory cortex and the parietal lobe and receives inputs from the cerebellum (through the deep nuclei and the thalamus) and projects to the spinal cord and to the cerebellum (through the Pons) and the nuclei.

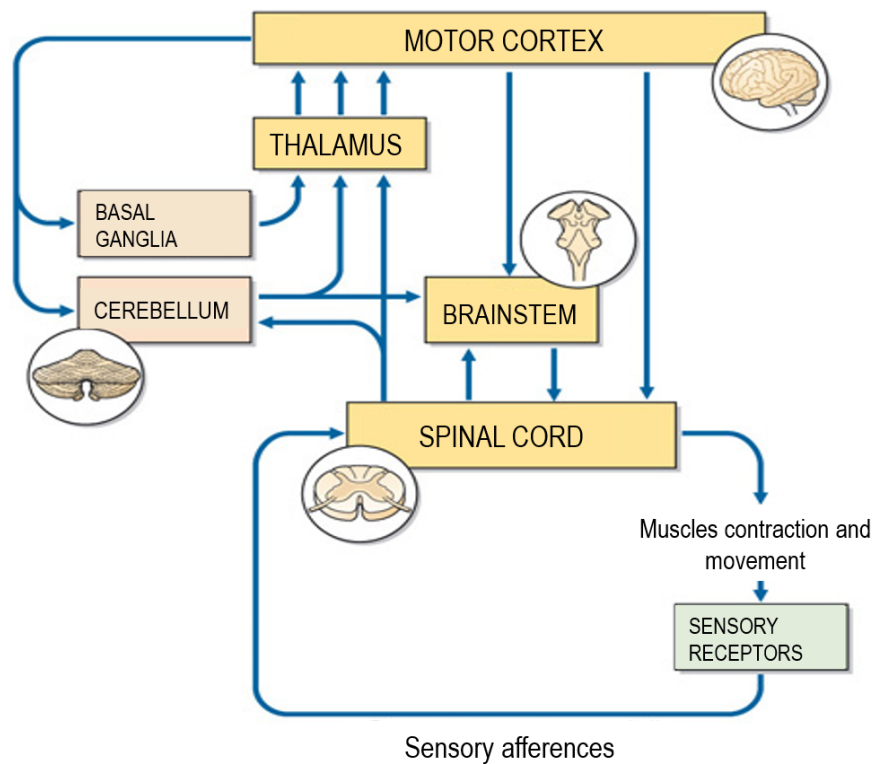


**Figure 2.1: Motor control system scheme** showing the main connections of each part of the brain concerned with motor control. (From [19]).

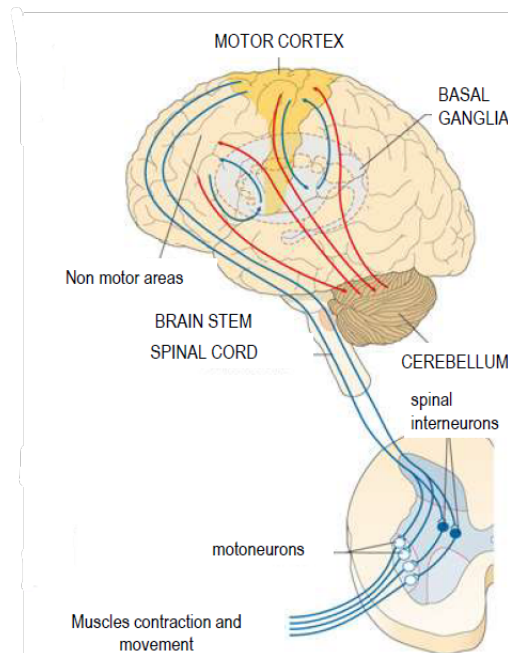


**Figure 2.2: Motor control system anatomy** (From [19]).

In the next sections, we will give an overview of the structures involved in motor control. In particular, we will focus on the primary motor cortex, the spinal cord, the supplementary motor cortices and the cerebellum. A more detailed focus on the

cerebellum will follow.

## 2.1 Primary Motor Cortex

The primary motor cortex, or M1, is located in the frontal lobe of the brain, along a bump called the precentral gyrus. The primary motor cortex is composed by 6 billion neurons it is thick 1/8 inch and it has a very uniform structure base of 6 layers of neurons, as shown in Figure 2.3. It can also be functionally divided into vertical formations, called columns, representing the functional units of the cortex. Each column is oriented perpendicular to the cortical surface and it consists of all the 6 different cellular layers. Neurons are tightly connected inside each column and they share connections both with the adjacent and distant columns and with the subcortical structures too. Thanks to this structure, each column can memorize relations and perform more complex operations than a single neuron.

**Histological Structure of the Cerebral Cortex**

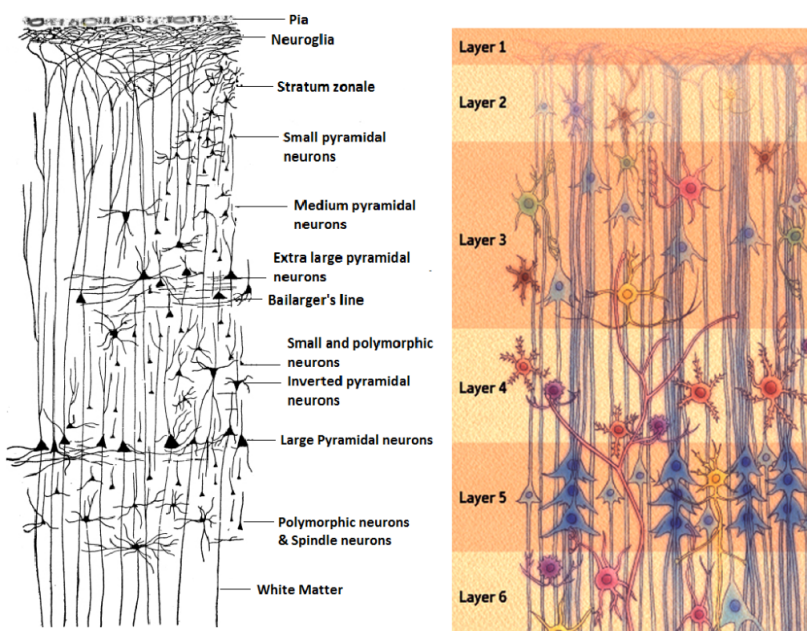


**Figure 2.3: Histological structure of the cerebral cortex:** I. **Molecular layer** (lamina molecularis) - consists only a few nerve cells. II. **External granular layer** (lamina granularis externa) - relatively thin layer consisting of numerous small, densely packed neurons. III. **Pyramidal layer** or external pyramidal layer (lamina pyramidalis externa) - is composed of medium-sized pyramidal nerve cells. IV. **Inner granular layer** (lamina granularis interna) - contains small, irregularly shaped nerve cells. V. **Ganglionic or inner pyramidal layer** (lamina pyramidalis interna) - includes large pyramidal cells. VI. **Multiform layer** (lamina multiformis) - small polymorphic and fusiform nerve cells. (From <https://imgur.com/gallery/xCAoW>).

The uniform organization would suggest that there might be a common computational principle operating across cortex that is still an open issue. Research in neuro-

science is aiming at proving answer to this issue (for example Human Brain Project EU Flagship and the US Brain Initiative).

Each part of the body is represented in the primary motor cortex and these representations are arranged somatotopically, which means that specific groups of muscles are innervated by specific groups of neurons.

The "amount of brain matter" devoted to any specific body part represents the "amount of control" that the primary motor cortex has over that body part. The size of these areas does not correspond to the size of the body parts they represent, rather to the complexity of the movements that those muscles can produce. So, areas of the body with more complex or more numerous sensory or motor connections are represented as larger, while those with less complex or numerous connections are represented as smaller. The schematic and distorted representation of the body parts in the way they are represented in the cortex gives an image of the so-called Motor Homunculus (Figure 2.4).

Somatotopic motor cortex organization allows the reconstruction of motor maps through electrical stimulation. The term 'map' refers to a population of neurons that first responds selectively to the presence of stimuli that sample from an underlying stimulus space, while the term 'somatotopic' is used because, in this case, the space is related to locations on the body, such that adjacent neurons in the neural tissue respond selectively to stimuli presented to adjacent locations on the body. While a less intense stimulus can evoke a single muscle contraction, a single muscle can always be activated through stimulation of multiple and different cortical districts. This demonstrates that neurons from different cortical districts project on the same muscle. Moreover, most stimuli activate more muscles, whereas we can only rarely observe single muscle activation. In fact, cortico-spinal terminations of a single axon diverge and they distribute over different motor neurons that innervates different muscles.  
***Somatotopic motor cortex organization is not fixed, but it can be modified with learning and after brain lesions.***

**From literature: Correspondence between M1 neurons and muscles [20]**

In 1979 Fetz showed, with spike triggered averaging technique, that single corticomotorneuronal cells monosynaptically project to more than one single motor nucleus, sometimes to muscles that control different joints as well. Furthermore, the use of several stimuli can bring to the activation of more muscles at the same time, which is the general condition most of the time. That is the reason why it is rare to observe the activation of only one muscle. Thus at the cortical level, muscles are not represented with a 1 to 1 relationship with output M1 neurons.

**From literature: Force Coding [21]**

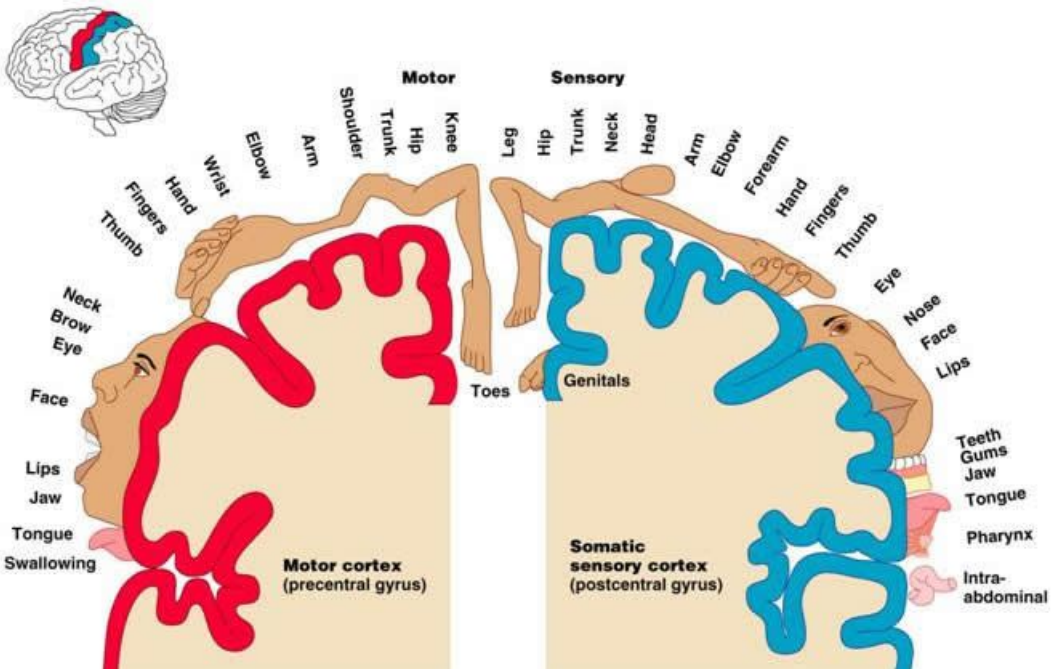


**Figure 2.4: Cortical Homunculus:** somatotopic organization (From <http://www.tulane.edu/~h0Ward/BrLg/Cortex.html#id38>)

In a classic experiment, Evarts showed that during wrist flexion, the firing frequency of M1 neurons change in relation to the force that the animal had to exercise rather than the amplitude of the movement [21]. In his experiment, he used monkeys performing operantly conditioned movements. In particular, Evarts recorded the activity of the monkey motor cortex related to the wrist movement when forcing the wrist flexion with three different load conditions, using an experimental set up as shown in Figure 2.5. In this way, he discovered that the activity of the recorded M1 Pyramidal Tract Neuron (PTN) codes direction and intensity of the force needed to produce a movement rather than joint angle variation.

In 1976, Tanji and Evarts found another unexpected property of M1 neurons: the activity recorded in M1 Basal neurons change when the mammal is waiting for the signal to start the movement in a given direction [22]. They discovered the presence of the “**set related activity**”, which shows that even just the movement intention, without performing it, modifies the firing of some neurons 100 milliseconds before the real movement execution.

**From literature:** *Cortico-motor cell activity is not directly correlated to the activity of target muscle* [23]

The multiplicity of motoneuron connection allows that activity is flexible and it

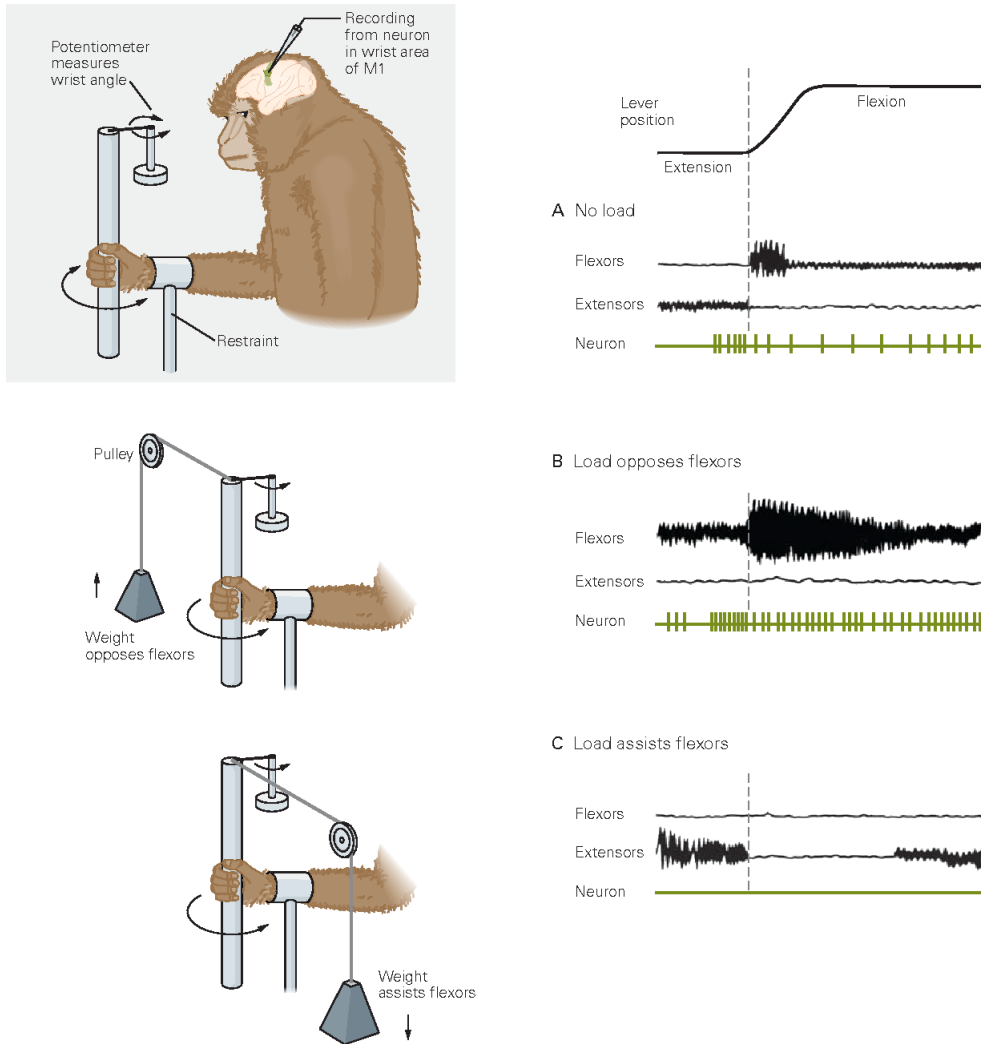


**Figure 2.5: Force Coding:** Activity in a corticospinal axon correlates with the direction and amplitude of muscle force rather than the direction of displacement. Records shown here were made while a monkey flexed its wrist under three load conditions. The wrist displacement was exactly the same across the three conditions (top trace). When no load was applied (A) the neuron fired before and during flexion. When a load-opposing flexion was applied, activity in the neuron increased (B). When a load-assisting flexion was applied, the neuron fell silent (C). In all three conditions the wrist displacement was the same but the neuronal activity changed as the load changed. **Thus the firing of the corticospinal neuron in this experiment is related to the force exerted during a movement and not to the displacement of the wrist.** (M1 single neurons activity is correlated to muscular force and it has been observed that there are some activities where the force-firing frequency relationship is quite linear. M1 corticospinal neuron (PTN Pyramidal tract Neuron) single neurons activity control movement execution and fit them to different environmental conditions. (From [1])

can well adapt to the motor task it has to execute. In fact, they demonstrated that depending on the movement objective (e.g. precision grip vs force grip), primates have a different cortical activation patterns [23].

#### From literature: *How motor cortex encode movement direction*

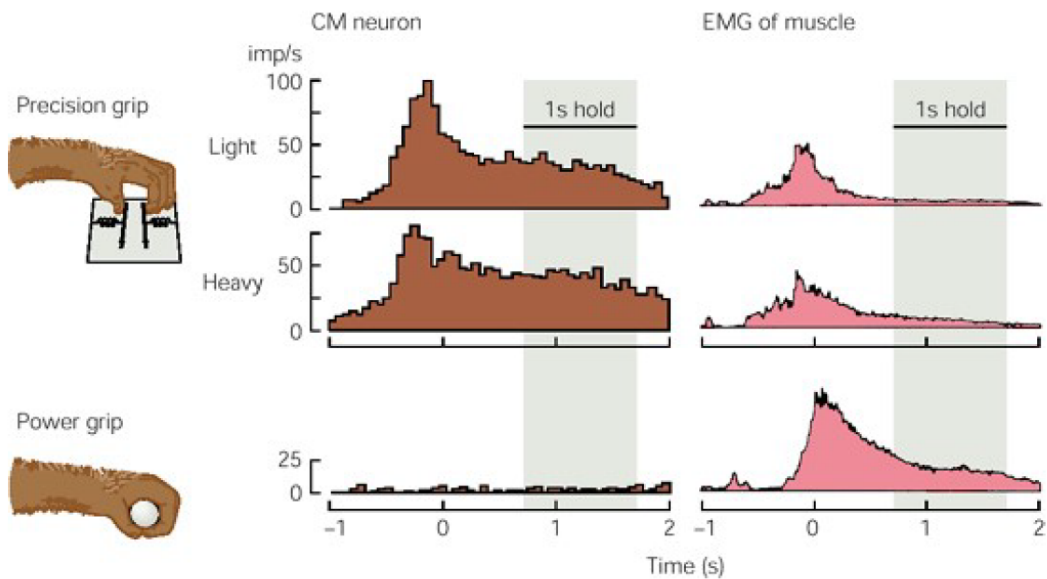


**Figure 2.6: Cortico-motor cell and target muscle activities are not directly correlated:** Whether an individual corticomotoneuronal (CM) cell is active depends on the motor task. The activity of a CM cell and the activity in its target muscle are not directly related. Cumulative histograms show the activity of a single neuron during a precision grip and a power grip. During the precision grip the neuron's activity is the same whether overall force is light or heavy and the level of electromyographic (EMG) activity in the target muscle is similar for both forces. During the power grip there is almost no activity in the neuron despite a greater amount of EMG activity in the muscle. Thus, even if a given motor neuron is monosynaptically connected to a given CM cell, their firing patterns do not have to parallel each other because the multiplicity of connections to motor neurons allows task flexibility (imp/s = impulses per second). (From [1]).

The largest part of movements involve many joints and they require synergistic, sequential and accurate muscle activations in time. Which movement aspects are coded in M1? Do M1 neurons code spatiotemporal characteristics?

Or do they code global movements aspect such as direction, amplitude and angle variation?

In 1982, Georgopoulos observed that a pool of neurons from an M1 area vivaciously fire before a movement starts and during its execution with a quite broad directional sensitivity [24]. Therefore, he formulated the hypothesis that movement direction is coded by a pool of neurons and not by a single neuron. By building a population vector, as in Figure 2.7. Georgopoulos represented single neuron contribution through vector whose amplitude indicates the activity level that is presented in the selected movement direction. Single neuron vector direction was selected as the one where the neuron has the highest firing rate. This direction was kept constant during movement direction variation, while its amplitude was modulated with firing rate (with respect to maximal one). Then for each movement direction, he summed the contribution of all neurons from the population, and he constructed the population vector. The population vector directions were surprisingly corresponding to movement directions.

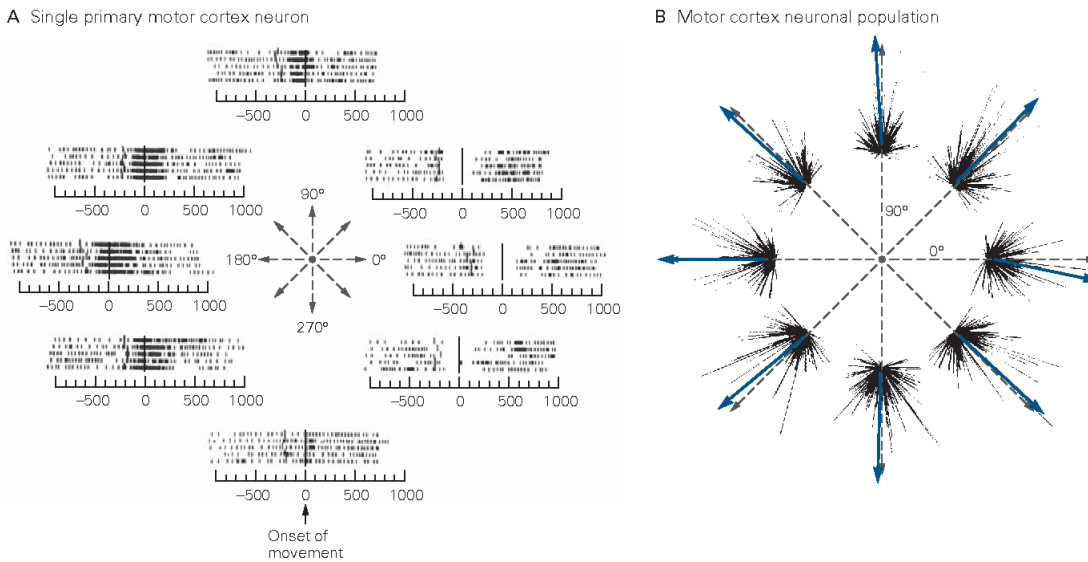


**Figure 2.7: How motor cortex encode movement direction:** Direction of movement is encoded in the motor cortex by the pattern of activity in an entire population of cells. A. Motor cortical neurons are broadly tuned to the direction of movement, but individual cells fire preferentially in connection with movement in certain directions. Raster plots of the firing pattern of a single neuron during movement in eight directions show the cell firing at relatively higher rates during movements in the range from 90 degrees to 225 degrees. Different cells have different preferred movement directions. For these recordings a monkey was trained to move a handle to eight locations arranged radially in one plane around a central starting position. Each row of tics in each raster plot represents activity in a single trial; the rows are aligned at zero time (the onset of movement). B. Cortical neurons with different preferred directions are all active during movement in a particular direction. The entirety of this activity results in a population vector that closely matches that of the direction of movement. The eight clusters shown here represent the activity of the same population of neurons during reaching movements in eight different directions. Solid arrows are the population vectors; dashed arrows are the direction of movement of the target limb. (From [1]).

**From literature: Motor Cortex codes for the force required to maintain a trajectory. [25]**

The spike frequency of a neuron increases if a load is applied against the arm movement in the neuron preferred direction; conversely it decreases if the load is applied in the direction preferred by the neuron itself. In [25] It has been demonstrated that activity of M1 neurons code lower level parameters (such as force) that muscles have to develop, and high level parameters (such as those related to hand trajectory) during reaching movements.

To sum up, in motor control, the primary motor cortex has a double-fold control:

1. A low level control of single muscles (homunculus)
2. A high level control of multiple muscles depending on High content motor parameters

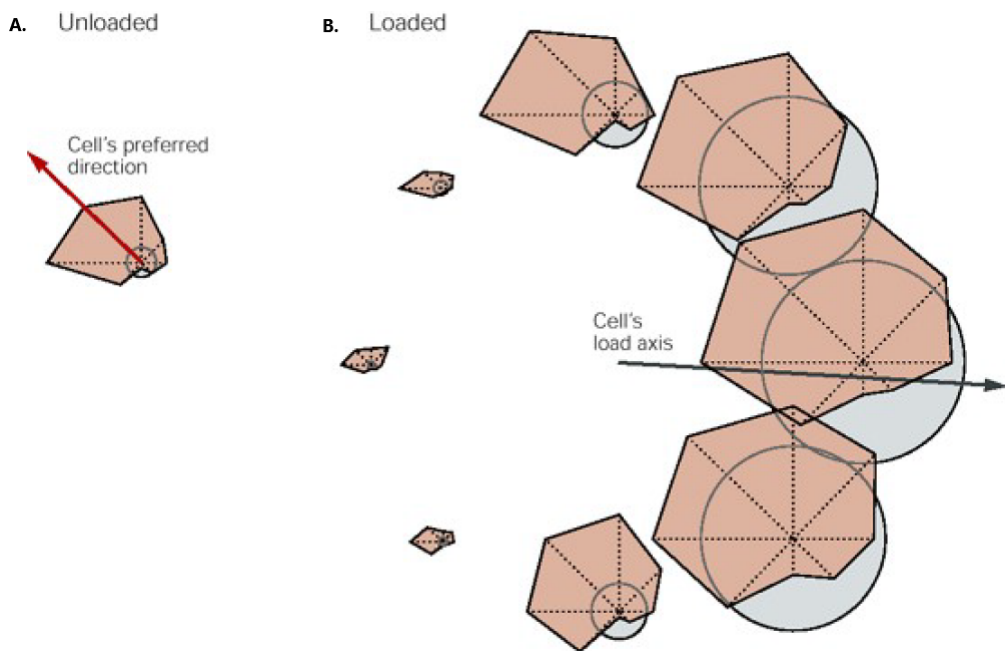


**Figure 2.8: Force required to maintain a trajectory:** Motor cortical cells can code for the force required to maintain a trajectory. A monkey was trained to reach in eight directions while external loads pulled the arm in one of these directions. Polar plots represent the activity of a single cell in the primary motor cortex while the arm moved with external loads. The magnitude of the cell's discharge is plotted as the length of a vector extending in the direction of the executed movement (dotted line). The tips of all vectors are joined by a solid line. The radius of the circle indicates the magnitude of cell activity while holding the arm at the central starting position before movement. A. Plot showing the preference of the cell for movement to the upper left during movements in eight directions without an external load applied to the arm. B. Polar plots for the same cell when loads are applied in eight directions. The position of each polar plot corresponds to the direction in which the load pulled the arm. The cell's firing rate increases in all directions when the arm is pulled right. This rightward direction is the load axis of the cell, which is approximately opposite to its preferred movement direction. Thus the cell's firing rate is related to the amount of force required to maintain an arm trajectory in a given direction, not just to the direction itself. (From [1]).

Exercise and training modify both functions.

## 2.2 Ventral Stream

The ventral stream is associated with object recognition and form representation. Also described as the "what" stream, it has strong connections to the medial temporal lobe (which stores long-term memories), the limbic system (which controls emotions), and the dorsal stream (which deals with object locations and motion). The ventral stream gets its main input from the parvocellular (as opposed to magnocellular) layer of the lateral geniculate nucleus (LGN) of the thalamus. These neurons project to V1. From there, the ventral pathway goes through V2 and V4 to areas of the inferior temporal lobe: PIT (posterior inferotemporal), CIT (central inferotemporal), and AIT (anterior

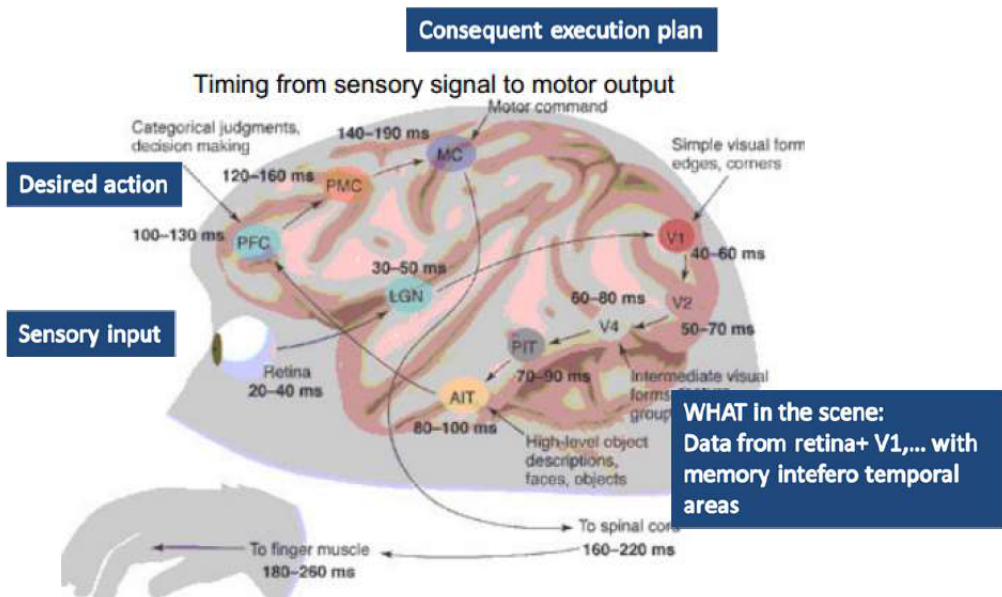


**Figure 2.9: Ventral Stream:** from object sight to motor action delays. (From [26]).

inferotemporal). Each visual area contains a full representation of visual space. That is, it contains neurons whose receptive fields together represent the entire visual field. Visual information enters the ventral stream through the primary visual cortex and travels through the rest of the areas in sequence. Moving along the stream from V1 to AIT, receptive fields increase their size, latency, and the complexity of their tuning. Once AIT got the “what” the information projects to the Prefrontal Cortex (PFC), which makes decision. The decision (desired action) is the converted into motor plan by the premotor Cortex (PMC) and then converted into motor commands by the motor cortex (MC).

## 2.3 Spinal Cord

Signals generated in the primary motor cortex reach the spinal cord through different descending motor pathways, which can be distinguished in two major groups (see Figure 2.10):

- Lateral pathway, also called pyramidal, which includes the lateral corticospinal tract and the rubrospinal tract. It manages both proximal and distal muscles.
- Medial pathway, also called extrapyramidal, made by vestibulospinal, reticulospinal, tectospinal and anterior corticospinal tract. They control axial muscles and handle posture and balance.

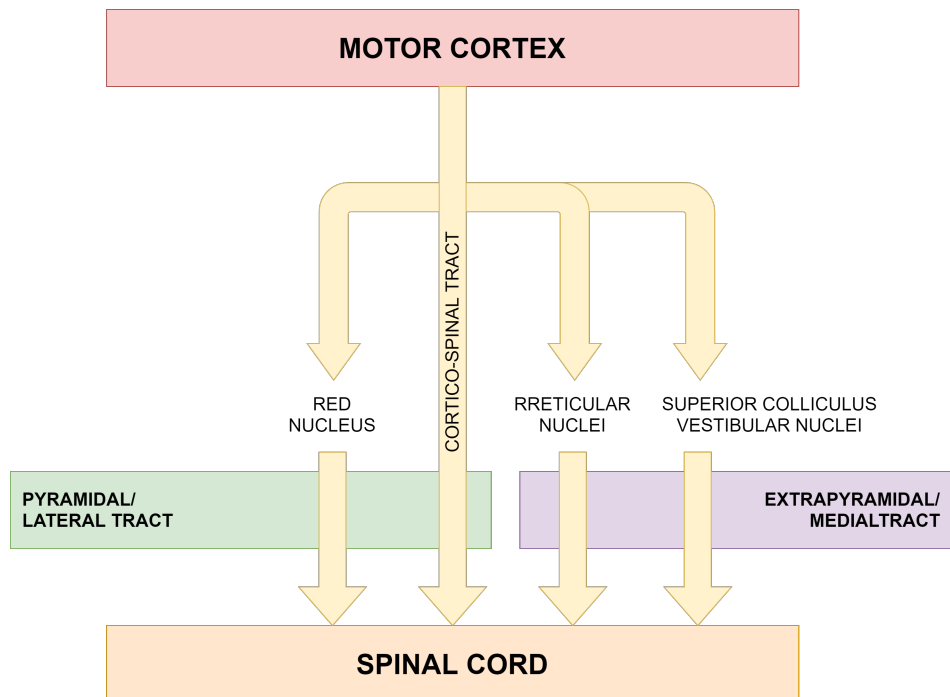


**Figure 2.10: Spinal Cord.Pyramidal/Lateral Tract:** The lateral pathway controls distal muscles and it is directly pilot by PMC or thought the Rubrospinal tract. **Extrapyramidal/Medial Tract:** The ventromedial pathway controls axial muscles and goes thought reticular nuclei and vestibular nuclei (part of posture control is also achieved by reflexes).

At general level, the spinal cord is responsible for the cyclic motor tasks. These tasks are the combination of voluntary tasks, which represent the trigger, and reflexes which maintain the cyclic motion. Its role is important in motor control because the rhythmic repetition of gestures and alternate coordination of two sides or of different body parts. They are controlled by spinal circuits and brain stem, under the supervision of cortex. A tonic action of the motor cortex is translated into oscillatory activity, central patter generators. Their existence at spine level is recognized but their functioning is still not fully understood.

## 2.4 Supplementary Motor Areas and Premotor cortex

Supplementary motor area and Premotor cortex are activated in case of complex motor tasks and to program sequences. Lesions to these area causes apraxia, i.e. Disorder in performing goal-directed tasks. The posterior parietal cortex takes part in the process of transforming visual information into motor commands. It sends this information on to the premotor cortex and the supplementary motor area. The premotor cortex lies just in front of the primary motor cortex. It is involved in the sensory guidance of

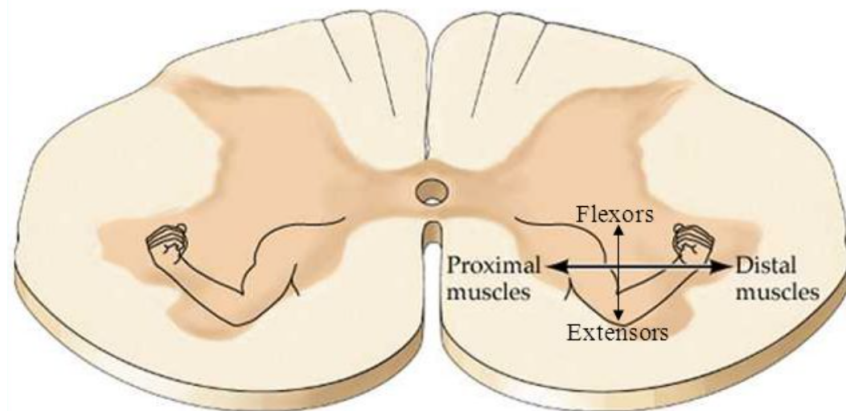


**Figure 2.11: Spatial Organization of Spinal Cord Neurons:** **Flexor-extensor rule:** motor neurons that innervate flexor muscles are located posteriorly to motor neurons that innervate extensor muscles. **Proximal-distal rule:** motor neurons that innervate distal muscles (e.g., hand muscles) are located lateral to motor neurons that innervate proximal muscles (e.g., trunk muscles). (From [https://personal.utdallas.edu/~tres/integ/mot1/display1\\_13.html](https://personal.utdallas.edu/~tres/integ/mot1/display1_13.html))

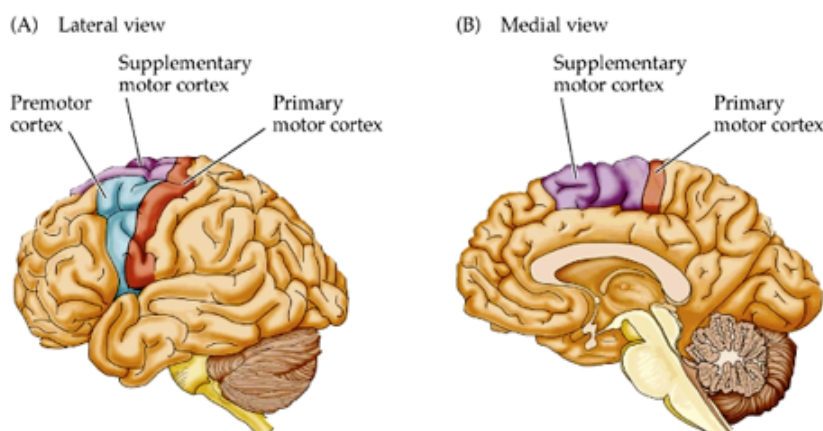


**Figure 2.12: Supplementary Motor Areas and Premotor cortex** (From [http://163.178.103.176/Temas/Temab2N/APortal/FisoNerCG/FisoNer0b5/MotorK/MotorIIK/display2\\_13.html](http://163.178.103.176/Temas/Temab2N/APortal/FisoNerCG/FisoNer0b5/MotorK/MotorIIK/display2_13.html))

movement and controls the muscles of the body defined as more proximal. Instead, the supplementary motor area lies above the premotor area, in front of the primary motor cortex. It is involved in the planning of complex movements and in coordinating two-handed movements. These two regions both send information to the primary motor cortex as well as to brainstem motor regions and they are activated in case of complex motor tasks and to program sequences.

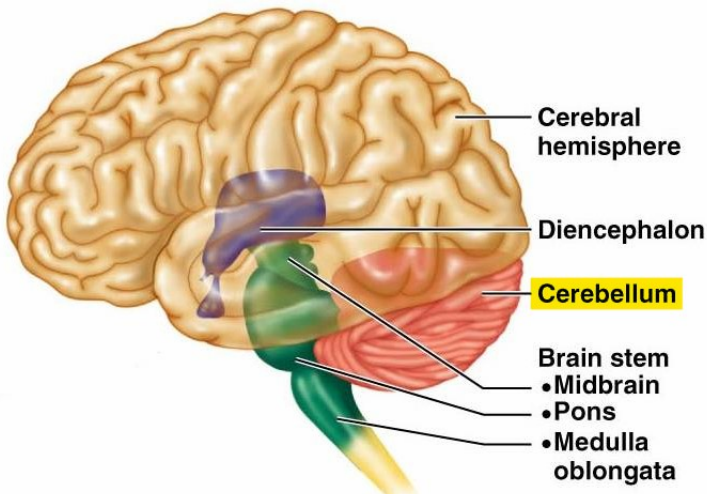


**Figure 2.13: Cerebellum** (From <https://teachmeanatomy.info/neuroanatomy/structures/cerebellum/>)

## 2.5 Cerebellum

The cerebellum is a structure located at the base of the skull, underlying the occipital and temporal lobes of the cerebral cortex. It lies at the same level of and posterior to the pons, from which it is separated by the fourth ventricle. Although the cerebellum accounts for only the 10% of the brain's volume, it contains about half of the total number of neurons of the brain, with a ratio of  $INPUT = 40 * OUTPUTS$  <https://courses.lumenlearning.com/boundless-ap/chapter/the-cerebellum/>. The cerebellum has an important role in motor control: it does not initiate movement but modifies the motor commands of the descending pathways to adapt movements and make them more accurate. In particular, the cerebellum is involved in different functions:

- **Maintenance of balance and posture:** through its input from vestibular receptors and proprioceptors, it modulates commands to motor neurons to compensate for shifts in body position or changes in load upon muscles.
- **Coordination of voluntary movements:** one major function of the cerebellum is to coordinate the timing and force of different muscle groups to produce fluid limb or body movements.
- **Motor learning:** the cerebellum plays a major role in adapting and fine-tuning motor programs to make accurate movements through a trial-and-error process.

Patients with cerebellar damage display uncoordinated voluntary movements and problems maintaining balance and posture. They are unable to produce coordinated and

smooth movements, also they produce an involuntary tremor when they make a movement to a target and they have difficulty to perform rapidly alternating movements [27].

**Final remarks on internal models: simplified distributed motor control:** Figure 2.14 gives a schematic representation of the connections between the different

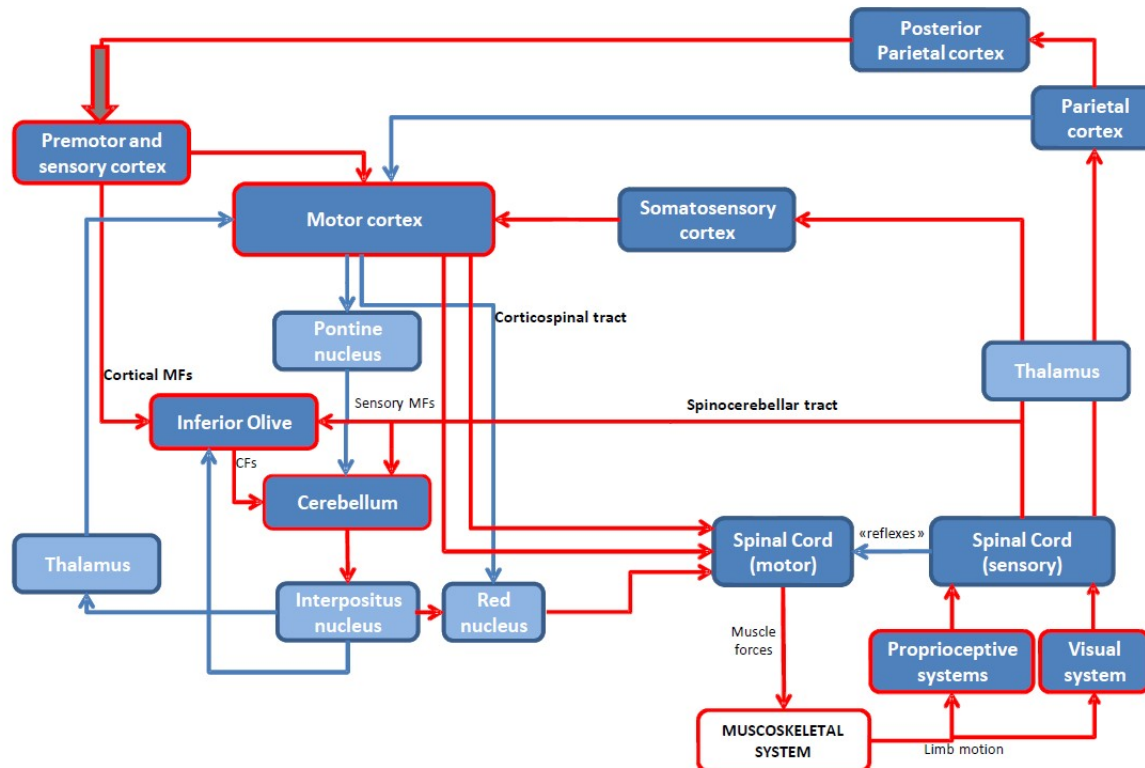


Figure 2.14: Simplified distributed motor control

brain areas involved in motor control. There are multiple simplifications in this scheme (for example there is not the ventral stream), but we can highlight some of the loops concurring to motor control. Motor cortex receives the desired trajectory from Premotor cortex and frontal lobe, receives information about sensory data from the Sensory Cortex and the parietal lobe and receives inputs from the cerebellum (through the deep nuclei and the thalamus) and projects to the spinal cord and to the cerebellum (through the Pons) and the nuclei.

# Focus on the Cerebellum

---

The most relevant property of the cerebellum is the modulation of the input/output connections (adaptation and motor learning thanks to synaptic plasticity).

## ***What does it receive as input?***

Information on the objective of motor actions;

Information on the current motor commands;

Sensorial feedback signals associated to the planning and execution of movements.

## ***What does it produce as output?***

The output projections of the cerebellum are toward "upward" cerebro areas, such as the premotor and motor systems of the cerebral cortex and "downward" through the brain stem, to the systems that control spinal interneurons, and eventually motor neurons .

## 3.1 Anatomical and Functional Structure

The cerebellum is composed of two hemispheres, separated by the **vermis**, a narrow midline zone. Most of its volume is made up of the cerebellar cortex, a tightly folded layer of grey matter. Underneath the grey matter of the cortex lies the white matter and embedded in it there are four cerebellar nuclei- deep cerebellar nuclei-, all composed of grey matter. The cerebellum is connected to different parts of the nervous system thanks to the presence of three paired cerebellar peduncles. These are identified as the superior cerebellar peduncle, the middle cerebellar peduncle and the inferior cerebellar peduncle, their name is related to the position they have respect to the vermis [28].

The cerebellum inputs are conveyed primarily through the **inferior** and **middle** cerebellar **peduncles**, whereas its outputs are conveyed primarily through the **superior** cerebellar **peduncle**. There are three anatomical lobes that can be distinguished

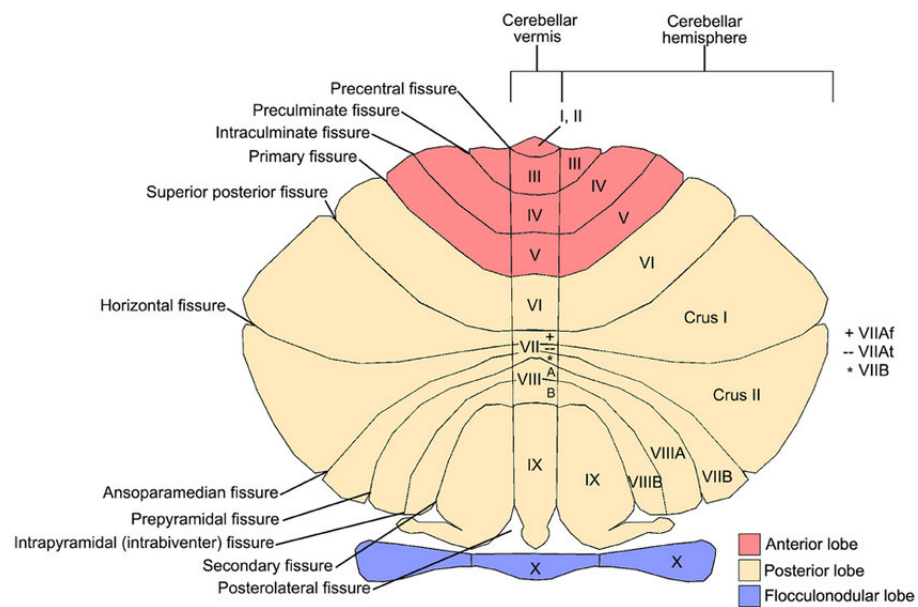


**Figure 3.1: Anatomical Structure of the Cerebellum (From [28])**

in the cerebellum: the **anterior lobe**, the **posterior lobe** and the **flocculonodular lobe**. These lobes are divided by two fissures – the primary fissure and posterolateral fissure <https://teachmeanatomy.info/neuroanatomy/structures/cerebellum/>.

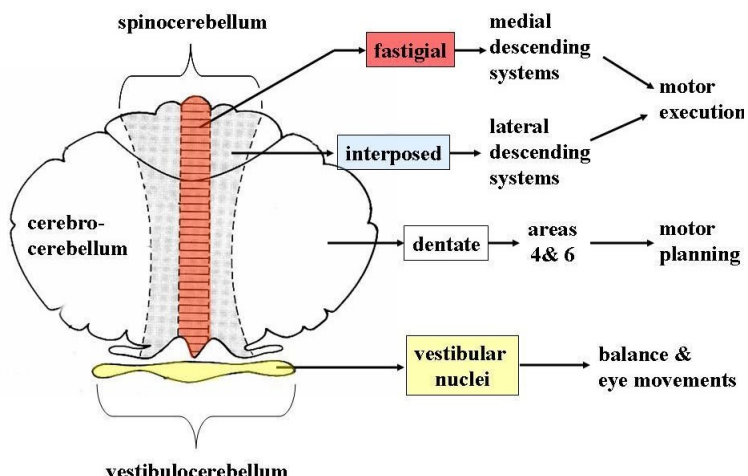


**Figure 3.2: Anatomical and Functional Structure of the Cerebellum (Adapted from <https://teachmeanatomy.info/neuroanatomy/structures/cerebellum/>).**

We can also identify three different functional areas of the cerebellum (Figure 3.2):

1. **Cerebro-cerebellum:** largest functional subdivision formed by the lateral hemispheres. It is involved in planning movements and motor learning. This area also regulates coordination of muscle activation and it is important in visually guided movements.

2. **Spino-cerebellum:** comprised of vermis and medial zone of the cerebellar hemispheres. It is involved in regulating body movements by allowing error correction and controlling muscular tone. It also receives proprioceptive information.
3. **Vestibulo-cerebellum:** functional equivalent to the flocculo-nodular lobe. It is involved in controlling balance and ocular reflexes, mainly fixation on a target. It receives inputs from the vestibular system and it sends outputs back to the vestibular nuclei.

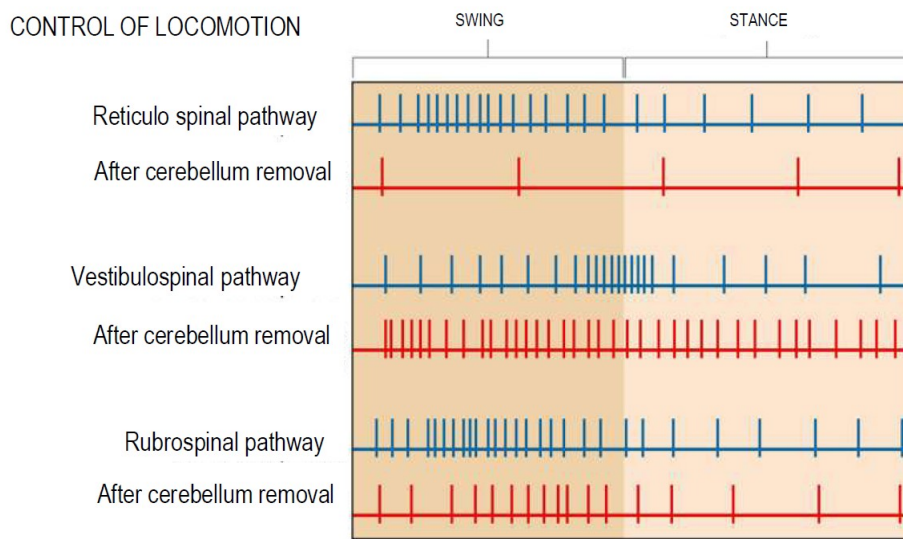


**Figure 3.3: Effects of Cerebellar Removal:** The activity of neurons of three major spinal pathways involved in locomotion control (reticulo, vestibulo and rubro-spinal) are compared in case of a physiological functioning of the cerebellum and after cerebellum removal. The overall activity is extremely modified by the removal of the cerebellum, even if the capability to walk is still preserved by the patient.

## 3.2 Cerebellar Microcircuit

The cerebellar circuit consists of cortical and subcortical sections. The cerebellar cortex is organized in three layers with different histological composition.

- The **Granular layer** that contains Granule cells (**GrC**) somata and Golgi cells (**GoC**), inhibitory interneurons.
- The **Purkinje layer** that contains Purkinje cells somata (**PC**).
- The **Molecular layer** that contains Basket cells (**BC**) and Stellate cells (**SC**), that are inhibitory interneurons, dendrites of Purkinje cells (**PC**) and parallel fibers (**pfs**). The parallel fibers are axons of Granule cells (**GrC**) that bifurcate in the molecular layer.

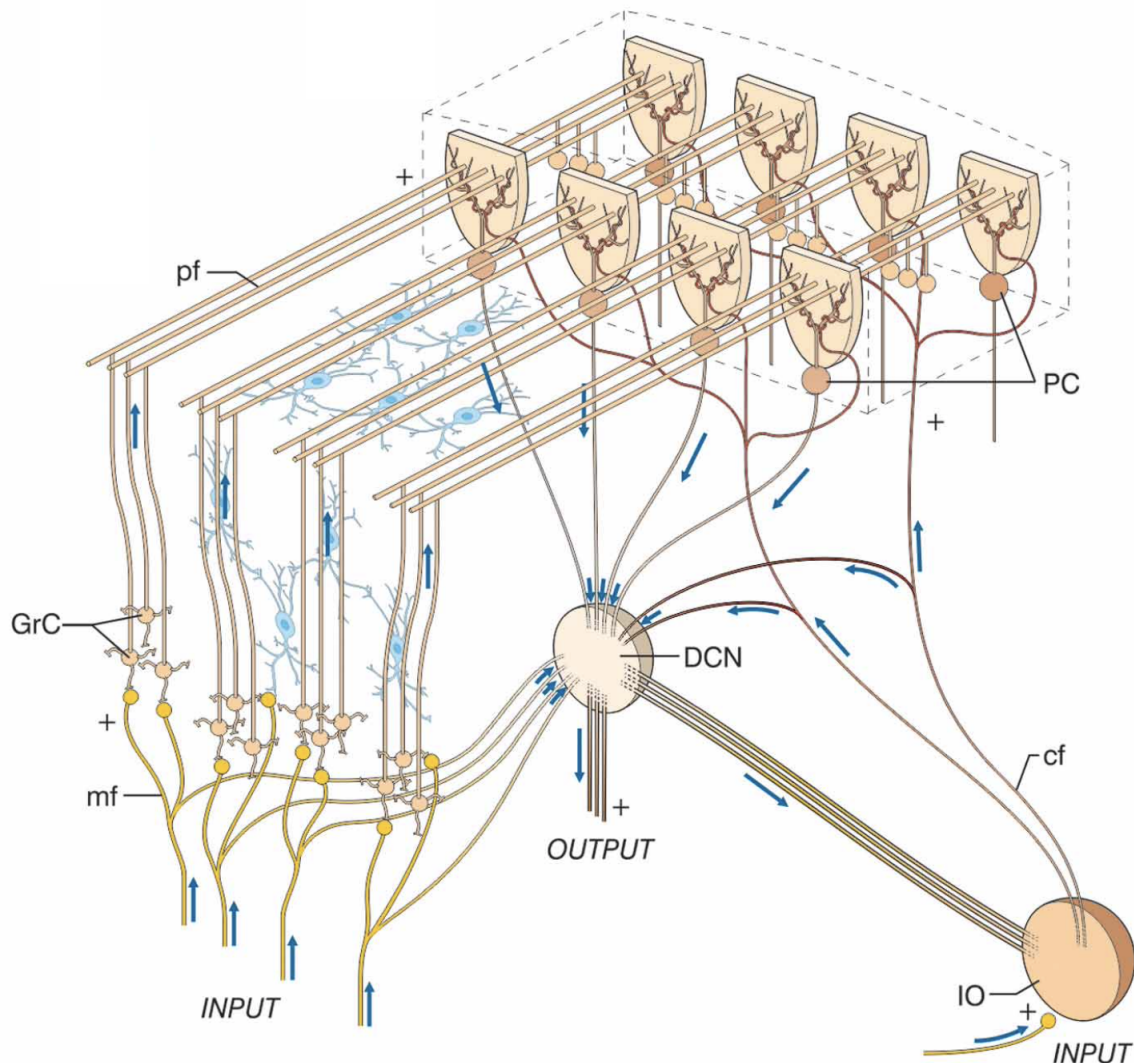


**Figure 3.4: Cerebellar Microcircuit.** The cerebellar circuit consists of cortical and subcortical sections. At subcortical level, the afferent fibers activate Deep Cerebellar Nuclei cells (DCN-C) and Inferior Olive cells (IO-C). The DCN emits the output and at the same time inhibits the IO. In the cerebellar cortex, there are a few different types of neurons including granule cells (GrC), Golgi cells (GoC), Purkinje cells (PC), stellate and basket cells (SC, BC), Lugano cells, and unipolar brush cells (not shown). The two main inputs are represented by mossy fibers (mf) originating in various brain stem and spinal cord nuclei, and by climbing fibers (cf) originating from the IO. Signals conveyed through the mossy fibers diverge to DCN and activate the granular layer (containing GrC and GoC). The ascending axon of the GrC bifurcates in the molecular layer (containing PC, SC, and BC) forming the parallel fibers (pf). The cerebellar cortical circuit is organized as a feedforward excitatory chain assisted by inhibitory loops: mfs excite GrCs, which activate all the other cortical elements. In the granular layer, inhibition is provided by GoCs, in the molecular layer by SC and BC. Finally, PCs inhibit DCN. The IO, which is also activated by brain stem and spinal cord nuclei, controls PC activity through a single powerful synapse. Thus, the whole system can be seen as a complex mechanism for eventually controlling the DCN output. (From [29])

The two inputs of the cerebellar circuit are the mossy fibers (**mfs**) and the climbing fibers (**cf**s), while the output is represented by the Deep Cerebellar Nuclei (**DCN**)

in the subcortical section. The cerebellar cortical circuit is organized as a feedforward excitatory chain assisted by inhibitory loops: mfs excite GrCs, which activate all the other cortical elements. In the granular layer, inhibition is provided by GoC, in the molecular layer by SC and BC. Finally, PCs inhibit DCN. The IO, which is also activated by brain stem and spinal cord nuclei, controls PC activity through a single powerful synapse. Thus, the whole system can be seen as a complex mechanism controlling the DCN output.

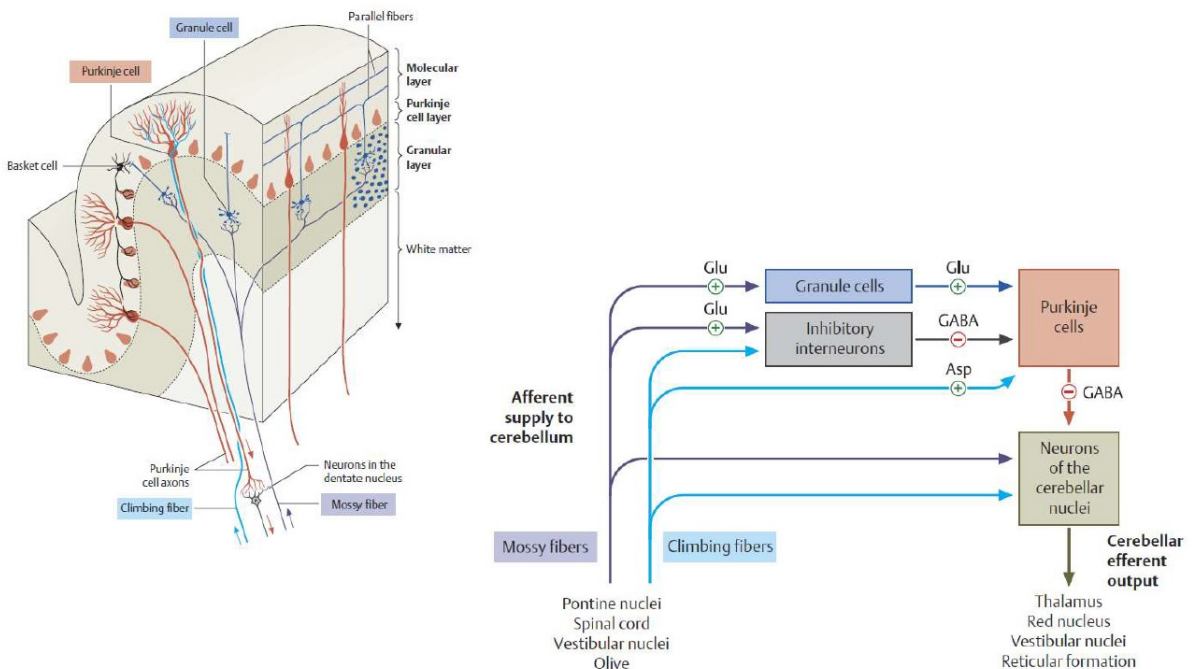


**Figure 3.5: Cerebellum Cytology (From [29])**

### 3.2.1 Cerebellar input: mossy fibers, Granule cells and climbing fibers.

The **mfs** can originate from different structures: nuclei in the **spinal cord** and **brain stem** carrying sensory information from the periphery and **cerebral cortex** (cortical mfs) carrying motor commands (efference copy). They have excitatory synapses on the dendrites of GrCs that are not-recurrent state generator and allow for sparse coding, having a high divergence rate of connections. GrCs are the most numerous neurons in the human brain.

The **GrCs** excite large numbers of **PC** inducing a constant simple spike (SS). The frequency of the SS could codify the intensity and the duration of peripheral information or behaviors generated by the CNS. One of the fundamental characteristics of GrC is their center-surround way coding information.

The *cfs* originate from the Inferior Olive nucleus (**IO**) and convey somatosensory, visual, or cerebral cortical information. They have excitatory synapses on the Purkinje cells, generating low frequency complex spike, CS. Each PC receives only one *cf*, while a single climbing fiber contacts a few PCs transversally orientated (wrt parallel fibers). The CS could codify the temporal features of the peripheral events and/or act as starting signals for behavioral actions.

**Note:** the *cfs* wrap the PC so that when it generates the CS, the PC is dominated by the electrical event induced by the *cf*.

### 3.2.2 Electrical Activity of Purkinje Cells

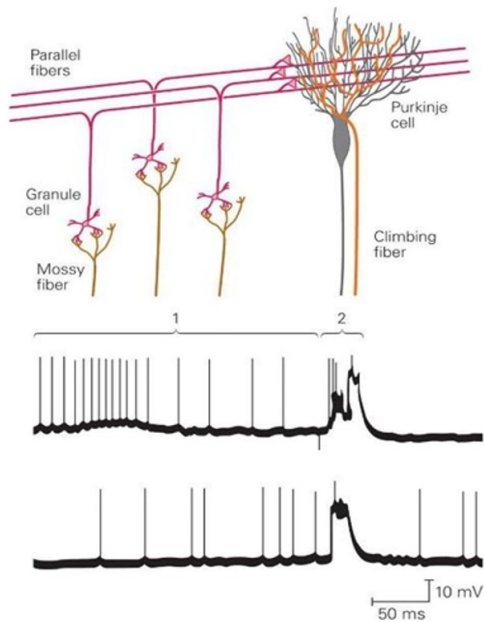


**Figure 3.6: Electrical Activity of Purkinje Cells:** Simple and complex spikes recorded intracellularly from a cerebellar Purkinje cell. Simple spikes are produced by mossy fibers input (1), whereas complex spikes are evoked by climbing fiber synapses (2). (From <https://neopsykey.com/the-cerebellum-2/>).

The connection of *pfs* and *cfs* with PCs and the way these connections influence the electrical activity of PCs is different. The PC dendrites intersect perpendicularly the *pfs*. In this way, each PC receives input from a large number of parallel fibers, and each parallel fiber can contact a very large number of PCs (on the order of tens of thousands). On the other hand, a single PC forms a synapse with a single climbing fiber [30]. Therefore, each PC processes a private input together with an input common to other PCs. Regarding the effect on the electrical activity, *pfs* activity induces in a PC the so-called simple spike, whose frequency encodes the magnitude and duration of peripheral stimuli or centrally generated behaviours. Inputs from many parallel fibers are needed to have a substantial effect on the frequency of simple spikes, as for each

postsynaptic potential the synaptic input is tiny. An action potential in the *cfs*, instead, induces in the PC a complex spike, composed by an initial large-amplitude action potential followed by a high-frequency burst of smaller-amplitude action potentials. The *cfs* spontaneously induce complex spikes at low rates, rarely more than one to three per second. The *cfs* system therefore seems specialized for event detection; the firing rate carries a few or no information. Although these fibers fire infrequently, the synchronous firing in multiple fibers enable them to find important events. Synchrony seems to arise because neurons in the IO nucleus often are connected to one another through gap junctions.

### 3.2.3 Cerebellar output: deep cerebellar nuclei

DCNs project directly to the red nucleus and indirectly to the primary motor cortex and premotor cortex via the thalamus. The cerebellum influences the regulatory action of these nuclei and cortices on the descending motor system, thereby contribute to motor coordination and accuracy.

## 3.3 Learning and Plasticity

The mechanism underlying the learning process of the cerebellum, and more in general of the brain, implies modifications in the strength of connections between neurons, namely the synaptic plasticity. The best experimental setup for exploring plasticity in a controlled manner is the *in vitro* setup. By using pairs of neurons clearly isolated and connected (using either brain slices or cultured neurons), one can patch the pre- and the post-synaptic neuron and observe the synaptic modifications between them according to their discharge.

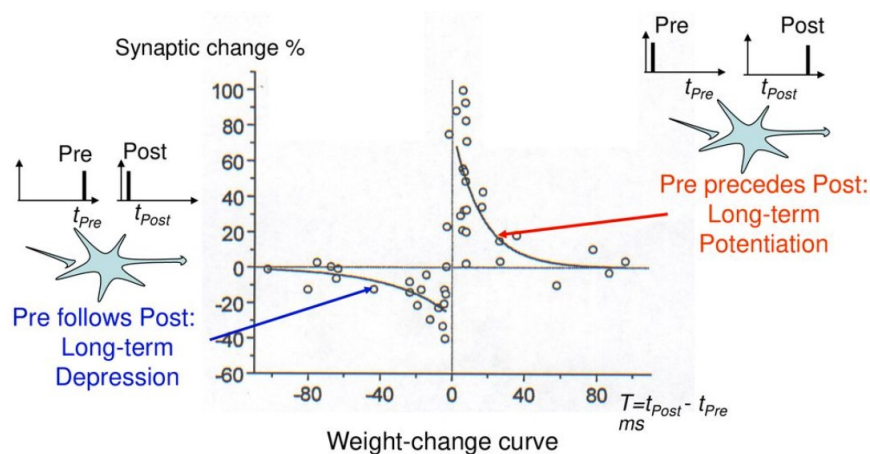


**Figure 3.7: Spike-Time Dependent Plasticity** (Adapted from [31])

There is indeed several evidence in many brain areas that the efficiency of a synaptic connection between two neurons may be regulated by the precise timing of the joint activity of the neurons [32, 33, 34]. This postulate, originally made by Hebb [6], has been demonstrated in a lot of in vitro experimental studies in the form of the **Spike Time Dependent Plasticity** (STDP) rule. Hebb did not, however, postulate the existence of synaptic weakening STDP is an associative rule.

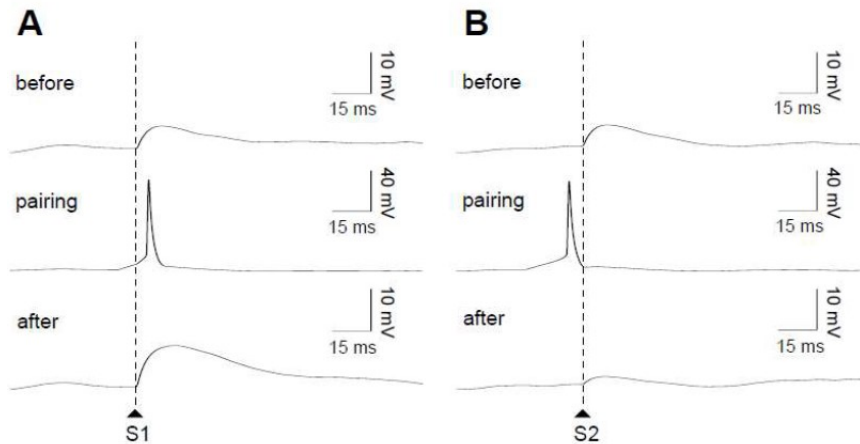


**Figure 3.8: Experimental protocol of STDP in vitro.** Pre and Post synaptic neurons are patched and forced to fire with a time difference, while the modification of the synaptic strength is monitored [32].

From Figure 3.8, when pre-post spikes pairings are made repeatedly at a fixed frequency of 1 Hz, with a particular time difference  $\delta t$  between pre and post spikes, synaptic modifications are observed, whose magnitude depends on  $\delta t$ . The weight of the synapse is measured as the amplitude (or initial slope) of the postsynaptic potential. For positive values of  $\delta t$ , when pre-synaptic spike occurs before the post, the synapse is potentiated (**Long Term Potentiation**, LTP). Oppositely, if  $\delta t$  is negative, the synapse is depressed (**Long Term Depression**, LTD). Both mechanisms occur in relatively short time windows of 20 ms circa. That 20 ms time scale is the time window for triggering a change, but the actual change happens much more slowly. The STDP phenomenon as seen in vitro is appealing from a theoretical point of view. Indeed STDP is the most recent and promising candidate to support unsupervised learning algorithms in the brain, based on neuronal activity.

In the cerebellum changes in the strengths of *pfs*-PC synapse could store **stimulus-response associations** by linking inputs with appropriate motor outputs, following a Hebbian learning approach but using the **supervision** of *cfs* discharge. *Cfs* provide a **teaching signal** that induces synaptic modification *pfs*-PC synapses.

In [35], Marr assumed that *cfs* input would cause synchronously activated *pfs* inputs to the same PC to be strengthened. However, the major part of the subsequent cerebellar-learning models has followed Albus theory, assuming that climbing fiber ac-

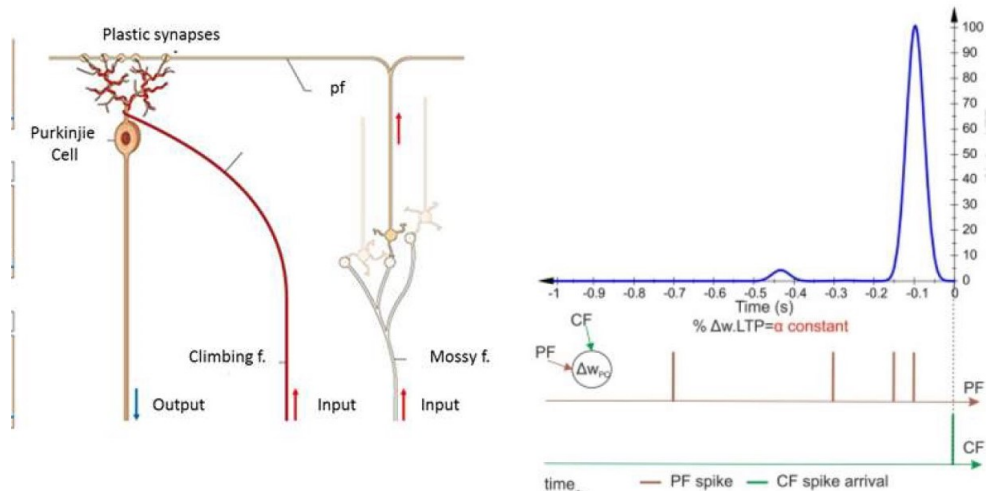


**Figure 3.9: Synaptic plasticity at parallel fiber– Purkinje cell**

tivity was an error signal and could cause synchronously activated parallel fiber inputs to be weakened [36]. Therefore, the modification of the synapse strength at the level of *pfs*-PC follows this learning rule: if, at a time  $t$ , the *cfs* fire, it induces LTD at the level of the *pfs* synapses that were active in a given time window before the time  $t$ . While LTP occurs when there is no *cfs* activity, which corresponds to a decrease or a cancellation of the teaching signal. For more detail see chapter 5.



# Modelling and Simulation: Single Neuron Modeling

---

The brain is part of a complex biological system (the nervous system) whose functional organization may be divided in many different levels, each operating at a different scale. Behaviour is the more general level of this complex hierarchical structure, and is the only level that can be observed with the bare eye. Its functional explanation, however, is strictly interconnected with all the other levels of this graded organization, from brain regions to single cells activity. Thus, the nervous system (and the brain itself) requires a multi-scale modelling approach in order to investigate its fundamental mechanisms.

Models are abstractions of real-world systems to investigate specific hypotheses in a quantitatively way. Multi-scale modelling may follow a top-down approach (from higher to lower scales) or a bottom-up approach (from lower to higher). This paragraph will first present ion channels and single neurons models and then generalize them to form neural networks models.

Neuron models can be divided by their morphological and electrical levels of detail. Single cell models are morphologically distinguished in multi-compartment models and point neuron models: the former mathematically model the electrical activity of each subcellular element taking into account morphological features, while the latter describe the electrical activity of neurons as collapsed in single points, representing the computational properties of neurons rather than their electrical activity and its spatial distribution.

When modelling single elements of brain models, like neurons, a fundamental issue emerges: the balance between biological plausibility and computational load. Choosing the most suitable level of realism depends on the scientific question and should take into account the drawbacks of oversimplification as well as the possible important results hidden by unnecessary complexity [19].

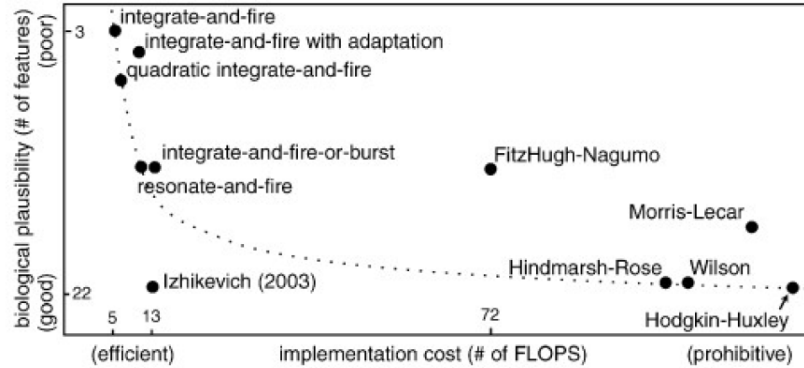


**Figure 4.1: Neuron Models:** balance between biological plausibility and computational load (From [37])

Single neuron models can show:

- **Different levels of morphological detail:** from compartmental models with different levels of detail to point models, in which the neuron collapse in a single point and all its morphological features are neglected.
- **Different levels of electrical detail:** from Hodgkin-Huxley model, which takes into account the contribution of the ion channels, to the Leaky Integrate and Fire model, which takes into account only the passive properties of the membrane. The first one is biologically plausible but computationally too heavy. The second one is computationally efficient, but it is not biologically plausible.

Despite the significant approximations of subcellular mechanisms, Leaky Integrate and Fire (LIF) neuron is the reference neuronal model in case of limited computational power. However, more advanced versions have been designed, with higher dimensionality and non-linear terms to account for the variety of electroresponsive behaviors of biological neurons. The main ones are the Izhikevich model, the Adaptive Exponential LIF model, the Generalized LIF model and the Extended-Generalized LIF model.

## 4.1 Hodgkin-Huxley Model

The Hodgkin-Huxley model, also called conductance-based model, is one of the most accurate neuronal models. It is a mathematical model made of a set of nonlinear differential equations whose solution gives the instantaneous value of the voltage across the membrane. The membrane of neurons contains voltage-gated ion-channels. These channels let through only one particular type of ion, typically Na or K, with a high selectivity. Due to an exquisite mechanism that relies on conformational changes, the open probability of the channel depends on the voltage across the membrane. The

cell can use these channels to modulate its input-output relation, regulate its activity level, and make the firing pattern history dependent (by adaptation). Consider a small membrane patch. The voltage equation is obtained by applying Kirchoff's law to the membrane and collecting all currents flowing through. In addition to the leak and capacitive currents (which flow in rest neurons), during spikes we need to include Na and K currents. Let us take the sodium current first (potassium is analogous). The current (per area) through the sodium channels is computed as in Equation 4.1

$$I_{Na}(V, t) = g_{Na}(V, t)[V(t) - V_{Na}^{rev}] \quad (4.1)$$

The current is proportional to the difference between the membrane potential  $V(t)$  and the Na reversal potential,  $V_{Na}^{rev}$ . The total conductance through the channels ( $g_{Na}$ ) is given by the conductance of the single Na channel multiplied by the number of open channels as in Equation 4.2.

$$g_{Na}(V, t) = g_{Na}^0 \rho_{Na} P_{open}(V, t) \quad (4.2)$$

where  $g_{Na}^0$  is the open conductance of a single Na channel,  $\rho_{Na}$  the density of Na channels per area,  $P_{open}$  a channel's open probability, which turns out to factorize as the product of three switches ( $m$ ) and one  $h$ :

$$P_{open}(V, t) = m^3(V, t)h(V, t) \quad (4.3)$$

where,

$$\frac{dm(V, t)}{dt} = \alpha_m(V)(1 - m) - \beta_m(V)m \quad (4.4)$$

$$\frac{dh(V, t)}{dt} = \alpha_h(V)(1 - h) - \beta_h(V)h \quad (4.5)$$

Microscopically, the gates behave as binary switches that flip state on the membrane voltage. In order for the sodium channel to conduct, all three  $m$  and the  $h$  have to be switched on. The gating variables describe the probability that the gate is open ("on") or closed ("off") state. The gating variables evolve as shown in Figure 4.2.

Time constants  $\tau_m$ ,  $\tau_h$  and  $\tau_n$ , reported in Figure 4.2, depend on the voltage across the membrane: as the voltage changes, the equilibrium shifts and the gating variables will try to establish a new equilibrium. The  $m$  opens with increasing voltage (called an activation variable), but  $h$  closes with increasing voltage (inactivating gating variable). Then, the inactivation causes the termination of the Na current. Because the inactivation is much slower than the activation, spikes can grow before being terminated. The  $n$  gating variable is for K channels. The complete HH equation for the voltage is:

The full HH model consists of this equation plus the equations for the conductances

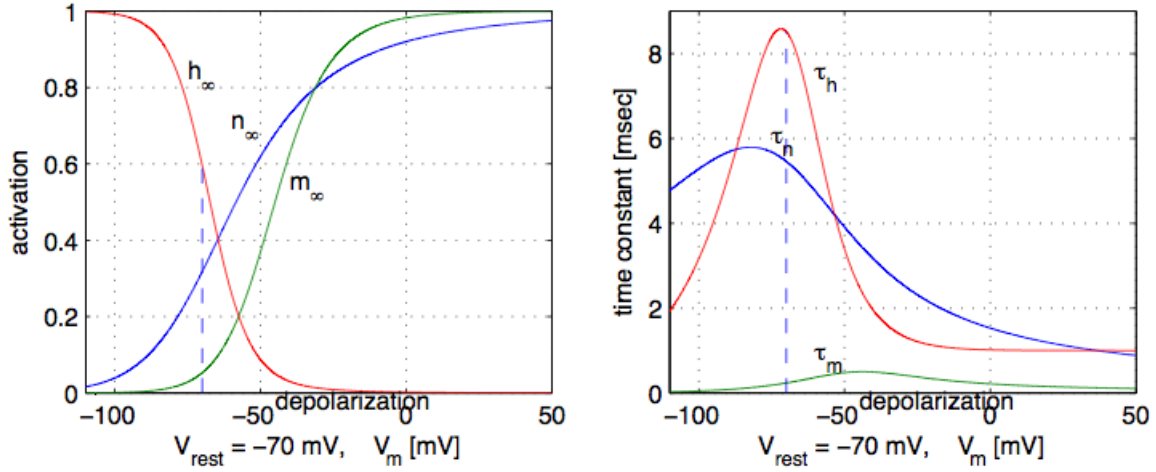


**Figure 4.2:** Hodgkin-Huxley model: Steady-state activation and inactivation functions (left) and time constants (right) are voltage-dependent. [38]

of Na, K and all the other ions for which V-gated channels are present. The circuital equivalent is reported in Figure 4.3.

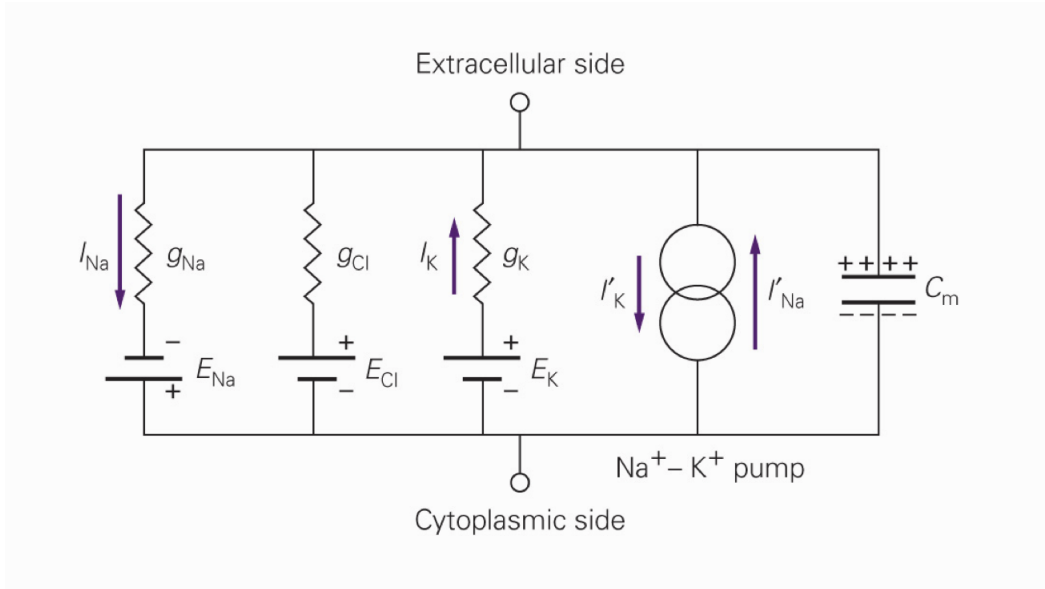


**Figure 4.3:** HH equivalent circuit [38]

To obtain the voltage equation we apply *Kirchoff's law* again and collect all currents: the capacitive, the leak, Na, and K currents.

$$C_m \frac{dV(t)}{dt} = g_{leak}[V(t) - V_{leak}] - g_{Na}(V, t)[V(t) - V_{Na}^{rev}] - g_K(V, t)[V(t) - V_K^{rev}] + I_{ext} \quad (4.6)$$

The full Hodgkin Huxley model consists of Equation 4.6, the equations for the Na current (Equation 4.1) and the similar equations for the K current and all other V-

gated ion-channels. Although the Na and K channels of the HH model are the prime channels for causing the spike, many other channel types are present. The cell can use these channels to modulate its input-output relation, regulate activity its activity level, and make the firing pattern history dependent (by adaptation). The HH model is a multi-dimensional, coupled equations (variables  $V, h, m, n$ ) model, with no analytical solutions. Solution is found by numerically integrating the equations.

#### 4.1.1 Markovian Stochastic Version

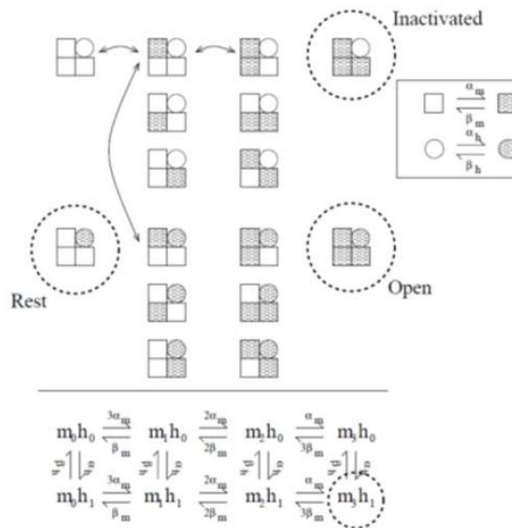


**Figure 4.4: Markovian Stochastic HH model** There are 4 gates in total (3  $m$ 's, and 1  $h$ ), which each can be independently in the up or down state. So in total there are  $2^4 = 16$  states, where one of the 16 states is the open state, top. However, it makes no difference which of the  $m$  gates is activated, and so it can be reduced to contain 8 distinct states, bottom.

In the Markovian model the neuron has a discrete number of channels each with activation variables ( $h, m, n$ ) that flip between on and off states, this in turns leads to a flickering of the conductances. In contrast, in the original HH model, all gating variable are continuous real quantities, not switches. The rate constants give the probability that channels flip. In the limit of a large number of channels, the stochastic description matches the original one.

## 4.2 Multi-Compartmental Models

The model can be applied to the whole cell by assuming constant properties along all the membrane. Otherwise, the model can be applied to a single compartment of the membrane with its specific characteristics. To describe propagation of the spike in the axon, coupling the compartments is necessary. An important problem is that

membrane characteristics are different along the structure of the neuron (dendrite or axon or soma...), therefore each one has different conductance properties. To take into account the shape of the neurons, we can think to divide it into elements called **compartments** and apply the cable equation on each of them (fig 4.5). In each

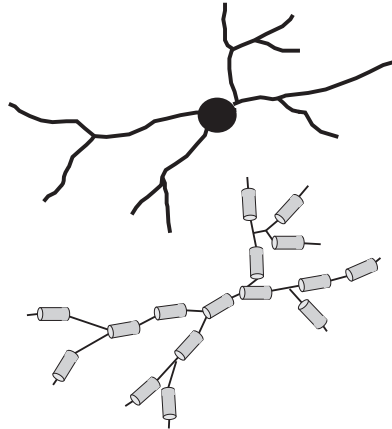


**Figure 4.5:** Neuron topology reconstruction using compartments [39]

compartment, membrane voltage was obtained as the time integral of the Equation 4.7 [40]:

$$\frac{dV_m}{dt} = -\frac{1}{C_m} * \left\{ \sum [g_i(V_m - V_i)] + I_{inj} \right\} \quad (4.7)$$

Adjacent compartments communicated through an internal coupling resistance [41].

#### From literature: *Electroresponsive properties of the Purkinje Cell model*

The PC model (with accurate representation of axonal compartments), reproduced auto rhythmicity, simple spike frequency modulation and complex bursting [42]. While Na channels allowed simple spike generation and sustained firing, dendritic Ca channels contributed to sustain pace-making and complex bursting, axonal K channels were critical for spike frequency filtering. Therefore, a coherent hypothesis on how ionic channel localization and function regulates action potential generation and propagation was made, highlighting the importance of axonal compartmentalization.

In order to develop the PC model, one must identify a series of different electrotonic compartments in the neuron: dendrites, soma, axon initial segment (AIS), paraAIS, myelin, ranvier nodes and collateral. Each of those is characterised by specific channel types, distribution and gating properties. Also, maximum conductance and reversal potential can be obtained. The free parameters of the model that need to be addressed are the maximum ionic conductances of voltage- and calcium-dependent channels: they were taken from estimations in literature and fine-tuned through genetic algorithms. Then, the testing phase followed: the matching between model output and experimental data was evaluated by comparing the voltage traces elicited in response to various

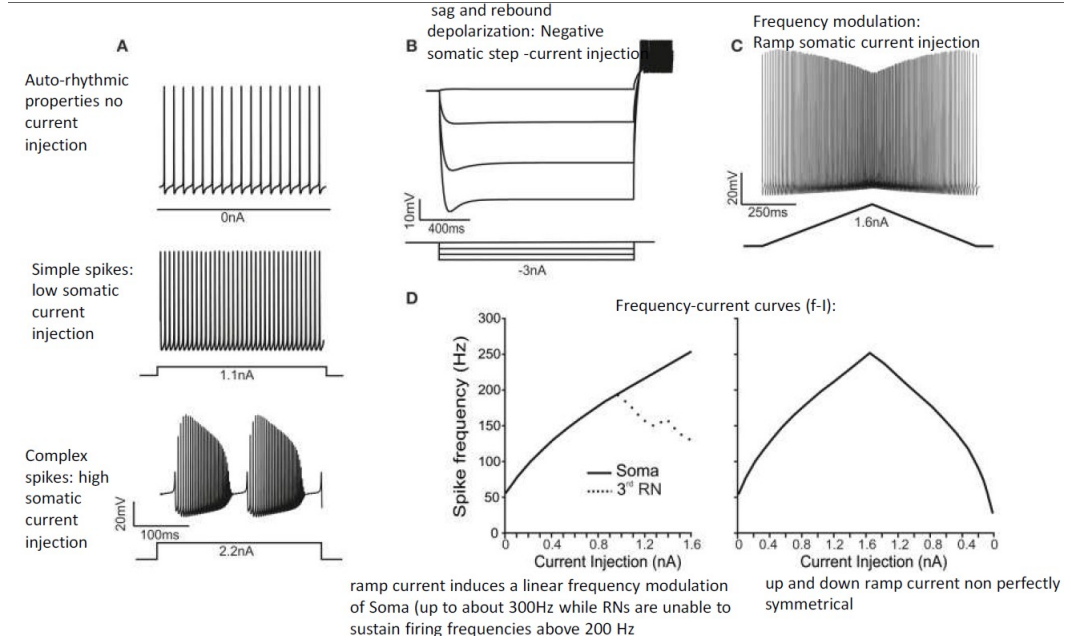


**Figure 4.6: Electoresponsive properties of the PC model.** (A) The traces show spikes in the soma during spontaneous firing (Protocol 1) and in response to moderate (1.1 nA) and high (2.2 nA) step-current injections in the soma (Protocol 2), demonstrating the transition from simple spikes to complex bursting. (B) A series of negative step-current injections in the soma determines voltage responses showing the typical sag and rebound depolarization generated by the H-current. (C) A ramp-current injection (from 0 to 1.6 nA and back) causes a frequency-modulated response in the PC model. (D) In response to step-current injection from 0 to 1.6 nA (0.1 nA steps), the PC model generates proportionately higher spike frequencies. Conversely, the RNs are unable to sustain firing frequencies above 200 Hz (dotted line). In response to ramp-current injection increasing from 0 to 1.6 nA, the f-I curve closely resembles that obtained using step-currents. However, on the way back, the f-I curve is asymmetrical. (From [42].)

sets of step-current injections including pulses from different holding potentials and responses to hyperpolarization.

To test the model, two experimentally-based protocols that reproduced the main PC properties were developed and performed after each conductance change. The first protocol was designed to test the ability of PCs to generate spontaneous firing and evaluate the PC model discharge in the absence of current injection. The second protocol was designed to evaluate the PC model electroresponsiveness upon somatic current injection.

A compartmental model like the one described allows to highlight the properties of a specific neuron with a very high accuracy. However, the level of complexity makes it unusable in a circuit since the computational cost would be unaffordable.

## 4.3 Leaky Integrate and Fire Model

Next step is to go from detailed compartmental models of cells to single point neurons to simulate the functional properties of microcircuits. The most common reduced model for reproducing spiking activity, as it generates only the spike event, is the leaky integrate and fire (LIF) model, an easy and efficient model introduced in 1907 by Lapicque [43]. It describes the sub-threshold behaviour with a simple passive circuit (Figure 4.7):

*Membrane potential dynamic*

$$\tau_m \frac{dV_m(t)}{dt} = -[V_m(t) - E_L] + R_m I_{in}(t) \quad (4.8)$$

*Spike condition*

$$If V_m > V_{th}, then V_m = V_{reset} \quad (4.9)$$

$\tau_m$  is the membrane time constant ( $\tau_m = R_m * C_m$ , where  $R_m$  and  $C_m$  are the membrane resistance and capacitance, respectively), and it accounts for how fast the  $V_m$  curve increases.  $E_L$  is the resting potential and it represents the steady-state value of  $V_m$  in absence of external input current.  $I_{in}$  is the input current. Action potentials are approximated as single spike instants: whenever  $V_m$  reaches a firing threshold  $V_{th}$ , the membrane potential is reset to a fixed value  $V_{reset}$ . After the spike,  $V_m$  remains at  $V_{reset}$  value (constant) during the refractory period and it is not possible to emit spikes.

The simplified model without the resistance ( $R_m$ ) is called the leak-less I&F model.

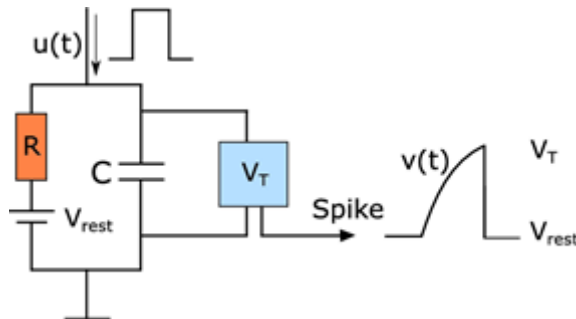


**Figure 4.7: Leaky Integrate and Fire circuit** when a rectangular pulse input is provided. The voltage across the membrane, starting from  $V_{rest}$ , raise until the threshold is reached and a spike is generated. The voltage is then reset to  $V_{rest}$ .

### 4.3.1 Izhikevich Model

The model consists of a system of two differential equations that describe the membrane potential  $V_m(t)$  and the membrane recovery variable  $u(t)$ :

$$\begin{cases} \frac{dV_m(t)}{dt} = 0.04 * V_m^2(t) + 5 * V_m] + 150 - u(t) + 1 & \text{Membrane potential dynamic} \\ \frac{du(t)}{dt} = a * b(V_m(t) - u(t)) & \text{Membrane recovery variable} \end{cases} \quad (4.10)$$

If  $V(t) > 30mV \rightarrow \text{Spikes.}$

$$\begin{cases} V_m(t+1) = c \\ u(t+1) = u(t) + d \end{cases} \quad (4.11)$$

The Izhikevich model was obtained from a simplification of HH models into a 2D IF system. The model, as the LIF, does not describe the shape of the action potential but just the time instant of the spike event. After the action potential, the membrane potential is reset to a value  $c$  while the recovery variable is incremented of a value  $d$ . The parameters  $a$  and  $b$  are coupling constants between  $V$  and  $u$ , while  $c$  and  $d$  are update constants. A quadratic term in  $V$  models the spike initiation, while the membrane recovery variable accounts for subcellular ionic mechanisms and summarizes all the properties of the single ion channels described in the HH model.

The recovery variable contributes to hyperpolarization of the neuron, therefore allows adaptation of the firing rate after a burst. Different spiking patterns can be obtained for different parameter sets  $(a,b,c,d)$  as shown in Figure 4.8. The model consistently represents cortical and thalamic neurons dynamics [44], that show always the same spiking pattern, but it does not suit well for neurons, like Golgi cells, that exhibit different behaviours according to different inputs.

### 4.3.2 Adaptive Exponential LIF Model

The model consists of a system of two differential equations that describe the membrane potential  $V(t)$  and the adaptive current  $w(t)$ :

$$\begin{cases} C_m \frac{dV_m(t)}{dt} = -g_L \cdot (V_m(t) - E_L) + g_L \cdot \Delta_T \cdot \exp \frac{V_m(t) - V_{th}}{\Delta_T} + I_{in}(t) & \text{Membrane potential} \\ \tau_m \frac{dw(t)}{dt} = a \cdot (V_m(t) - E_L) - w(t) & \text{Adaptive current} \end{cases} \quad (4.12)$$

If  $V(t) > V_{th} \rightarrow \text{Spikes.}$

$$\begin{cases} V_m(t+1) = V_r \\ w(t+1) = w(t) + b \end{cases} \quad (4.13)$$

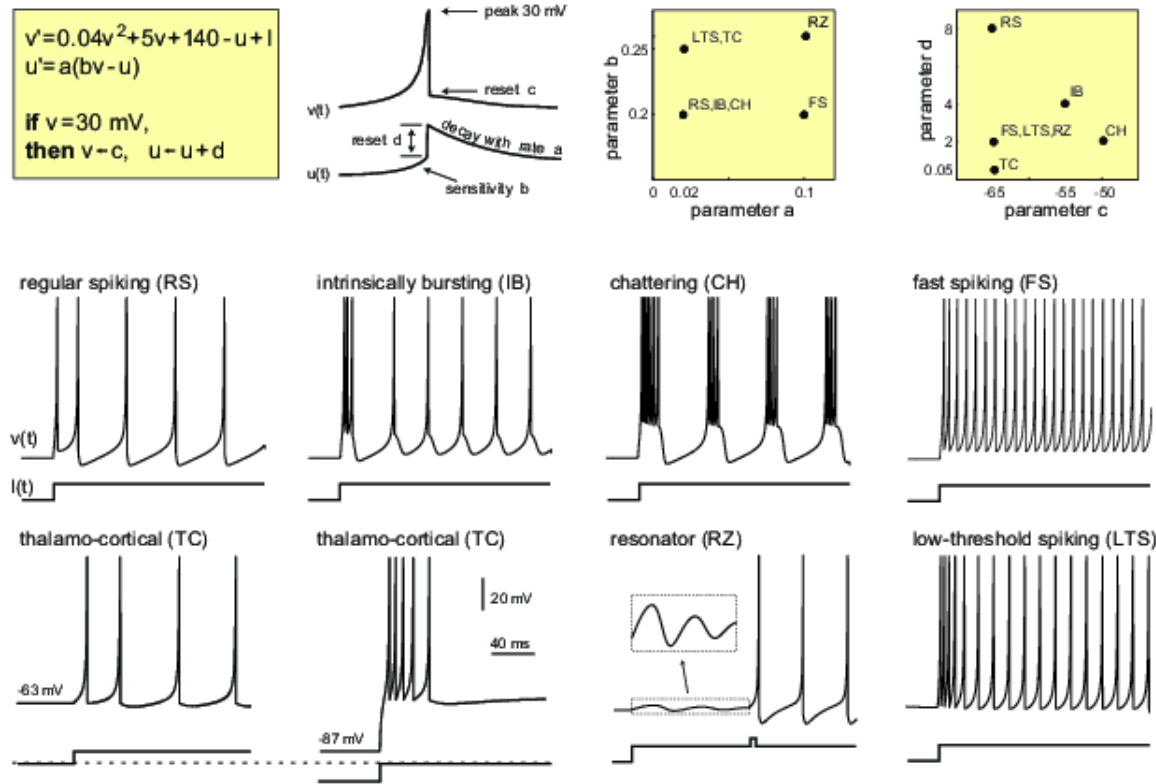


**Figure 4.8:** Different firing dynamics of the Izhikevich neuron model corresponding to different sets of the free parameters.

The Adaptive Exponential Integrate and Fire is another example of non-linear bidimensional IF model, including two state variables:  $V_m$  and an adaptive current coupled with  $V_m$ , which accounts for adaptation or bursting, depending on the value of the coupling constant,  $a$ . An exponential term allows a realistic representation of the action potential initiation and shape [45].

The most relevant properties of this model are:

- multiple electroresponsive properties based on parameter values;
- replacement of the strict voltage threshold by a more realistic smooth spike initiation zone;
- subthreshold resonances or adaptation as in the Izhikevich model.

### 4.3.3 Generalized LIF Model

The Generalized LIF (GLIF) model is a linear multi-dimensional version of the basic LIF [46, 47]. It consists of a system of three differential equations that describe the

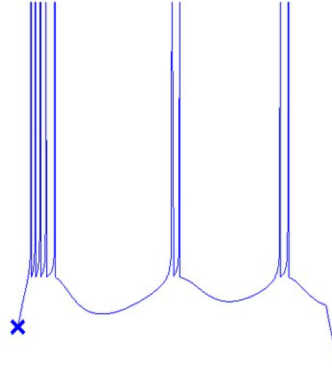


**Figure 4.9: Regular bursting as response of the Adaptive Exponential model to a current step:** (left) voltage as a function of time; (right) trajectories in the 2-dimensional space of voltage (horizontal axis) and adaptation variable (vertical axis). Resting potential marked by cross; sequence of reset values marked by squares. Nullclines  $w'(t) = 0$  (green line) and  $V'(t) = 0$  before (black dashed line) and after the current step (black line). (From [45])

membrane potential  $V(t)$  (as in the basic LIF), the spike-triggered currents  $I_j(t)$  with different dynamics and reset rules to account for fast and slow subcellular mechanisms and the spike-triggered firing threshold  $V_{th}$  with own dynamics.

$$\begin{cases} C_m \frac{dV_m(t)}{dt} = -g_L \cdot (V_m(t) - E_L) + \sum_j I_j(t) + I_e & \text{Membrane potential} \\ \frac{dI(t)}{dt} = -k_j \cdot I_j(t) & \text{Spike-triggered current} \\ \frac{dV_{th}}{dt} = a \cdot (V_m(t) - E_L) - b \cdot (V_{th}(t) - V_\infty) & \text{Spike-triggered threshold} \end{cases} \quad (4.14)$$

Moreover, here we have an escape-rate non-linear rule for probabilistic spike emission. At each spike, state variables are updated according to:

$$\begin{cases} V_m(t+1) = V_r \\ I(t+1) = R_j \cdot I_j(t) + A_j \\ V_{th}(t+1) = \max(V_\infty, V_{th}(t)) \end{cases} \quad (4.15)$$

The model consists of a linear differential equation and an update rule for each variable. The coefficients of the differential equations form a triangular matrix, which allows sequential solving of the set of equations. Internal currents are exponentially decaying and do not depend on other variables, the evolution of the membrane voltage depends on the internal currents, and the evolution of the threshold depends on the membrane voltage.

The GLIF model accurately predicts the occurrence of individual spikes with millisecond precision. As an example, to evaluate the predictive power of the GLIF model,

the response of a L5 pyramidal neuron to a fluctuating input current has been recorded intracellularly. The same protocol was repeated nine times to assess the reliability of the neural response. The GLIF model (with parameters extracted using a different dataset) was able to accurately predict both the subthreshold and the spiking response of the cell. See [46] for more details. After automatic fitting of parameters based on experimental data, the GLIF model has been proven capable to reproduce cortical neurons spiking patterns with high accuracy [46].

#### 4.3.4 Extended Generalized LIF Model

The Extended Generalized LIF (E-GLIF) [48] model consists of a system of differential equations (Equation 4.16) that describe the membrane potential  $V_m(t)$ , the adaptive current  $I_{adap}$  and the spike-triggered depolarizing current  $I_{dep}$ :

$$\begin{cases} \frac{dV_m(t)}{dt} = \frac{1}{C_m} \cdot \left( \frac{C_m}{\tau_m} \cdot (V_m(t) - E_L) + I_{stim} + I_e + I_{dep} - I_{adap}(t) \right) & \text{Membrane potential} \\ \frac{dI_{adap}(t)}{dt} = k_{adap} \cdot (V_m(t) - E_L) - k_2 I_{adap}(t) & \text{Adaptive current} \\ \frac{dI_{dep}(t)}{dt} = -k_1 I_{dep}(t) & \text{Depolarizing current} \end{cases} \quad (4.16)$$

Spike generation at  $t_{spk}$  is described by Equation 4.17

$$\begin{cases} t_{spk} \notin \Delta t_{ref} & \text{Refractory period} \\ rng < (1 - \exp -\lambda(t_{spk})t_{spk}) & \text{Stochasticity} \end{cases} \quad (4.17)$$

being:

$$\lambda(t) = \lambda_0 \cdot e^{\frac{V_m(t) - V_{th}}{\tau_V}} \quad (4.18)$$

When a spike occurs, the variables are updated as follows:

$$\begin{cases} V_m(t_{spk}) \leftarrow V_r \\ I_{dep}(t_{spk}) \leftarrow A_1 \\ I_{adap}(t_{spk}) \leftarrow I_{adap}(t_{spk} - 1) + A_2 \end{cases} \quad (4.19)$$

In addition to the leaky current term  $\frac{C_m}{\tau_m} \cdot (V_m(t) - E_L)$ , each one of the membrane currents defined in the model ( $I_e$ ,  $I_{adap}$ ,  $I_{dep}$ ) accounts for a different mechanism that can be properly parameterized.

- $I_e$  is an endogenous current modeling the net contribution of depolarizing ionic

$I_{stim}$	external stimulation current	-
$C_m$	membrane capacitance	Biological
$\tau_m$	membrane time constant	Biological
$E_L$	resting potential	Biological
$I_e$	endogenous current	Artificial
$k_{adap}, k_2$	adaptation constants	Artificial
$k_1$	$I_{dep}$ decay rate	Artificial
$V_{th}$	threshold potential	Biological
$\lambda_0, \tau_V$	escape rate parameters	Artificial
$t_{spk}^+$	time instant immediately following the spike time $t_{spk}^+$	-
$V_r$	reset potential	Biological
$A_2, A_1$	model currents update constants	Artificial

**Table 4.1: E-GLIF parameters**

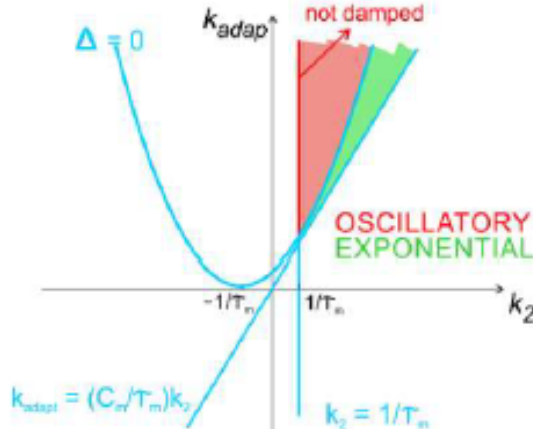
currents generating autorhythmicity [47]

- $I_{adap}$  is an adaptive current, usually hyperpolarizing, which is characterized by a small spike-triggered increment ( $A_2$ ) that decays thereafter according to  $k_{adap}$  and  $k_2$ .  $I_{adap}$  models the activation of potassium channels generating a slow hyperpolarizing current. Since  $I_{adap}$  activates slowly while  $I_{dep}$  is already decaying, the balance between the two currents generates spike-frequency adaptation and after hyperpolarization. Moreover, by being coupled with  $V_m$  by  $k_{adap}$ ,  $I_{adap}$  endows the model with the capability of generating post-inhibitory rebound bursting, intrinsic subthreshold oscillations and resonance [45] [49].
- $I_{dep}$  is a depolarizing spike-triggered current, which has a larger spike-triggered increment ( $A_1$ ) and faster decay ( $k_1$ ) compared to  $I_{adap}$ .  $I_{dep}$  mimics the fast (almost instantaneous) activation and deactivation of sodium channels.  $I_{dep}$  can generate depolarization-induced excitation and sustain post-inhibitory rebound bursts.

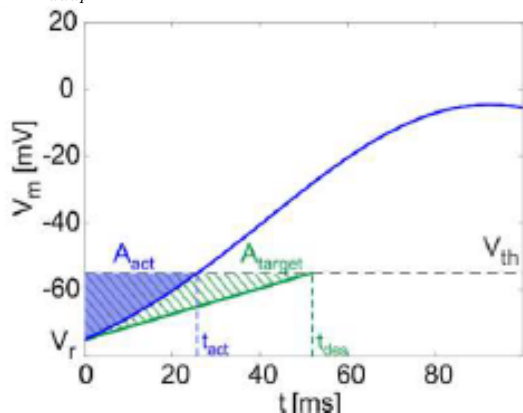
The parameters (listed in Table 4.1) in the model include those directly related to **neurophysiological** quantities ( $C_m, t_m, E_L, t_{ref}, V_{th}, V_r$ ), that are fixed for each specific cell type and their values can be taken from literature or available from animal experiments or databases [50]; and the more **abstract** ones related to neuron-specific functional mechanisms ( $k_{adap}, k_2, k_1, A_2, A_1, I_e$ ), that need to be optimized.

### Optimization

For the other neuron-specific functional parameters (tunable parameters), we developed an optimization strategy based on a desired input-output relationship, considering a current step  $I_{stim}$  as the input and spike times as the output. By computing the analytical solution of the model, we were able to associate different regions in the



(a) Different solution regimes depending on parameters  $k_2$  and  $k_{adap}$



(b) Model analytical solution (blue) vs simplified target area (green)

**Figure 4.10: Parameters optimization (From [48])**

parameter space to different system responses (i.e. exponential or oscillatory and stable or unstable). Specifically, as reported in Figure 4.10a, the  $k_2 - k_{adap}$  plane includes an area corresponding to exponential and stable solutions (in green) and an area with oscillatory stable solutions (in red). Within the latter, the red line corresponding to  $k_2 = \frac{1}{\tau_m}$  defines the condition for not-damped oscillatory solutions, which allow to reproduce self-sustained oscillations of the membrane potential. This was used to constrain the parameter space. To define the cost function, the input-output features listed in Table 4.1 were considered, to evaluate different properties:

- $I_{stim} = 0 \text{ pA}$ : zero current ( $zero_{stim}$ ) generating spikes at frequency  $tonic_{freq}$  to evaluate **autorhythym**;
- $I_{stim}$  at three increasing excitatory current steps ( $exc_1 < exc_2 < exc_3$ ) producing firing with increasing frequency ( $freq_1 < freq_2 < freq_3$ ) to reproduce the

$f - I_{stim}$  relationship and spike-frequency adaption (i.e. steady-state decreased frequency with  $gain_1 > gain_2 > gain_3$ );

- $I_{stim} = inh$ , an inhibitory input current to evaluate the occurrence of an inhibition induced silence followed by rebound burst, made of at least 2-spikes.

To compute the corresponding cost function, we exploited the analytical tractability of the model and we evaluated the model solution  $V_m(t)$ , within the most significant time windows (initial, transitory, and steady state) during each stimulation current step. For each  $I_{stim} = (i) = zero_{stim}, exc_1, exc_2, exc_3$ , the three time windows taken into account were:  $\Delta t_1^{(i)}$ , from  $t_{start}^{(i)}$  to first spike  $t_1^{(i)}$ ,  $\Delta t_2^{(i)}$  between  $t_1^{(i)}$  and second spike time  $t_2^{(i)}$  and  $\Delta t_{ss}^{(i)}$  between two spikes at Steady-State (ss).

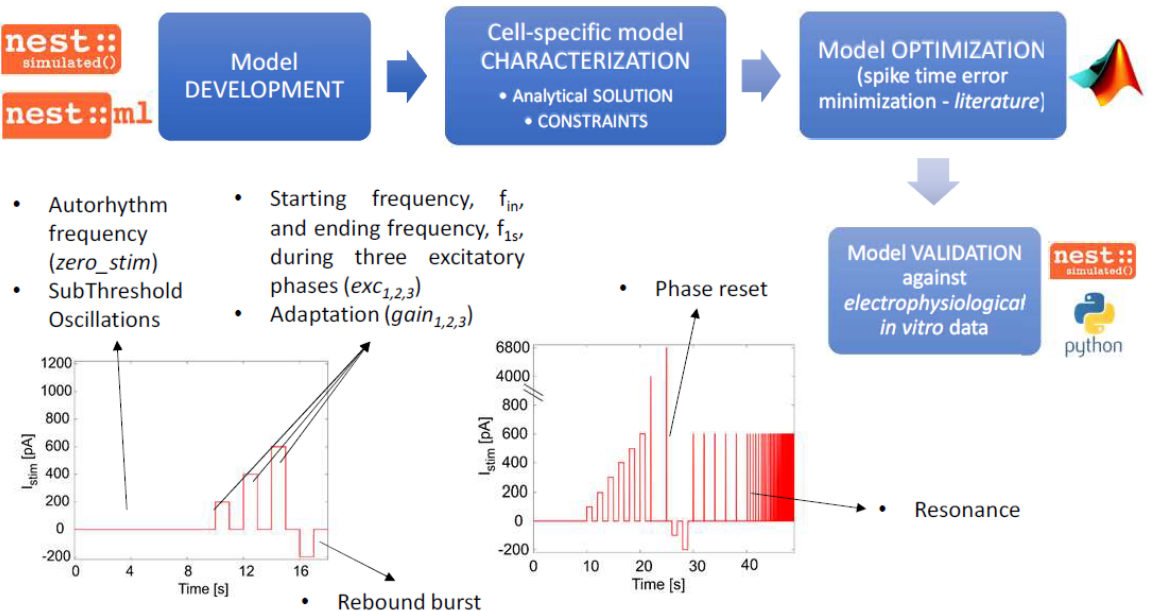


Figure 4.11: E-GLIF – implementation, optimization and validation

#### 4.3.5 E-GLIF Model: Reproducing Golgi Cell Electoresponsiveness

In [48], E-GLIF model and optimization were applied to reproduce the complex electoresponsiveness of cerebellar Golgi cells (GoCs). GoCs are the main inhibitory neurons in the cerebellum granular layer and contribute to filter and reshape the input signals coming from mossy fibers. In single-cell recordings, GoCs show **spontaneous firing** around 8 Hz, a **nearly-linear input-output relationship** (about 0.25 Hz/pA), **input-dependent spike-frequency adaptation** when depolarization is maintained, **rebound bursting** after hyperpolarization, **phase-resetting**, **subthreshold self-sustained oscillations** and **resonance** in the theta band (around 3-6 Hz) [51, 52].

A multi-compartmental realistic model [51]. assumed that dendrites were passive and used them to redistribute the passive electrotonic load while placing all the ionic channels in the soma, suggesting that an appropriate single point model could have been effective as well. In the present E-GLIF model, all electrical properties are collapsed into a point and gating kinetics of ionic channels is substituted by lumped and simplified membrane mechanisms. Parameter associated to passive membrane properties were set to experimental values from literature. Following the algorithm introduced in the previous paragraph, the remaining ones were optimized to reproduce the key electroresponsive features of cerebellar GoCs, fitting the input-output patterns reported in [?].  $k_2$  and  $k_{adap}$  were constrained to reproduce self-sustained subthreshold oscillations of the membrane potential as in Figure 4.10a. The optimal parameter set was obtained from the median of final values from 10 optimization runs.

The model was then validated against *in vitro* recordings from mouse acute cerebellar slices applying also additional current values with respect to those used in the optimization.

The target firing rates were properly reproduced during spontaneous, excitatory and post-inhibitory phases, with increasing spike-frequency adaptation for higher input current values.

In addition, the GoC E-GLIF model was able to reproduce phase reset, subthreshold oscillations of the membrane potential and resonance in theta band, as found in experimental recordings.

## 4.4 Cerebellar Neurons Modelling

Cerebellar neurons have been almost fully characterized in terms of electroresponsive properties. They exhibit different spiking patterns that are fundamental for the network dynamics, noise filtering, plasticity and communication within/among areas.

- **Autorhythm:** spontaneous firing at a certain frequency, with no need of an external stimulation. GoCs, PCs, and DCNs exhibit this property. Autorhythmicity of a cells population at a given frequency can be important in determining the overall intrinsic rhythmicity of the network.
- **Spontaneous subthreshold oscillations:** sinusoidal oscillations of the membrane potential around the threshold value. IO cells, GRCs and GoCs exhibit this property. (In GoCs subthreshold oscillations are present if the spontaneous generation of action potentials is blocked). A stimulation is amplified if it has the same frequency and phase of the subthreshold oscillations, otherwise is filtered out.

- **Depolarization induced bursting:** increased firing rate (burst) following the begin of a depolarizing external stimulation. GoCs, PCs and DCNs exhibit this property.
- **Linear current-frequency relationship.**
- **Spike-frequency adaptation:** decrease in the neuron's firing rate when stimulated with a constant input. GoCs and DCNs exhibit this property.
- **Phase reset:** reset of the spikes train's phase in an autorhythmic cell after receiving a sufficiently high impulse stimulation. Thanks to this property a group of cells firing at the same frequency but with different phases can return to be in phase after a proper stimulation. GoCs and IO cells exhibit this property.
- **Post-inhibitory rebound burst:** increased firing rate following the end of a negative hyperpolarizing input. GoCs and DCNs exhibit this property.
- **Resonance:** maximum firing response at a preferred frequency of the input current stimulus. GoCs and GRCs exhibit this property, and both show the maximum response for frequency of the stimulus in the theta band (1-4 Hz).



# Modelling and Simulation: Cerebellum

---

In network simulations, neurons are represented as computational units mapping inputs into outputs. The inputs are often given by synaptic currents and processed by an internal operator that integrates them and compares the result to a threshold that determines the neuron activation. Links between neurons are weighted, where the *weight*  $w_j$  represents the efficiency (strength) and type of individual synapses  $j$  (i.e. excitatory, inhibitory or null) (Figure 5.1).

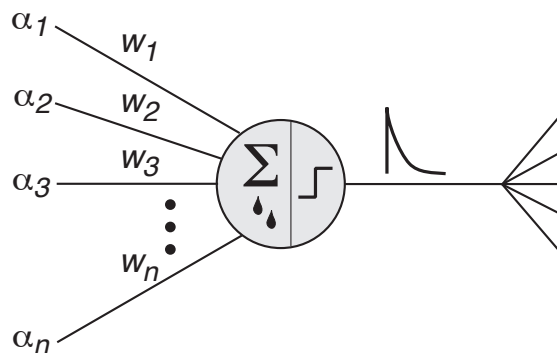


**Figure 5.1:** Schematic of a leaky integrate-and-fire neuron [39]

Note that the weight value of individual synapses represents the type of synapse, which in turn depends on receptor type, and as such shouldn't change sign. This is different for models that describe the average behaviour of neurons or populations.

The modeling of neural networks is still facing many open problems, particularly for realistic modeling of neural connectivity and dynamics, giving birth to different projects such as the *Human Brain Project*, the *Blue Brain Project* and others [29]. Realistic modeling requires to satisfy biophysical rules, biological validations and it also needs new tools for analysis, computation and simulation.

After choosing the appropriate neuron species, they become the building elements to construct neuronal microcircuits of several thousand units. Microcircuits can generate complex dynamics and exhibit a variety of properties such as learning, pattern recognition, signal processing, storing of information and more. In realistic modeling these properties emerge from the network, in a bottom-up approach. Differently, in *theoretical modeling* the model is artificially designed to achieve a particular known function. Eventually, microcircuits can be joined together forming interconnected and feedback subsystems.

Since the cerebellar network operates based on implicit computations with spikes, a biorealistic approach to sensorimotor learning modelling and control requires to develop adaptive Spiking Neural Networks (SNNs). SNNs are artificial neural networks that more closely mimic natural neural networks. In addition to neuronal and synaptic state, SNNs incorporate the concept of time into their operating model. The idea is that neurons in the SNN do not fire at each propagation cycle (as it happens with typical multi-layer perceptron networks), but rather fire only when a membrane potential reaches a specific value.

When a neuron fires, it generates a signal that travels to other neurons which, in turn, increase or decrease their potentials in accordance with this signal. Artificial neural networks are usually fully connected, receiving input from every neuron in the previous layer and signalling every neuron in the subsequent layer. Although these networks have achieved breakthroughs in many fields, they are biologically inaccurate from the point of view of how the single neurons are represented, since they do not mimic the operation mechanisms of neurons in the brain of a living thing. Since biological organisms set up effective control systems using ensembles of interconnected firing neurons, SNNs clearly do have the potential to produce effective bioinspired control systems for robots. Generic SNNs were applied to control sensorimotor tasks in simulations ranging from eye to multi-joint arm movements.

The cerebellum represents a relevant bench-test for computational neuroscience. It has significant **plasticity** properties, that makes it a key element in **motor learning**. Simple simulations can be done to test robot controller based on cerebellum properties (as illustrated in section 5.3), such as pavlovian association protocols. Moreover, the cerebellum can be quite easily studied, thanks to the much higher level of knowledge with respect to other brain areas, that also have more complex cellular architectures.

Specialization of **cerebellum**, **basal ganglia** and **cerebral cortex** for different types of learning rules is illustrated in Figure 5.2 .

The **cerebral cortex** is specialized for **unsupervised learning**, which is guided by the statistical properties of the input signal itself, but may also be regulated by the ascending neuromodulatory inputs. Possible role as learning module:

- Concise representation of sensory state, context, and action

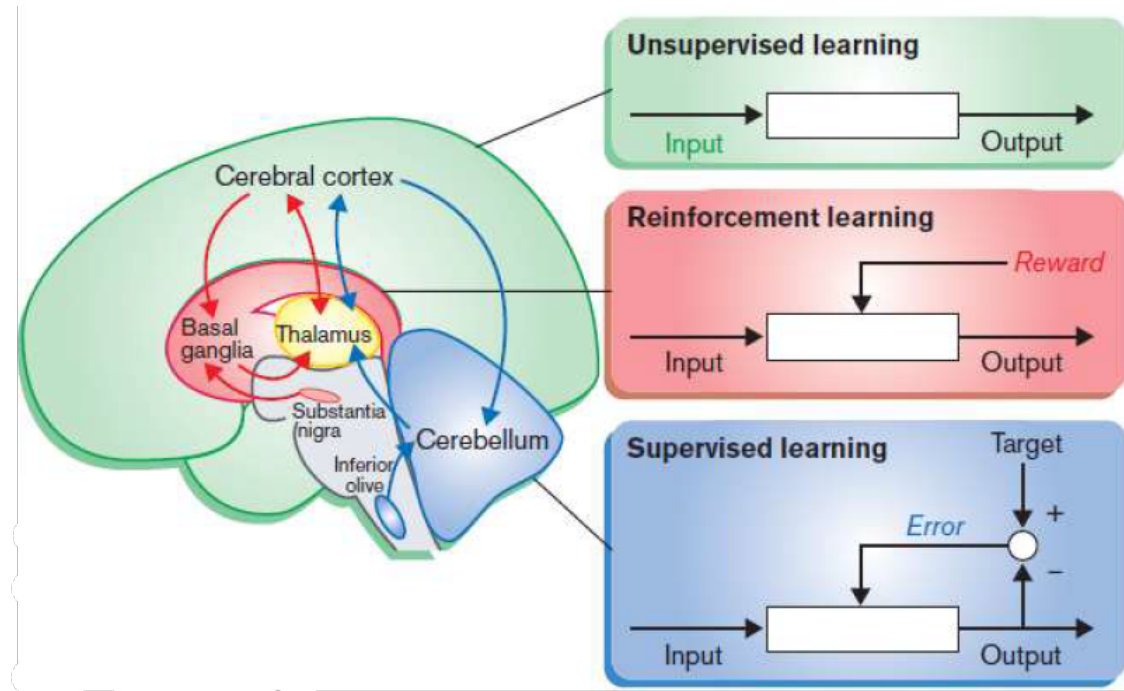


**Figure 5.2: Possible roles of different learning modules: Cerebellum, Basal Ganglia, Motor Cortex (From [53]).**

- Finding appropriate modular architecture for a given task [53].

The **basal ganglia** are specialized **reinforcement learning**, which is guided by the reward signal encoded in the dopaminergic input from the substantia nigra. Possible role as learning module:

- Evaluation of current situation by prediction of reward.
- Selection of appropriate action by evaluation of candidate actions [53].

The **cerebellum** is specialized for **supervised learning**, which is guided by the error signal encoded in the climbing fiber input from the inferior olive. Possible role as learning module:

- Internal models of the body and the environment.
- Replication of arbitrary input-output mapping that was learned elsewhere in the brain [53].

Based on novel experimental evidence, the update and validation of cerebellar model elements, can lead to more realistic simulations of mechanisms at multiple scales: single neuron dynamics, network responses and, eventually, sensorimotor signal encoding. This is of paramount importance if we want to use computational models to help neuroscientists understanding the neural bases of behaviour and also to explain pathological conditions.

Being involved in motor control, major characteristics of cerebellum function are **timing** and **sensory prediction**. For this reason, both feed-forward and feedback circuits are needed. Indeed, cerebellar cortex is organized as a feed-forward excitatory

chain assisted by inhibitory loops (fig. 5.3).

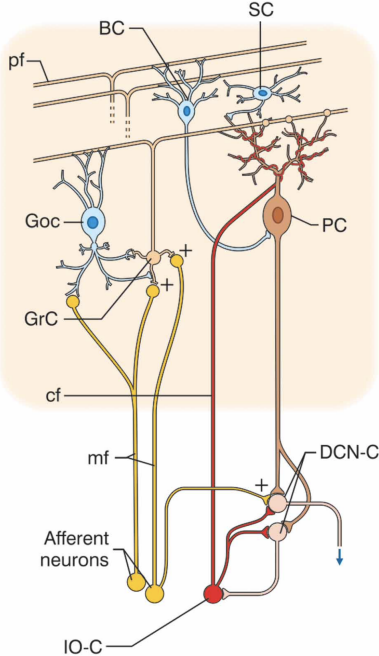


**Figure 5.3: Simplified Cerebellar microcircuit [29]**

The cerebellum can be seen as a **mapping network**, predicting output from input patterns, where the inputs are represented by different sources entering the cerebellum through the *mossy fibers*, that contact the Granular layer. Granule Cells are connected to the Purkinje Cells through *parallel fibers*, and PCs in turn provide an inhibitory action on the output of the cerebellum, the Deep Cerebellar Nuclei. PCs also receive input from *climbing fibers* from the Inferior Olivary nucleus.

To test and validate the impact of network architecture and functioning on computation and behaviour, models can be integrated into robotic simulators or real robots, being both effectors of cerebellar output and feedback controllers of the network. The robot may be involved in multiple protocols regarding various aspects of cerebellar function (see section 5.3).

## 5.1 Cerebellum as an Inverse Model

The possibility that the cerebellum contains an internal model or models of the motor apparatus has been investigated by [17]. As already anticipated, acquiring an inverse dynamics model through motor learning is generally a complex task because the error in the model's output, i.e. the motor command error, which could provide a training signal, is not directly available to the CNS.

If the motor command error were known, there would be no need to learn the inverse

dynamics as the correct control signal would already be known. Instead, movement errors are initially represented in sensory coordinates and these sensory errors need to be converted into motor errors before they can be used to train an inverse model.

Kawato and colleagues have proposed a cerebellar feedback-error learning model [17].

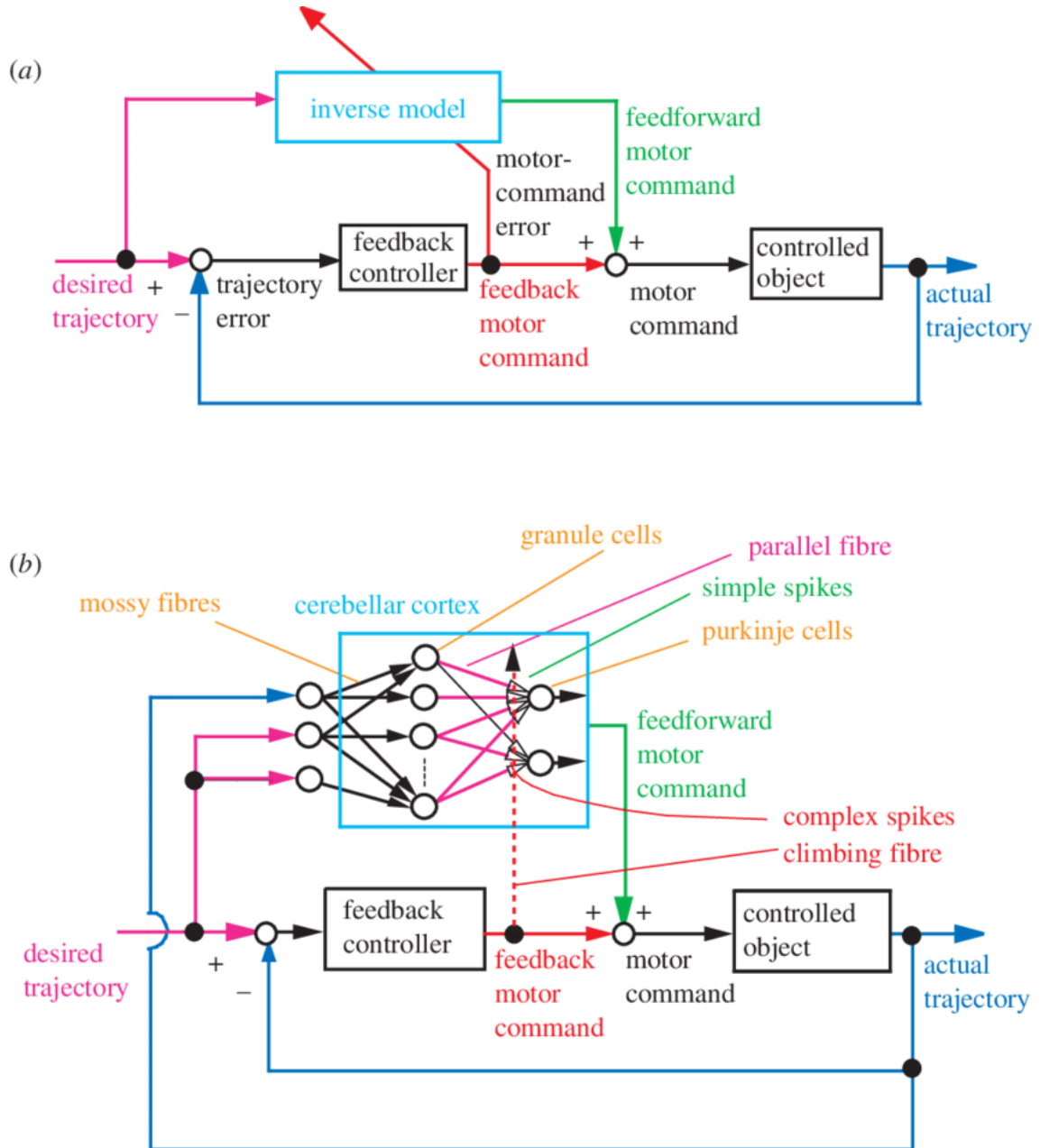


Figure 5.4: Cerebellum as an Inverse Model (From [17])

The ‘controlled object’ is a physical entity that needs to be controlled by the central nervous system (CNS), such as the eyes, hands, legs or torso.

The feedback controller transforms the trajectory error into a feedback motor command, which is then used to train the inverse model. This training signal therefore

represents the sensory error converted into motor command coordinates. Then, the sum of the feedforward and feedback motor commands acts on the controlled object. If a desired trajectory is given to the inverse model, at the end of the cascade the actual trajectory will be close to the desired trajectory. Thus, accurate inverse models can be used as ideal feedforward controllers.

According to this model hypothesis, in the cerebellar circuit simple spikes (SS) represent feedforward motor commands, and the parallel fiber inputs represent the desired trajectory as well as the sensory feedback of the current state of the controlled object. A microzone of the cerebellar cortex constitutes an inverse model of a specific controlled object, such as the eye or arm. *Cf* inputs are assumed to carry a copy of the feedback motor commands generated by a crude feedback control circuit. Thus, the complex spikes (CS) of PC activated by *cf* inputs are predicted to be sensory error signals already expressed in motor command coordinates (see Figure 5.4b).

## 5.2 Plasticity

Plasticity is the capacity of the nervous system to modify its structure and functionalities depending on neural activity. The operative mechanisms of synaptic plasticity are:

- Generation and selective removal of connections, changing the *topology* of the network (*Structural* plasticity).
- Variation in strength of synaptic signals (*Functional* plasticity)
- Spatial position and morphology variation of synapses
- Molecular and chemical variations

At synaptic level, plasticity consists in the modification of the efficiency of neural signal transmission. This process has a direct effect on specializing the function of **neuron populations** that become coherent and synchronized. We can also distinguish two kinds of plasticity: **long-term plasticity** requires a wide temporal span to establish and reinforce/weaken interconnections, but lasts longer; **short-term plasticity**, on the other hand, represents only a temporary variation of synaptic connection.

The central role of associative learning and plasticity as an organizing principle in the brain is essentially captured by the **Hebbian rule**. In a nutshell, it states that if an input coming from a neuron contributes to the firing of it, the synapse from which the input is transmitted should be strengthened. Instead, if the input signal fails to excite the neuron, the connection is weakened.

In artificial neural networks, plasticity is described as a functional plasticity, with weight modifications happening in a discretized time dimension and function of time

and weight itself:

$$w_{ij}(t + \Delta t) = w_{ij}(t) + \Delta w_{ij}(t_i^f, t_j^f, \Delta t, w_{ij}) \quad (5.1)$$

Where  $w_{ij}$  is the strength of the connection from neuron  $j$  to neuron  $i$ , while  $t_i^f$  and  $t_j^f$  represent the firing times of neuron  $i$  and  $j$ .

The relative timing of pre- and postsynaptic spikes plays a critical role in synaptic plasticity, when considered in a time window of about  $\pm 50ms$ . For spiking neurons plasticity is commonly described through **Spike Timing Dependent Plasticity** (STDP) rules. By considering isolated spike pairings, presynaptic spikes that precede postsynaptic action potentials produce **Long Term Potentiation** (LTP), while **Long Term Depression** (LTD) is induced if presynaptic spikes follow postsynaptic action potentials.

The strength of synaptic modification depends on the temporal proximity of the two spikes ( $t_i^n - t_j^f$ ):

$$\Delta w_{ij} = \sum_{f=1}^N \sum_{n=1}^N W(t_i^n - t_j^f) \quad (5.2)$$

Where  $W$  is the STDP function or *learning window*, commonly an exponential function (for more see [http://www.scholarpedia.org/article/Spike-timing\\_dependent\\_plasticity](http://www.scholarpedia.org/article/Spike-timing_dependent_plasticity)). Moreover, as repeated stimuli might lead to instability of the weights, other terms can be employed to introduce weight dependency.

Other types of plasticity can be exploited by three learning procedures:

- **supervised learning:** inputs of a neuron or network are associated with a desired output *target* which can be directly assigned or given by another "teaching" network
- **unsupervised learning:** the network self-organizes depending on plasticity rules and the nature of inputs.
- **reinforcement learning:** combines the previous mechanisms by providing a feedback to the network (reward or punishment), that is used to control plasticity.

### 5.2.1 Plasticity Models in Cerebellar SNN

**Pf-PC** plasticity model:

In the cerebellum changes in the strengths of *pf-PC* synapse could store stimulus-response associations by linking inputs with appropriate motor outputs, following a Hebbian learning approach but using the supervision of *cfs* discharge.

*Cfs* provide a sort of teaching signal that induces synaptic modification in *pf*-PC synapses. Marr ([35]) assumed that *cfs* input would cause synchronously activated *pf* inputs to the same PC to be strengthened. However, the major part of the subsequent cerebellar-learning models has followed Albus theory [36], assuming that *cfs* activity was an error signal and could cause synchronously activated *pf* inputs to be weakened.

Therefore, the modification of the synapse strength at the level of *pf*-PC synapse follows this learning rule: if, at a time  $t$ , the *cfs* spikes, there is a LTD at the level of the synapses with the *pfs* that were active in a given time window before the time  $t$ . If the same *mfs* pattern is provided, trial after trial, the cerebellar network will be capable to learn the correlation between a particular input state and the presence of an error signal, related to *cfs*. The opposite mechanism, the LTP, occurs when there is no *cfs* activity, which corresponds to a decrease or a cancellation of the error signal.

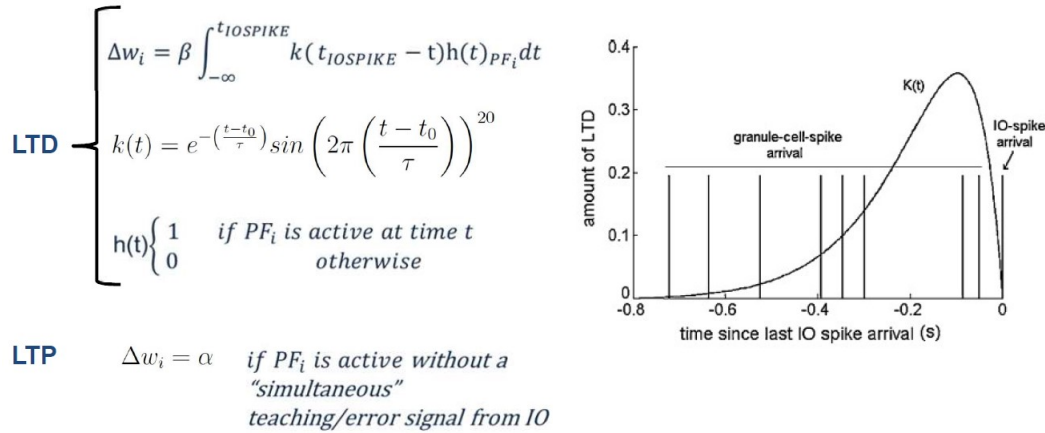


Figure 5.5: Modelling *pf*-PC plasticity

### 5.3 Neurorobotics

Neurorobotics is the research field where neural controllers (controllers based on neurophysiology studies or on neural structures) are embedded into the control of robots with the purpose of investigating the consequent behaviour. The cerebellar controller interacts with the body, for instance a robot, in a closed loop: receiving sensory signals, for example from the motors encoders or from visual systems, and to react to the input generating an action, changing the robot's behavior.

In [54] a cerebellar inspired SNN was built exploiting the Event-Driven simulator based on Look-Up Table (EDLUT), which is an open-source computer application for simulating SNNs. This SNN is composed of 100 *mossy fibers* as inputs, which connect to 2000 Granule Cells of granular layer. Each GrC receives four excitatory input connections selected randomly from *mfs* with constant synaptic weights. There

are 24 Inferior Olive (IO) cells, each IO sends a *climbing fiber* (CF) to one Purkinje Cell (PC). Each GrC is connected to 80% of the PCs, through the *parallel fibers*. PCs inhibit the 12 Deep Cerebellar Nuclei cells (DCN), which are excited by all the *mfs*.

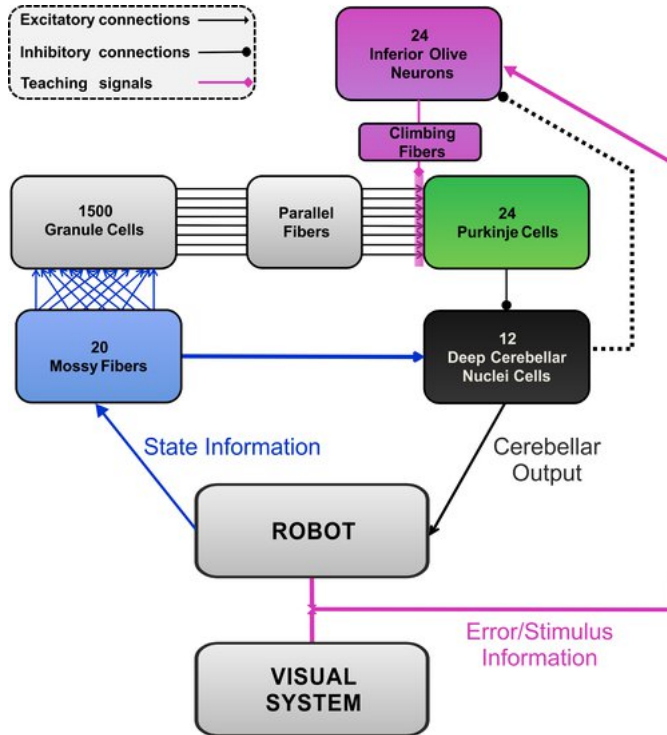


Figure 5.6: *Cerebellar Spiking Neural Network scheme*, from [29]

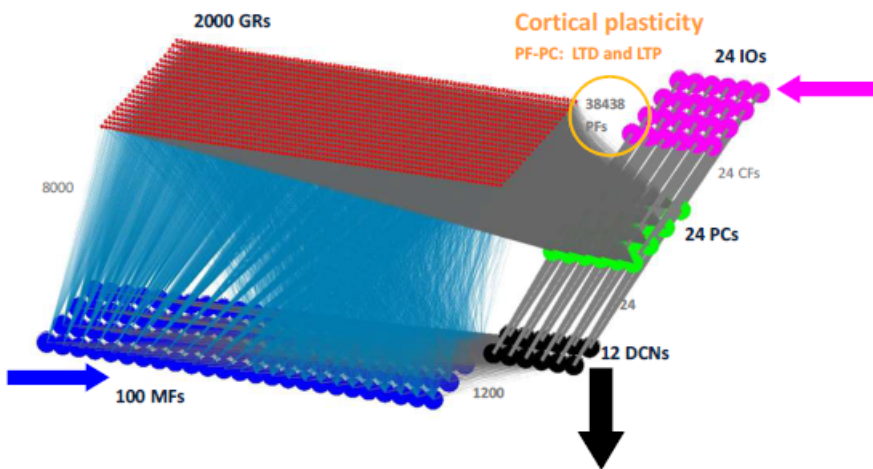


Figure 5.7: *Cerebellar Spiking Neural Network* from [29]

In the SNN, synaptic adaptation occurs at *pf*-PC connections as a change in synaptic conductance through a spike- timing dependent plasticity rule (see details in section 5.2) inducing either Long-Term Depression (LTD) or Long-Term Potentiation (LTP). LTD results from coincident *pf* and *cf* activation, considering all the *pf* spikes

falling within a given time window preceding the *cf* spikes. Conversely, LTP results from *pf* stimulation alone.

The cerebellar SNN was embedded in the robot controller, and the robot was tested in three different protocols, that take inspiration from human physiological paradigms in which the cerebellum has a crucial role. The cerebellar controller interacts with the robot in a closed loop: receiving sensory signals and reacting to the input generating robot control signals, thus actions that change the robot's behaviour.

The same cerebellar architecture can be tested in multiple protocols in order to validate the generalizability of the model to express learning.

Testing protocols can be inspired by human physiological paradigms in which the cerebellum has a crucial role. The **Eye Blinking Classical Conditioning** (EBCC) is a pavlovian associative learning in which the cerebellum is involved in timing association between two stimuli. Other protocols, such as the **Vestibulo-Ocular Reflex** (VOR) and the **reaching perturbed by force fields** involve both timing and gain modulation. In the VOR, the cerebellar output is a continuous cerebellar action that generate the reflex, and in the reaching perturbed by force fields the cerebellar action is added to the feed-back controllers in order to exhibits fine motor control.

### 5.3.1 Eye Blinking Classical Conditioning

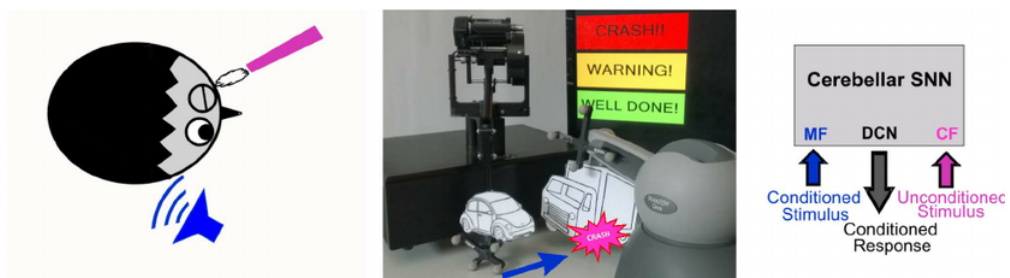


**Figure 5.8: EBCC-like Pavlovian task:** is reproduced into the robotic platform as a collision-avoidance task. The CS onset is based on the distance between the moving robot end-effector and the fixed obstacle placed along the trajectory, detected by the optical tracker. The US is the collision event. US is fed into the *cf* pathway, CS into the *mf* pathway; the DCNs trigger the conditioned response (anticipated stop). (From [54]).

During the EBCC physiological protocol, a human subject receives two stimuli: one **conditioned stimulus** (CS), for example a tone, followed after a well defined interval called inter stimulus interval, for example 400 ms, by a second stimulus, the **unconditioned stimulus** (US), for example an air puff toward the subject's eye. At the beginning of the protocol, the subject close the eye in response to the US: this blinking action is called **unconditioned response** (UR). After repeating some acquisition trials, with the presentation of CS and US paired, the subject learns to

anticipate the eye closure before the US onset, generating a so called **conditioned response** (CR). In [54] they translated this protocol with a collision avoidance task.

### 5.3.2 Vestibulo-Ocular Reflex



**Figure 5.9:** **VOR** is reproduced into the robotic platform by using the second joint of the robotic arm as the head (imposed rotation) and the third joint (determining the orientation of the second link, on which the green laser is placed) as the eye. The disalignment between the gaze direction (i.e. second link orientation) and the environmental target to be looked at (hold and eventually moved by another robotic device) is computed through geometric equations from the optical tracker recording. The image slip is fed into the *cf* pathway, the vestibular stimulus about the head state into the *mf* pathway; the DCNs modulate the eye compensatory motion. (From [54]).

The vestibulo-ocular reflex (VOR) consists of eye movements stabilizing images on the retina during head motion, and its tuning is ascribed mainly to the cerebellar flocculus. It is a paradigm of time-dependent gain learning in reflex movements, in which phase and gain of eye movements must be finely tuned in order to obtain image stabilization during head rotation. In [54], The VOR protocol was reproduced in real robot by using the 2nd joint as the head, on which a desired joint displacement was imposed, and the 3rd joint as the eye, driven only by the cerebellar SNN. The head rotation generating the vestibular input was provided to the 20 *ms*. The visual error was computed as the disalignment between the actual gaze direction, i.e. the orientation of the second link of the robot, and the desired one, aligned with the object to be fixed. This error was provided to the *cfs*. The DCNs modulate the eye compensatory motion. The protocol consisted of a sequence of 400 repetitions where a head turn was imposed and the target object was fixed, followed by 200 repetitions with the same head turn but with the target moving in the same direction as the head, thus requiring a strong VOR gain-down.

### 5.3.3 Reaching Perturbed by Force Fields



**Figure 5.10:** *Perturbed Reaching protocol* is reproduced into the robotic platform by applying a viscous force field on the moving robotic arm by means of the other robotic device attached at its end-effector. The joint error is fed into the *cf* pathway, the desired plan into the *mf* pathway; the DCNs modulate the anticipatory corrective torque. (From [54]).

Force field compensation during arm reaching movements critically depends on the cerebellum, since it acts as a comparator of predicted and perceived state of the limb, adapting to new dynamics. The perturbed reaching is a paradigm of time-dependent gain learning in voluntary multi-joint movements. The cerebellum produces an accurate compensation to external force. It is added to the feedback motor commands, which are not able to learn and anticipate the perturbation effects. In [54], the protocol consisted of a baseline phase of 50 trials, after which the disturbing force lasted 400 repetitions (acquisition phase), followed by 200 extinction trials in which the force field was removed. The perturbed reaching is reproduced into the robotic platform by applying a viscous force field on the moving robotic arm by means of the other robotic device attached at its end-effector. The joint error is fed into the *cf* pathway, the desired plan into the *mf* pathway; the DCNs modulate the anticipatory corrective torque.

---

# List of Figures

---

1	As easy as drinking a glass of water . . . . .	1
1.1	Kinematic and Dynamic transformation . . . . .	5
1.2	Sensorimotor transformations in a reaching movement . . . . .	6
1.3	Perception . . . . .	7
1.4	Reaching task . . . . .	9
1.5	Velocity and Acceleration of the hand movement . . . . .	10
1.6	Motor equivalence: writing . . . . .	11
1.7	Reaction time . . . . .	12
1.8	Fitt's law . . . . .	13
1.9	Learning induced by repetitive training . . . . .	14
1.10	Synapses in adult human neocortex rapidly recover from depression . . . . .	16
1.11	Feedback and Feedforward motor control . . . . .	17
1.12	Inverse and Forward model . . . . .	18
1.13	Forward model . . . . .	19
1.14	Localize a visual object . . . . .	19
1.15	Two eyes for one eye experiments . . . . .	20
1.16	Two eyes for one eye experimental results . . . . .	21
1.17	Why can't you tickle yourself . . . . .	22
1.18	Why can't you tickle your self results . . . . .	22
1.19	Why can't you tickle your self pathological condition . . . . .	23
1.20	Inverse model. . . . .	24
1.21	General feedback-error-learning model. . . . .	25
1.22	Re-afference and Kalman Filter . . . . .	26
1.23	Multiple Paired Forward-Inverse Model . . . . .	27
2.1	Motor control system scheme . . . . .	30
2.2	Motor control system anatomy . . . . .	30
2.3	Histological structure of the cerebral cortex . . . . .	31
2.4	Homunculus . . . . .	33
2.5	Force coding . . . . .	34
2.6	Cortico-motor cell and target muscle activities are not directly correlated . . . . .	35
2.7	How motor cortex encode movement direction . . . . .	36
2.8	Force required to maintain a trajectory . . . . .	37
2.9	Ventral Stream . . . . .	38
2.10	Spinal Cord . . . . .	39
2.11	Spatial Organization of Spinal Cord Neurons . . . . .	40
2.12	Supplementary Motor Areas and Premotor cortex . . . . .	40
2.13	Cerebellum . . . . .	41
2.14	Simplified distributed motor control . . . . .	42

3.1	Anatomical Structure of the Cerebellum . . . . .	44
3.2	Anatomical and Functional Structure of the Cerebellum . . . . .	44
3.3	Effects of Cerebellar Removal . . . . .	45
3.4	Cerebellar Microcircuit . . . . .	46
3.5	Cerebellum Cytology . . . . .	47
3.6	Electrical Activity of Purkinje Cells . . . . .	48
3.7	Spike-Time Dependent Plasticity . . . . .	49
3.8	Experimental protocol of STDP in vitro. . . . .	50
3.9	Synaptic plasticity at parallel fiber– Purkinje cell . . . . .	51
4.1	Neuron Models: biological plausibility vs computational load . . . . .	54
4.2	Hodgkin-Huxley model: Steady-state activation and inactivation functions (left) and time constants (right) are voltage-dependent. [38] . . . . .	56
4.3	HH equivalent circuit . . . . .	56
4.4	Markovian Stochastic HH model . . . . .	57
4.5	Neuron topology reconstruction using compartments . . . . .	58
4.6	Electroresponsive properties of the PC model . . . . .	59
4.7	Leaky Integrate and Fire circuit . . . . .	60
4.8	Izhikevich model dynamics . . . . .	62
4.9	Regular bursting as response of the Adaptive Exponential model to a current step . . . . .	63
4.10	EGILIF Parameters Optimization . . . . .	66
4.11	E-GLIF – implementation, optimization and validation . . . . .	67
5.1	Schematic of a leaky integrate-and-fire neuron [39] . . . . .	71
5.2	Learning Module . . . . .	73
5.3	Simplified Cerebellar microcircuit . . . . .	74
5.4	Cerebellum as an Inverse Model . . . . .	75
5.5	Modelling <i>pf</i> -PC plasticity . . . . .	78
5.6	Cerebellar Spiking Neural Network scheme . . . . .	79
5.7	Cerebellar Spiking Neural Network . . . . .	79
5.8	Robotic EBCC . . . . .	80
5.9	Robotic VOR . . . . .	81
5.10	Robotic Perturbed Reaching task . . . . .	82

---

## List of Tables

---

4.1 E-GLIF parameters . . . . .	65
---------------------------------	----



# Bibliography

---

- [1] E. R. Kandel, J. H. Schwartz, T. M. Jessell, D. of Biochemistry, M. B. T. Jessell, S. Siegelbaum, and A. Hudspeth, *Principles of neural science*, vol. 4. McGraw-hill New York, 2000.
- [2] A. P. Eleanor Gibson, *An ecological approach to perceptual learning and development*. Oxford University press, 2000.
- [3] J. Piaget, “How children form mathematical concepts,” *Scientific American*, vol. 189, no. 5, pp. 74–79, 1953.
- [4] C. von Hofsten, “Structuring of early reaching movements: a longitudinal study,” *Journal of motor behavior*, vol. 23, no. 4, pp. 280–292, 1991.
- [5] K. S. Lashley, “The problem of cerebral organization in vision.,” 1942.
- [6] D. Hebb, *The Organization of Behavior: A Neuropsychological Theory*. John Wiley and Sons, 1949.
- [7] R. S. Woodworth, “Accuracy of voluntary movement.,” *The Psychological Review: Monograph Supplements*, vol. 3, no. 3, p. i, 1899.
- [8] R. A. Schmidt, H. Zelaznik, B. Hawkins, J. S. Frank, and J. T. Quinn Jr, “Motor-output variability: a theory for the accuracy of rapid motor acts.,” *Psychological review*, vol. 86, no. 5, p. 415, 1979.
- [9] G. Testa-Silva, M. B. Verhoog, D. Linaro, C. P. De Kock, J. C. Baayen, R. M. Meredith, C. I. De Zeeuw, M. Giugliano, and H. D. Mansvelder, “High bandwidth synaptic communication and frequency tracking in human neocortex,” *PLoS Biol*, vol. 12, no. 11, p. e1002007, 2014.
- [10] H. H. T. S. Mitsuo Kawato, Shogo Ohmae, “50 years since the marr, ito, and albus models of the cerebellum,” *Neuroscience*, vol. Jun, 2020.

- [11] M. Kawato and D. Wolpert, "Internal models for motor control," *Novartis Found Symp*, vol. 218, pp. 291–307, 1998.
- [12] D. M. Wolpert and J. R. Flanagan, "Motor prediction," *Current biology*, vol. 11, no. 18, pp. R729–R732, 2001.
- [13] G. M. Gauthier, D. Nommay, and J.-L. Vercher, "The role of ocular muscle proprioception in visual localization of targets," *Science*, vol. 249, no. 4964, pp. 58–61, 1990.
- [14] S. S. Shergill, P. M. Bays, C. D. Frith, D. M. Wolpert, *et al.*, "Two eyes for an eye: the neuroscience of force escalation," *Science*, vol. 301, no. 5630, pp. 187–187, 2003.
- [15] S.-J. Lakemore, D. Wolpert, and C. Frith, "Why can't you tickle yourself?," *Neuroreport*, vol. 11, no. 11, pp. R11–R16, 2000.
- [16] D. M. Wolpert and Z. Ghahramani, "Computational principles of movement neuroscience," *Nature neuroscience*, vol. 3, no. 11, pp. 1212–1217, 2000.
- [17] M. Kawato, "Internal models for motor control and trajectory planning," *Curr Opin Neurobiol*, vol. 9, p. 718–727, 1999.
- [18] D. Wolpert and M. Kawato, "Multiple paired forward and inverse models for motor control," *Neural Networks*, vol. 11, no. 7-8, pp. 1317–1329, 1998.
- [19] P. Dayan and L. F. Abbott, *Theoretical neuroscience: computational and mathematical modeling of neural systems*. Computational Neuroscience Series, 2001.
- [20] E. Fetz and P. Cheney, "Muscle fields and response properties of primate corticomotoneuronal cells," in *Progress in brain research*, vol. 50, pp. 137–146, Elsevier, 1979.
- [21] E. V. Evarts, "Relation of pyramidal tract activity to force exerted during voluntary movement," *J Neurophysiol*, vol. 31, no. 1, pp. 14–27, 1968.
- [22] J. Tanji and E. V. Evarts, "Anticipatory activity of motor cortex neurons in relation to direction of an intended movement," *J Neurophysiol*, vol. 39, no. 5, pp. 1062–1068, 1976.
- [23] M. A. Maier, K. M. Bennett, M. C. Hepp-Reymond, and R. N. Lemon, "Contribution of the monkey corticomotoneuronal system to the control of force in precision grip," *J Neurophysiol*, vol. 69, no. 3, pp. 772–785, 1993.
- [24] A. P. Georgopoulos, J. F. Kalaska, R. Caminiti, and J. T. Massey, "On the relations between the direction of two-dimensional arm movements and cell discharge in primate motor cortex," *J Neurosci*, vol. 2, no. 11, pp. 1527–1537, 1982.
- [25] J. F. Kalaska, D. A. Cohen, M. L. Hyde, and M. Prud'Homme., "A comparison of movement direction-related versus load direction-related activity in primate motor cortex, using a two-dimensional reaching task," *J Neurosci*, vol. 9, no. 6, pp. 2080–2102, 1989.

- [26] S. J. Thorpe and M. Fabre-Thorpe, “Seeking categories in the brain,” *Science*, vol. 291, no. 5502, pp. 260–263, 2001.
- [27] E. D’Angelo and S. Casali, “Seeking a unified framework for cerebellar function and dysfunction: From circuit operations to cognition,” *Frontiers in Neural Circuits*, vol. 6, no. 116, 2012.
- [28] A. M. D’Mello and C. J. Stoodley, “Cerebro-cerebellar circuits in autism spectrum disorder,” *Frontiers in neuroscience*, vol. 9, p. 408, 2015.
- [29] E. D’Angelo *et al.*, “Realistic modeling of neurons and networks: towards brain simulation,” *Funct Neurol*, vol. 28, no. 3, pp. 153 – 166, 2013.
- [30] Y. Zang and E. D. Schutter, “Climbing Fibers Provide Graded Error Signals in Cerebellar Learning,” *Front. Syst. Neurosci.*, vol. 13, no. 46, 2019.
- [31] G.-q. Bi and M.-m. Poo, “Synaptic modification by correlated activity: Hebb’s postulate revisited,” *Annual review of neuroscience*, vol. 24, no. 1, pp. 139–166, 2001.
- [32] G. qiang Bi and M. ming Poo, “Synaptic modifications in cultured hippocampal neurons: dependence on spike timing, synaptic strength, and postsynaptic cell type,” *J Neurosci*, vol. 18, no. 24, pp. 10464–10472, 1998.
- [33] H. Markram, J. Lübke, M. Frotscher, and B. Sakmann, “Synaptic modifications in cultured hippocampal neurons: dependence on spike timing, synaptic strength, and postsynaptic cell type,” *Science*, vol. 275, no. 5297, pp. 213–215, 1997.
- [34] W. Gerstner, R. Kempter, J. L. V. Hemmen, and H. Wagner, “A neuronal learning rule for sub-millisecond temporal coding,” *Nature*, vol. 383, no. 6595, pp. 76–78, 1996.
- [35] D. Marr, “A theory of cerebellar cortex,” *The Journal of Physiology*, 1969.
- [36] J. S. Albus, “A theory of cerebellar function,” *Mathematical Biosciences*, 1971.
- [37] E. M. Izhikevich, “Which model to use for cortical spiking neurons?,” *IEEE transactions on neural networks*, vol. 15, no. 5, pp. 1063–1070, 2004.
- [38] A. L. Hodgkin and A. F. Huxley, “A quantitative description of membrane current and its application to conduction and excitation in nerve,” *The Journal of Physiology*, vol. 117, no. 4, pp. 500 – 544, 1952.
- [39] T. P. Trappenberg, *Fundamentals of Computational Neuroscience*. Oxford university press, 2010.
- [40] W. M. Yamada, C. Koch, and P. R. Adams, *Methods in Neuronal Modeling: From Synapses to Networks*, ch. Multiple channels and calcium dynamics. Cambridge, MA: Bradford Book, The MIT Press, 1989.

- [41] S. Diwakar, J. Magistretti, M. G. M, G. Naldi, and E. D'Angelo, "Axonal na<sup>+</sup> channels ensure fast spike activation and back-propagation in cerebellar granule cells," *J Neurophysiol*, vol. 101, no. 2, pp. 519–32, 2009.
- [42] S. Masoli, S. Solinas, and E. D'Angelo, "Action potential processing in a detailed purkinje cell model reveals a critical role for axonal compartmentalization," *Frontiers in Cellular Neuroscience*, vol. 9, 2015.
- [43] L. Lapicque, "Recherches quantitatives sur l'excitation électrique des nerfs traitée comme une polarization," *J Physiol Pathol Gen*, vol. 9, p. 620–635, 1907.
- [44] E. Izhikevich and G. M. Edelman, "Large-scale model of mammalian thalamocortical systems," *PNAS*, vol. 105, no. 9, pp. 3593–8, 2008.
- [45] R. Brette and W. Gerstner, "Adaptive exponential integrate-and-fire model as an effective description of neuronal activity," *J Neurophysiol*, 2005.
- [46] P. C, M. S, H. O, N. R. K. C, and G. W, "Automated high-throughput characterization of single neurons by means of simplified spiking models," *PLoS Comput Bio*, vol. 11, no. 6, p. e1004275, 2015.
- [47] S. Mihalaş and E. Niebur, "A generalized linear integrate-and-fire neural model produces diverse spiking behaviors," *PLoS Comput Bio*, vol. 21, no. 3, pp. 704–18, 2009.
- [48] A. Geminiani, C. Casellato, F. Locatelli, F. Prestori, A. Pedrocchi, and E. D'Angelo, "Complex dynamics in simplified neuronal models: Reproducing golgi cell electroresponsiveness," *Frontiers in Neuroinformatics*, vol. 12, no. 88, 2018.
- [49] L. Hertäg, J. Hass, T. Golovko, and D. Durstewitz, "An approximation to the adaptive exponential integrate-and-fire neuron model allows fast and predictive fitting to physiological data," *Frontiers in computational neuroscience*, vol. 6, p. 62, 2012.
- [50] P. Tripathy, B. Sahoo, A. Priyadarshini, S. Das, and D. Dash, "Standardization of kharif onion cultivars," *International Journal of Bio-resource and Stress Management*, vol. 5, no. 2, pp. 269–274, 2014.
- [51] S. Solinas, L. Forti, E. Cesana, J. Mapelli, E. De Schutter, and E. D'Angelo, "Fast-reset of pacemaking and theta-frequency resonance patterns in cerebellar golgi cells: simulations of their impact in vivo," *Frontiers in cellular neuroscience*, vol. 1, p. 4, 2007.
- [52] C. E. M. J. . D. E. Forti, L., "Ionic mechanisms of autorhythmic firing in rat cerebellar golgi cells," *The Journal of physiology*, vol. 574, no. 3, p. 711–729, 2006.
- [53] K. Doya, "Complementary roles of basal ganglia and cerebellum in learning and motor control," *Current opinion in neurobiology*, vol. 10, no. 6, pp. 732–739, 2000.

- [54] C. Casellato, A. Antonietti, J. A. Garrido, R. R. Carrillo, N. R. Luque, E. Ros, A. Pedrocchi, and E. D'Angelo, "Adaptive robotic control driven by a versatile spiking cerebellar network," *PLoS one*, vol. 9, no. 11, p. e112265, 2014.